DOKUZ EYLÜL UNIVERSITY
GRADUATE SCHOOL OF NATURAL AND APPLIED SCIENCES

THE IMPROVEMENT OF MECHANICAL PROPERTIES OF STRUCTURAL REPAIR MORTARS BY WASTE PLASTICS

by
Dheya Mohammed Ali GHILAN

March, 2018
İZMİR

THE IMPROVEMENT OF MECHANICAL PROPERTIES OF STRUCTURAL REPAIR MORTARS BY WASTE PLASTICS

A Thesis Submitted to the
Graduate School of Natural and Applied Sciences of Dokuz Eylül University
in Partial Fulfillment of the Requirements for the Master Degree
in Civil Engineering, Structural Engineering Program

by
Dheya Mohammed Ali GHILAN

March, 2018
İZMİR

M.Sc THESIS EXAMINATION RESULT FORM

We have read the thesis entitled **"THE IMPROVEMENT OF MECHANICAL PROPERTIES OF STRUCTURAL REPAIR MORTARS BY WASTE PLASTICS"** completed by **DHEYA MOHAMMED ALI GHILAN** under supervision of **ASSOC. PROF. EGEMEN TEOMETE** and we certify that in our opinion it is fully adequate, in scope and in quality, as a thesis for the degree of Master of Science.

....

Assoc. Prof. Egemen TEOMETE

Supervisor

....

Prof. Dr. Serap KAHRAMAN

Jury Member

....

Doç. Dr. Ninel ALVER

Jury Member

Prof. Dr. Kadriye ERTEKİN

Director

Graduate School of Natural and Applied Sciences

ACKNOWLEDGMENT

I would like express my gratitude to my supervisor, Associated Professor Egemen TEOMETE, who guided and encouraged me from the initial to the final level and motivated me to understand of the subject. His help was priceless to the progress of my education and the construction of this thesis.

I am also thankful to Batıçim Batı Anadolu Çimento Sanayii A.Ş., Sika Yapı Kimyasalları A.Ş. and Narsan Plastik San. Tic. Ltd. for supporting this research with materials.

I would also like to thank my supporting friends specially Cihan Karademir who never ceased helping me in the laboratorial work.

I am grateful to the Presidency of Turks Abroad and Related Communities who made it possible for me to come and study my MSc degree in Turkey under the Turkiye Scholarships program.

I am thankful to my great mother and the rest of my family for all the great support and encourage they gave me through this journey.

Dheya Mohammed Ali GHILAN

THE IMPROVEMENT OF MECHANICAL PROPERTIES OF STRUCTURAL REPAIR MORTARS BY WASTE PLASTICS

ABSTRACT

This research presents an experimental study on the mechanical performance of repair mortar by incorporating waste plastic as fiber reinforcement. Waste plastic fibers used were; 1) Waste polyethylene terephthalate (PET) fibers produced in the laboratory by shredding post-consumer PET bottles in the dimensions of 5×10, 5×15 and 5×20 mm. 2) Waste polyethylene laminated PET (PET/PE) fibers were produced in the laboratory by chopping waste PET/PE sheets in the dimensions of 5×10 and 5×15 mm. PET and PET/PE were incorporated into the mortar with volume ratios of 0.2, 0.5, 0.8, 1, 1.5 and 2 percentage. 3) Industrial waste polypropylene (PP), polyethylene (PE) and polyamide (PA) and chemically surface-treated waste PP and PE with volume ratios of 0.2, 0.5, 0.8, 1 and 1.5 percentage. A total of 55 mixtures were designed. From each mixture in the study, 3 prismatic samples of 4×4×16 cm dimension were cast and tested with 3-point bending test. Compression test was applied to the sides of the samples; thus, six compression tests were done for each mixture. Load and stroke were recorded during the mechanical tests and flexural and compressive strength and toughness were analyzed and discussed. Waste plastic fiber reinforced self-compacting mortar (SCM) was designed and concrete repairing tests were conducted. Bonding between concrete and SCM was studied through 3 different ways; drilling, nail planting and roughening the concrete surface. Total of 18 concrete beam specimens of the dimensions 30.5×7.5×7.5 cm was tested with 3-point bending and compression tests, and a total of 39 concrete cube specimens of the dimensions 7.5×7.5×7.5 cm was tested with split tensile and compression tests. Results show a magnificent increase in flexural toughness for waste plastic fiber reinforced mortar.

Keywords: Chemical treatment, fiber reinforced, mechanical properties, repair mortar, recycling, waste plastic

YAPISAL TAMİR HARÇLARININ MEKANİK ÖZELLİKLERİNİN PLASTİK ATIKLARIYLA İYİLEŞTİRİLMESİ

ÖZ

Bu çalışmada, atık plastiklerin, tamir harcın mekanik özelliklerine etkisi üzerine bir deneysel çalışmadır. Kullanılan atık plastik lifler; 1) Atık polietilen tereftalat (PET) lifleri, PET şişeleri 5×10, 5×15 ve 5×20 mm boyutlarında kesilerek laboratuvarda elde edildi. 2) Atık polietilen lamineli PET (PET/PE) lifleri, PET/PE poşetleri 5×10 ve 5×15 mm boyutlarında kesilerek laboratuvarda elde edildi. PET ve PET/PE lifleri 0,2, 0,5, 0,8, 1, 1,5 ve 2 oranında hacim oranları ile harç içine dahil edildi. 3) hacim oranları ile yüzde 0,2, 0,5, 0,8, 1 ve 1,5 endüstriyel atık polipropilen (PP), polietilen (PE), poliamid (PA), kimyasal yüzey-işlemli endüstriyel atık PP ve PE. Toplam 55 karışım tasarlandı. Çalışmanın her karışımından 4×4×16 cm boyutunda 3 prizmatik numune döküldü ve 3-nokta eğilme testi ile test edildi. Basınç testi, eğilme testinde çıkan örneklerin her iki kenarına uygulanmıştır; böylece, her karışım için altı basınç testi yapıldı. Mekanik testler sırasında yük ve deplasman kaydedildi. Plastik atıkların eğilme ve basınç dayanımı ve tokluğuna etkileri belirlendi. Atık plastik elyafı ile güçlendirilmiş kendiliğinden yerleşen harç (KYH) tasarımı ve beton güçlendirme deneyleri yapıldı. Beton ve KYH arasındaki aderans, beton yüzeyi delme, çivi dikme ve pürüzlendirme 3 farklı yöntemle incelendi. 30,5×7,5×7,5 cm boyutlarında toplam 18 beton kiriş numune 3-nokta eğilme ve basınç testleri ile test edildi. 7,5×7,5×7,5 cm boyutlarında toplam 39 beton küp numune yarmada çekme ve basınç testleri ile test edildi. Plastik atıkların, harcın eğilme tokluğunu önemli ölçüde arttırdığı ve tamir harcının beton güçlendirme performansını olumlu etkilediği tespit edildi.

Anahtar Kelimeler: Atık plastik, elyaf takviyeli, geri dönüşüm, kimyasal yüzey işlemi, mekanik özellikler, tamir harcı

CONTENTS

LIST OF FIGURES

LIST OF TABLES

Page

CHAPTER ONE
INTRODUCTION

In the last decades, plastics have been increasing magnificently in usage area and quantities due to their economical, high durability, easy to apply and other features. As a result, plastic waste is considered to be one of the major sources of pollution hazards on environment in consequence of its non-biodegradable nature and its content of several toxic chemicals, stabilizers, pigments, and colorants (Siddique, Khatib, Kaur, 2008; Gu, Ozbakkaloglu, 2016).

Plastics are very difficult to degrade in nature due to their chemical structure. These features cause environmental pollution in large scale. Some insufficient practices were applied to dispose of plastic waste including incineration, which produces dangerous gases that affect human life, and landfilling that means preserving harmful materials in our environment continually. These kinds of remedies lead to environmental deterioration that brings up the need to exploit this material in environmentally friendly way and to develop an effective recycling process (Saikia, de Brito, 2012; Sharma, Bansal, 2015).

Since construction industry is considered as one of the largest fields that expend natural resources, it was intuitive to search for an alternative process to dispose of plastic waste in a beneficial way in this industry. Incorporating plastics into construction elements results in significant benefits such as less density of construction elements which leads to smaller cross sections and to reducing the size of foundations. Added to that, enhancing the ductility, which will affect in a positive manner to prevent or at least to limit the propagation of micro and macro cracks of concrete and to decrease shrinkage (Saikia, de Brito, 2014; Choi, Moon, Kim, Lachemi, 2009; Choi, Moon, Chung, Cho, 2005; Foti, 2011).

We can differentiate between four major ways of recycling waste plastic into construction materials. First, producing polymer cementitious composites by contributing unsaturated polyester resin depolymerizing waste plastics. The cost of producing these polymers is considered high; in addition to its sensitivity to be affected by temperature. The second method is producing lightweight cementitious composites by substituting a portion of the aggregate for dosages of treated granular plastics. This method has positively affected producing lightweight cementitious composites but the results show weaker mechanical characteristics due to the prominent decrease of compressive strength, splitting tensile strength, and modulus of elasticity. The third method is to melt plastic by heat process and using it directly as a binder. More research is needed in this field. The fourth method is to use waste plastic fibers to reinforce concrete or mortar. It has a good result in reducing shrinkage and cracking but it still consumes a small quantity of plastic waste (Saikia et al., 2012; Ge, Sun, Zhang, Gao, Li, 2013).

In search works related to using plastics as a substitute of aggregates in cementitious composites, the mortars had good insulation properties with a decrease in mechanical compression performances when polyethylene (PE) polypropylene (PP) and polyethylene terephthalate (PET) based fiber polymeric wastes are used as aggregate replacement in lightweight mortar (Verdolotti, Iucolano, Capasso, Lavorgna, Iannace, Liguorib, 2014). Although the incorporation of plastics aggregates has proven to be unfavorable for certain properties, such as mechanical and adhesive strength, or water absorption, other properties obtained a considerable improvement in mortar's performance, such as water vapor permeability and impact resistance (da Silva, de Brito, Veiga, 2014). PET waste can be used successfully as a fine aggregate in self-compacting mortars despite the 28th compressive strength of self-compacting mortar containing up to 50% of plastic waste was reduced by 33% (Safi, Saidi, Aboutaleb, Maallem, 2013). Examining different plastic forms has demonstrated that the most efficient plastic aggregate used in a concrete mix should have using a rough surface, be irregular in shape, and have sufficiently small size at the same time graded similar to the sand it substitutes (Thorneycroft, Orr, Savoikar, Ball, 2018). The flexural strength, compressive strength and splitting tensile of normal and high strength concrete decreased with recycled plastic aggregate content (Ozbakkaloglu, Gu, Gholampour, 2017).

In search works related to using plastics as a reinforcing fiber, it was reported that mortar samples containing 1.5% of 50 mm long recycled PET fibers show substantial increase in flexural toughness and a significant increase in flexural strength compared to control mortar prisms without fibers (Al-Tulaian, Al-Shannag, Al-Hozaimy, 2016). The fraction of fiber volume affected the control of plastic shrinkage cracking regardless of the fiber geometry. Relatively low fiber fractions of up to 0.25% by volume had a significant ability to control plastic shrinkage cracking, whereas fiber fractions greater than 0.5% had almost identical characteristics regardless of fiber geometry (Kim, Park, Lee, Lee, Won, 2008). Flexural toughness of ultra-lightweight cement composites is increased linearly with the fiber dosage up to 0.5% by volume when combinations of the PE and steel fibers were used as reinforcement (Wang, Chia, Liew, Zhang, 2013). Monofilaments of polypropylene are more effective in reinforcing a cementitious matrix than split film and bundled multifilament strands (Peled, Guttman, 1992).

A large number of researchers attribute the decrease in some characteristics of cementitious composites incorporating plastics to the weak bonding between the cementitious matrix and plastic surface. So, many experiments were applied in attempt to improve the adhesion in the interfacial area, thus enhancing the properties of the cementitious composites.

High drop in contact angle of PP when treated by low frequency cold plasma of argon and oxygen gases and noticed a substantial improvement in the flexural strength and toughness of polypropylene fiber reinforced cementitious composites (Felekoglu, Tosun, Baradan, 2009). Peled et al. concluded that the dipping monofilaments of PP fibers into a bath of sulphuric acid and sodium dichromate solution or dipping monofilaments of PP fibers in a solution of nonionic detergent are effective in enhancing the first crack stress and the post-cracking behavior of the composites. And that the dipping of monofilaments of PP fibers in a Br2+H20 solution and then placing in an ammonia solution enhanced the first crack stress but did not the improve the post-cracking behavior. PVAC treatment of monofilaments (dipping fibers in a 5% polyvinyl acetate solution after they are dipped in a Br2+H20 solution and then placed in an ammonia solution) was not efficient and may was detrimental to the performance in the post-cracking zone. A decrease in contact angle value from 120 to 96 degrees was observed when PP fibers are treated by the alkaline surface treatment. Flexural strength is increased for concrete containing treated PP fibers. Treated PP fibers acted as anti-cracking agents impeding the propagation of cracks once load is applied (López-Buendía, Romero-Sánchez, Climent, Guillemb, 2013). The influence of chemical treatment on the mechanical properties of polymer FRC was investigated using Chromic acid, Potassium permanganate, and Hydrogen peroxide. the different surface treatment techniques showed decrease in contact angle, slight improvements in flexural residual strength and significant increase of toughness, slight decrease in the 7th and 28th day compressive strength peak strength (Payrow, Nokken, Banu, Feldman, 2011).

The main purpose of the study is to investigate the effects of using different waste plastics as reinforcing fiber for mortar in order to reduce waste and harmful effects of recycling waste plastics and to enhance specific properties of mortar. In this study, the effects of waste plastics fibers on the mechanical properties of mortar were investigated by contributing certain proportions of different types of waste plastic fibers, with and without chemical treatment, into mortar. Waste plastic fiber reinforced self-compacting mortar (SCM) and its ability to repair conventional concrete was also researched.

CHAPTER TWO
MATERIALS AND METHOD

This chapter presents materials, concrete design, equipment, and preparation methods for all laboratorial experiments used in this research.

2.1 Materials

2.1.1 Coarse Aggregates

Coarse aggregates were of crushed limestone with 5-15 mm granule size, supplied from BATIBETON Company. The results of the sieve analysis are presented in Figure 2.1. Sand was tested in the material laboratory in compliance with the TURKISH STANDARD (TS) 3526 “Test Method for Specific Gravity and Water Absorption of Aggregates for Concrete". The moisture content of the gravel was 0.23%, the water absorption rate was 0.5% and the saturated surface-dry (SSD) specific gravity was found as 2.7.

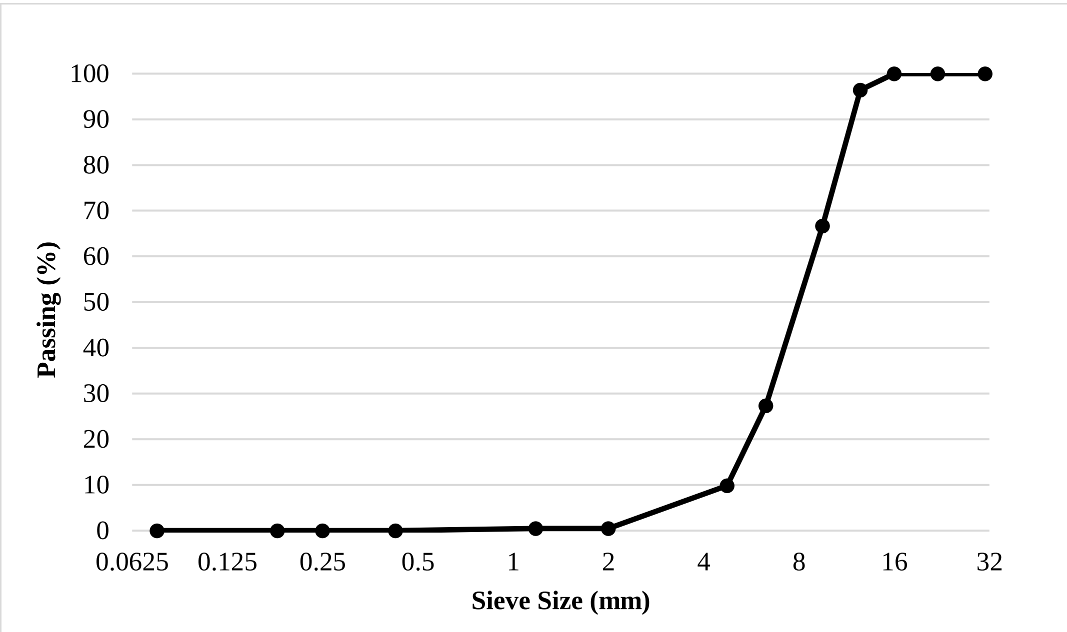

Figure 2.1 Sieve analysis of the coarse aggregates (5-15 mm) used in the study

2.1.2 Fine Aggregates

Fine aggregates were of crushed limestone with 5 mm maximum granule size supplied from BATIBETON Company. The results of the sieve analysis are presented in Figure 2.2. Sand was tested in the material laboratory to fulfill the TS 3526 “Test Method for Specific Gravity and Water Absorption of Aggregates for Concrete". The moisture content of the gravel was 0.55%, water absorption rate was 1.67% and SSD specific gravity was determined as 2.63.

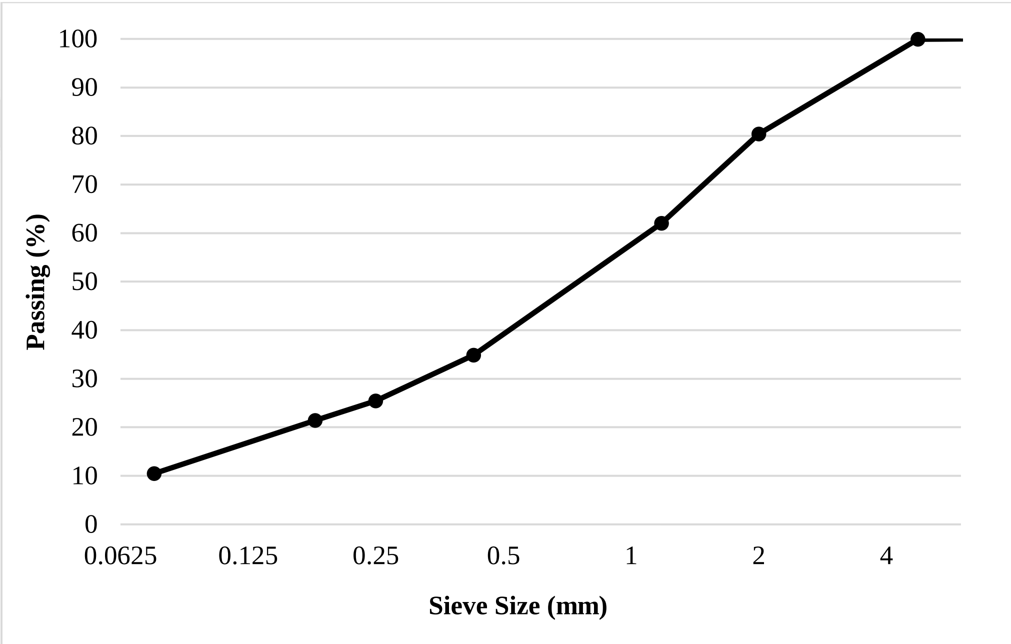

Figure 2.2 Sieve analysis of the fine aggregates (0-5 mm) used in the study

2.1.3 Cement

In the literature different cement types were used. In this study CEM II / B-M (L-W) 42.5 R was used. This type of cement is used widely in ready mixed concrete and precast fabricated structures. It was supplied from BATIÇİM Batı Anadolu Çimento Sanayii A.Ş. The physical properties of the cement used were as follows; the specific gravity was 2.98, and the specific surface was 4607 gr/cm^2. Cement was kept in plastic drums to prevent it from being affected by air humidity.

2.1.4 Silica Fume

MasterROC MS610 silica fume was used in the mixtures. It was supplied from BASF Türk Kimya San. and Tic. Ltd. Granule size of silica fume was identified by microscope images and shown in Figure 2.3. It was ranging from 200 to 300 nm. Technical specifications of the product are shown in Table 2.1.

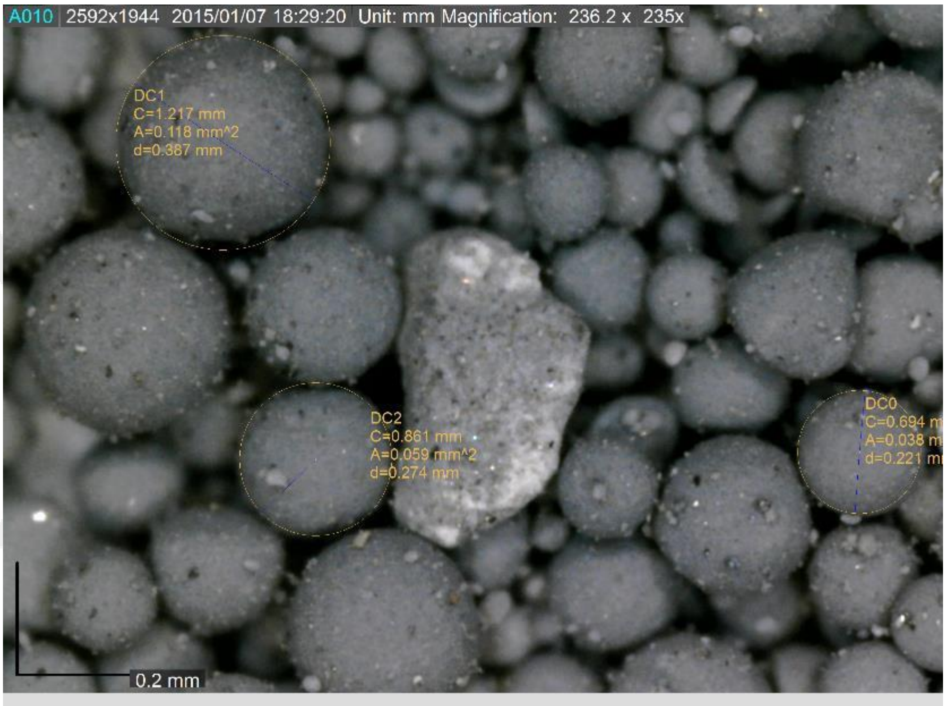

Figure 2.3 Microscope image of the silica fume 235 times magnified (Kolatar, 2016)

Table 2.1 Silica fume MasterROC MS610’s specifications (Manufacturer data)

Form	Powder
Color	Grey
Density	0.55 - 0.7 kg/l
Chloride content	<0.1%

2.1.5 Plasticizer

Sika Viscocrete Hi-Tech30 superplasticizer was used in the mixtures. It was supplied from Sika Yapı Kimyasalları A.Ş. Product specifications are given in Table 2.2.

Table 2.2 Sika Viscocrete Hi-Tech30 superplasticizer's specifications (Manufacturer data)

Chemical Base	Modified polycarboxylates based polymer
Density	1.07 – 1.11 kg/l, 20 °C
pH Value	3 – 7
Freezing point	-9 °C
Soluble in Water Chloride Ion Content % w/w	Max. %0.1, Chloride-free
Equivalent Sodium Oxide as % Na2O	Max. % 4

2.1.6 Water

Potable water was used in mixing and curing processes to make sure not to exceed the limits of the chemical constituents present in water that may actively participate in the chemical reactions.

2.1.7 Waste Plastic

In this research, used waste plastic fibers can be mainly sorted into two categories; artificially produced and industrial waste plastic fibers.

2.1.7.1 Artificially Produced Waste Plastic Fibers

Two types of regularly shaped waste plastic fibers were used; bottles of polyethylene terephthalate (PET), and sheets composed of polyethylene terephthalate and polyethylene (PET/PE).

Used waste PET bottles were with identical properties. They were made into rectangular strips of the dimensions 5×20 mm, 5×15 mm and 5×10 mm to obtain waste PET fibers. Cutting process of the fibers is shown in Figure 2.4.

Figure 2.4 Cutting process of the used PET waste plastic fibers (Personal archive, 2016)

Used waste PET/PE sheets were plastic fruit packaging rolls that are used in food packaging sector. They are composed of polyethylene terephthalate and polyethylene (PET/PE). They were cut manually in the sizes of 5×15 mm and 5×10 mm to be used as fiber in this work (Figure 2.5).

2.1.7.2 Industrial Waste Plastic Fibers

Waste Polypropylene (PP), waste polyethylene (PE) and waste polyamide (PA) plastics were also used in this work. They were supplied from Narsan Plastik San. Tic. Ltd. recycling factory in Izmir city. Fibers are shown in Figure 2.6. These waste plastics

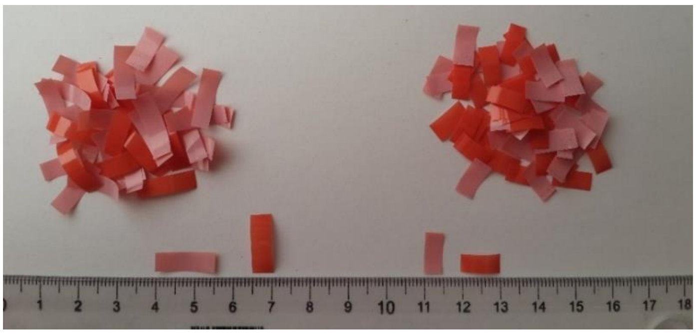

Figure 2.5 Representative samples of the used waste plastic PET/PE fibers (Personal archive, 2016)

were collected to be recycled and were passed through cutting and washing processes as shown in Figure 2.7. Then the collected wastes were sorted according to their types. The length of the PP fibers ranges between 0.5 cm and 3 cm and the width varies between 0.2 cm and 0.4 cm. PA fibers have their dimensions ranging between 0.5 cm and 1.5 cm for the length, and the width was between 0.7 cm and 0.3 cm. PE fibers' dimensions were approximately between 1 and 3 cm.

a) b) c)

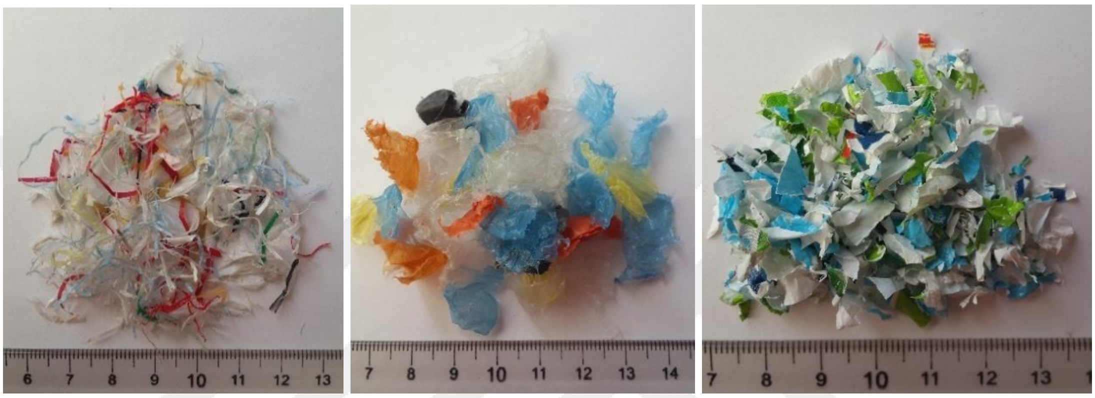

Figure 2.6 Representative samples of the used PP (a), PE (b) and PA (c) fibers (Personal archive, 2017)

Specific gravity tests were conducted to find the density of fibers using ASTM D 792-13, as shown in Figure 2.8. Densities of waste plastics used in this work are shown in Table 2.3.

Figure 2.7 Washing and cutting process (Personal archive, 2016)

Figure 2.8 Density measurement (Personal archive, 2016)

Table 2.3 Densities of waste plastic materials

	Polypropylene	Polyethylene	Polyamide	PET	PET/PE
Density (Kg/m³)	904	917	1132	1340	1025

2.2 Contact Angle Measurements

Contact angle is defined as the angle formed by a drop of adhesive in contact with the surface of the substrate. The value of this angle will indicate the degree of the adhesion of the adhesive on the substrate therefor the hydrophilicity. The apparatus used in this research is shown in Figure 2.9. It was used to determine the hydrophilicity of waste plastic surface which is correlated with the mechanical characteristics of plastic incorporated mortars.

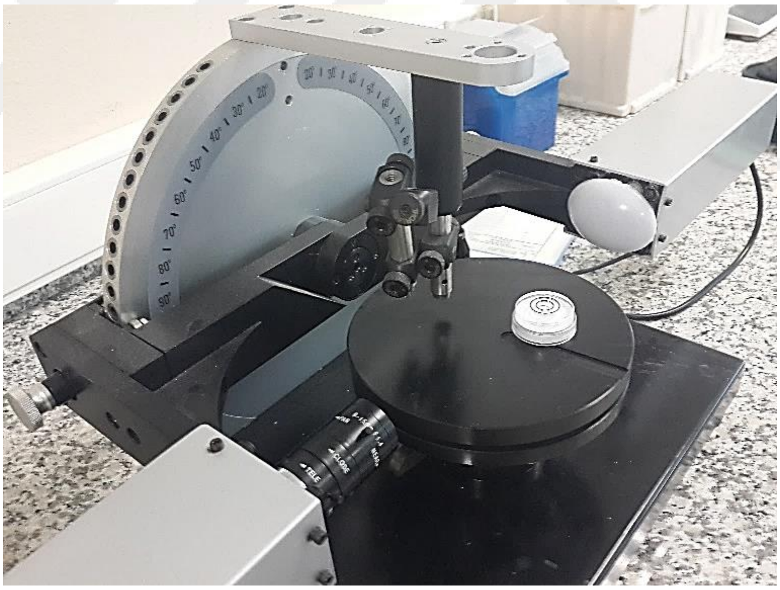

Figure 2.9 Contact angle apparatus (Personal archive, 2016)

2.3 Flow Test

Mortar Flow tests were carried out in order to maintain a design of repairing self-compacting mortar. Test was applied in accordance with the TS 13395-1. Used apparatus is shown in Figure 2.10 which is conforming to the specifications of the standard ASTM C230/C230M – 14.

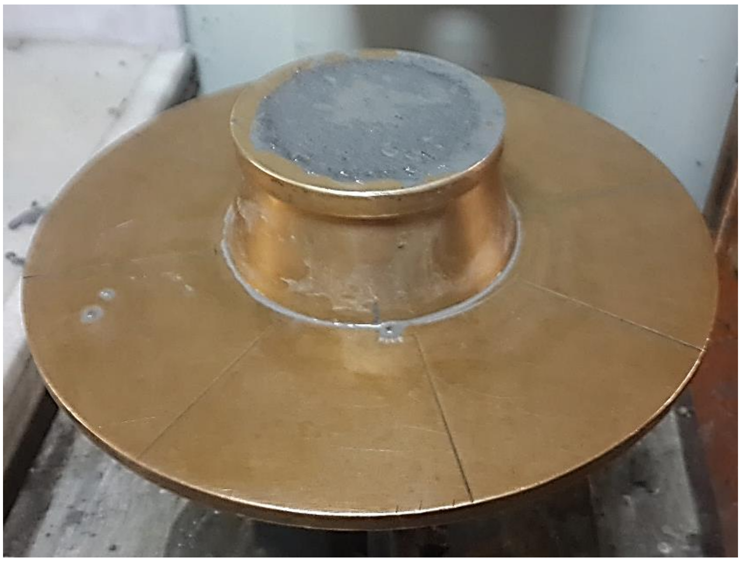

Figure 2.10 Mortar flow test apparatus (Personal archive, 2017)

2.4 Design of Mortar Mixtures

Two stages of mortar design were conducted in this study. The first stage was designed to study the mechanical properties of waste plastic fiber incorporated mortar specimens. Waste PET, PET/PE, PP, PE and PA plastic fibers were used in the design of the mixtures. Then, it was decided to increase the poor chemical bond between the concrete matrix and the hydrophobic surface of PP, PE and PA plastic fibers. So, fiber surface was treated by being immersed into a solution of 5% isopropanol + 95% distilled water for 5 minutes, then fibers were exposed to room temperature and humidity for 120 minutes before using. Contact angle measurements were conducted before and after treatment and the results are demonstrated in Table 2.4. The table

Table 2.4 Contact angle results of the irregular waste plastic fibers

Treatment	Contact Angle (degrees)
Polypropylene (PP)	86.2
Treated Polypropylene (TPP)	59.2
Polyethylene (PE)	90.1
Treated polyethylene (TPE)	83.8
Polyamide (PA)	79.1
Treated Polyamide (TPA)	82.7

shows enhancing in the hydrophilicity of PP and PE fibers after treatment but PA fibers did not show the desirable improvement. So, it was decided to carry out mortar mixture designs that include only treated PP (TPP) and treated PE (TPE).

Then, for the intension of producing waste plastic fiber reinforced self-compacting mortar, designs of self-compacting mortar and concrete were initiated and discussed below.

2.4.1 Mortar Design for Mechanical Tests

In order to determine the change in the mechanical properties of mortar by changing fiber volume % incorporated in, mortar mixtures were designed based on TS 802 "Design of concrete mixes". The following steps were carried out while designing the mixtures:

- The target compressive strength of the non-air entrained mortar was selected as 45 MPa.
- Water / binder ratio for non-air entrained 45 MPa mortar was 0.37.
- The value of mortar slump was taken as 8 - 10 cm, therefore water content was found as 220 kg / m^3.
- The largest grain size of aggregate was 5 mm and depending on climatic conditions, the suitable air content to be used in concrete mixtures for non-air entrained mortar was taken as 2.2%.
- Using the product data sheet of the company that produces the plasticizer, plasticizer / binder ratio was taken as 1%.
- With reference to the product data sheet of plasticizer producer, and taken into account the water retarding, 10% of water was cut.
- Using the instructions of silica fume producer, silica fume / total binder ratio was taken as 10%.
- Amount of materials used by kilograms in 1 cubic meter of the mixture are shown in Table 2.5.
- 56 mixtures were designed and named according to three changing parameters; type of waste plastic, dimensions of the fibers, and fibers' volume

percent incorporation in mortar matrix. Table 2.6 shows the used 55 fiber incorporated mixtures. One more traditional mortar M0 was also designed as a reference.

Table 2.5 Amount of materials used by kg/m^3 in fiberless conventional mortar mixture

Cement	**Aggregate**	**Silica Fume**	**Plasticizer**	**Water**
499	1339	55.5	5.6	220

Table 2.6 Mortar mixtures used for mechanical tests

Plastic type	**Dimensions (mm)**	**Volume percent incorporation**					
		0.2%	**0.5%**	**0.8%**	**1%**	**1.5%**	**2%**
PET	**5×10**	✓	✓	✓	✓	✓	✓
	5×15	✓	✓	✓	✓	✓	✓
	5×20	✓	✓	✓	✓	✓	✓
PET/PE	**5×10**	✓	✓	✓	✓	✓	✓
	5×15	✓	✓	✓	✓	✓	✓
PP	**-**	✓	✓	✓	✓	✓	
PE	**-**	✓	✓	✓	✓	✓	
PA	**-**	✓	✓	✓	✓	✓	
TPP	**-**	✓	✓	✓	✓	✓	
TPE	**-**	✓	✓	✓	✓	✓	

2.4.2 Self-Compacting Mortar Design

Self-compacting mortar with and without the incorporation of waste plastic fibers were designed for concrete repair purposes. So, another set of mixtures' designing was also performed in this research starting from TS 802. Names of the mixtures are shown in Table 2.7. The following steps were carried out while designing the mixtures:

- The target compressive strength of the non-air entrained mortar was selected as 45 MPa.
- Water / binder ratio was designed as 0.42.
- Water content was taken as 300 kg / m^3.
- The largest grain size of aggregate was 3 mm and depending on climatic conditions, the suitable air content to be used in concrete mixtures for non-air entrained mortar was taken as 4.4%.
- Using the product data sheet of plasticizer producer, plasticizer / binder ratio was taken as 1%, 1.25% and 1.5%.
- Using product data sheet of plasticizer producer, taken into account the water retarding, 25% of water was cut and designed to be replaced by plasticizer.
- Amount of materials by kilograms in 1 cubic meter of the mixture containing 1% plasticizer are shown in Table 2.7.
- According to the mechanical properties results shown by PP fibers, it was chosen as plastic fiber to reinforce self-compacting mortar.
- 10 mixtures were designed and named according to two changing parameters; plasticizer / binder ratio and fibers' volume percent incorporation in mortar matrix. Table 2.8 shows naming manner.

Table 2.7 Amount of materials used in the mixtures of self-compacting mortar tests (kg/m^3)

Mixture Name	Cement	Fine Aggregate	Water	Plasticizer
1Mix0%	536	1478	224	5.4

2.4.3 Design of Concrete Mixtures

In order to measure the mechanical properties of repairing self-compacting mortar, concrete mixture was designed to be repaired. It was designed in accordance with the TS 802 instructions. The following steps were carried out while designing the concrete mixture:

Table 2.8 Mixtures used to design self-compacting mortar

		Plasticizer ratio by weight of binder		
		1%	**1.25%**	**1.5%**
PP fibers incorporation in the mixtures by volume%	**0%**	1Mix0%	1.25Mix0%	1.5Mix0%
	0.2%	1Mix0.2%	1.25Mix0.2%	1.5Mix0.2%
	0.3%		1.25Mix0.3%	
	0.4%		1.25Mix0.3%	
	0.5%	1Mix0.5%		1.5Mix0.5%

- The target compressive strength of the non-air entrained concrete was 20 MPa.
- Water / binder ratio for non-air entrained 20 MPa concrete was found as 0.69.
- The value of concrete slump was taken as 8 - 10 cm, therefore water content was found as 236 kg / m^3.
- The largest grain size of aggregate was 15 mm and depending on climatic conditions, the suitable air content to be used in concrete mixtures for non-air entrained concrete was taken as 2.3%.
- Amount of materials by kg in 1 m^3 of the mixture are shown in Table 2.9.

Table 2.9 Amount of materials used in the concrete mixture (*kg/m^3*)

Mixture Name	Cement	Coarse Aggregate	Fine Aggregate	Water
C20	342	675	115	236

2.5 Preparation of Mixtures

Casting molds were prepared before the preparation of materials. All molds used were from steel to make certain not to absorb water or react with concrete. Molds hold their shape under laboratory conditions. Their inside surfaces were smooth and free from indentations. Concrete prismatic molds for bending tests were of the dimensions

30.5×7.5×7.5 cm. Mortar prismatic molds’ dimensions were 16×4×4 cm. Also, 7.5 × 7.5 × 7.5 molds were used for cubes compression and tensile splitting tests. Molds are shown in Figure 2.11 and Figure 2.12. They were coated with a thin layer of mineral oil before being cast into.

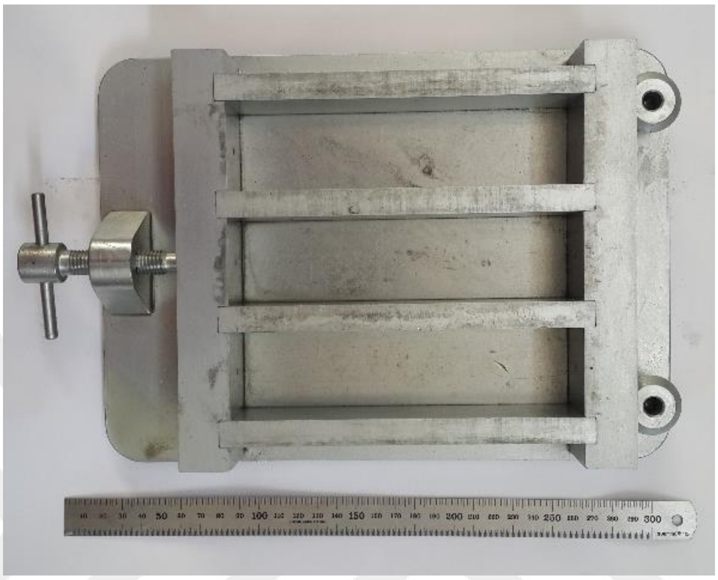

Figure 2.11 Molds of the dimensions 16×4×4 cm (Personal archive, 2017)

a) b)

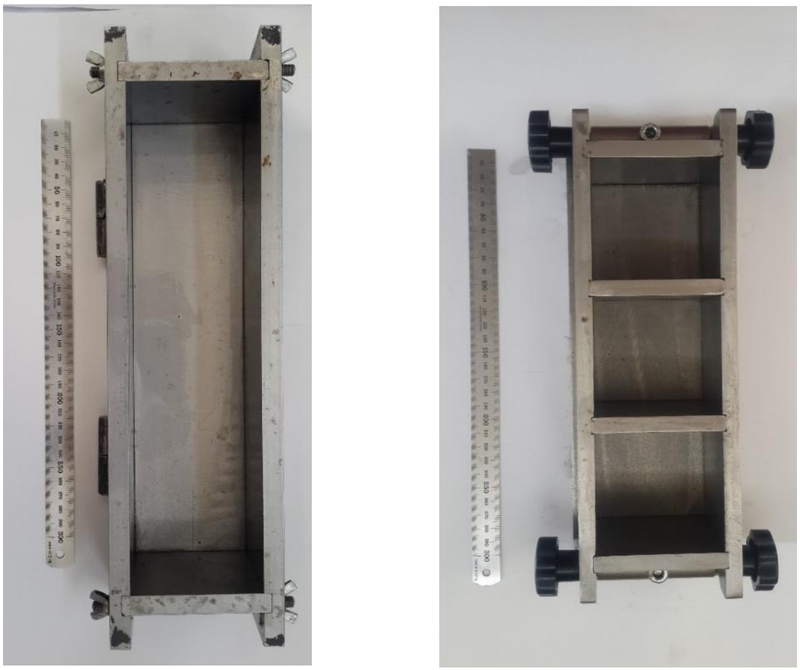

Figure 2.12 **a)** Beam mold of 30.5×7.5×7.5 cm dims. **b)** Cube molds of 7.5×7.5×7.5 cm dims. (Personal archive, 2017)

Materials composing mixtures were prepared according to the prescription design. Sensitive digital scale of 6 kg capacity and 0.1 gr sensitivity was used to maintain accurate material quantities. Specimens were cast in two layers. Every layer was tamped using a round, straight steel rod of the diameter 1 cm and of the length 20 cm.

2.5.1 Preparation of Mortar Mixtures

Casting mortar and self-compacting mortar starts by mixing fine aggregate with cement and silica fume in a mixer's stainless-steel bowl. After homogeneity was provided in the dry mixture, plasticizer and water were mixed together in a separate beaker. After ensuring that they were thoroughly mixed, the plasticizer-water mixture was added to the dry mixture at 1/3 dosages of total liquid each time. Then, mortar was mixed in the 5-liter capacity mixer (Figure 2.13) for 5 minutes until its consistency was attained.

Figure 2.13 5-liter capacity mixer (Personal archive, 2017)

The desired plastic fiber was gradually added and stirred into the mixture in a way that does not create clumping. The mixture was then cast manually to molds, each mold was filled in two layers and every layer was rod 20 times. The mortar then was vibrated in vibration table for 30-60 seconds, depending on the ratio of fibers in the mixture. Then the exposed surface of the mortar was leveled using an appropriate spatula. Sample of mortar prisms is shown in Figure 2.14.

Figure 2.14 Sample of mortar prisms (Personal archive, 2017)

2.5.2 Preparation of Concrete Mixtures

Casting concrete started by mixing coarse and fine aggregate with cement in a 125-liter capacity portable tilting mixer (Figure 2.15) until it turns into a homogeneous mixture. Then, water was added to the dry mixture at 1/3 of total water each time. After that, concrete was mixed for 5 minutes.

Figure 2.15 125-liter capacity portable tilting mixer (Personal archive, 2017)

The mixture was cast manually into greased molds using trowels, each mold was filled in two layers and every layer was rod 25 times. The molds were tapped lightly with a mallet 20 times to close any holes left by rodding and to release any large air bubbles that may have been trapped. The gaps that might appear on surface were filled. Then the exposed surface of the mold was leveled using a suitable spatula.

2.5.3 Preparation of Repairing Self-Compacting Mortar Mixtures

Self-compacting mortar mixtures had the same procedure of mixing, casting, and consolidating of traditional mortar except that they do not get vibrated or rod.

Concrete and mortar specimens were removed from the molds after 24 hours from casting. The test surfaces of the specimens were corrected with spatula so that they do not get subjected to any oblique loading during the mechanical tests. Sample names were written on the surfaces of the specimens. Then they get put into the water-filled curing tank shown in Figure 2.16. The water temperature of the curing tank was fixed at 20 °C. After 28 days curing period, the samples were removed from the tank and get prepared for their objective.

Figure 2.16 Curing tank (Personal archive, 2017)

2.6 Mortar-Repaired Concrete Tests

Experiments were conducted to produce concrete repairing waste plastic fiber reinforced self-compacting mortar. First, it was planned to design conventional concrete specimens. Then, flow test experiments of self-compacting mortar with and without waste plastic fibers designs shown in Table 2.8 were conducted using the instructions of ASTM C1437 − 15. Results of flow tests of self-compacting mortar are displayed in Table 2.10. Goal was set to achieve a flow value of at least 250 mm that contains the largest proportion of PP fibers without segregation. Results in Table 2.10 express that the most optimistic incorporation ratio by volume was 0.3% waste PP plastic fiber. So, it was decided to initiate a new set of repairing concrete experiments. These experiments were divided chronologically into three groups (A, B and C):

Table 2.10 Determination of flow value of waste PP fiber reinforced self-compacting mortar

Mixture name	Flow value (mm)	Note
1Mix0%	282	
1Mix0.2%	235	
1Mix0.5%	125	
1.25Mix0%	297	
1.25Mix0.2%	275	
1.25Mix0.3%	255	
1.25Mix0.4%	232	Segregated
1.5Mix0%	285	Segregated
1.5Mix0.2%	260	Segregated
1.5Mix0.5%	180	Segregated

2.6.1 Group A Tests

This group contained 3 concrete flexural beam specimens; the 1st specimen was cast in the mold's dimensions of 30.5×7.5×7.5 cm. The other two specimens were cast in the dimensions of 30.5×7.5×5.5 cm by sticking polystyrene foam boards of the width

2 cm inside the side wall of the molds as shown in Figure 2.17. After casting concrete, the specimens were kept in the molds for 24 hours at the room temperature. Then, the specimens were demolded and kept for 27 days in the curing tank at a temperature of 20 °C. At the 28^{th} day from casting, all specimens were removed from water. In order to achieve a rough concrete surface that have a good adherence with repair mortar, the 2^{nd} and 3^{rd} specimens were drilled with diameter of 8 mm, distance of 20±2 mm between each bore and bores' depth was set to be 5±1 mm as shown in Figure 2.18. Then, the 2 specimens' surfaces were cleaned by air compressor, then the will-be-repaired surfaces were submerged in water for 5 seconds, and after then, placed into their old molds and the rest gaps of the molds were cast by self-compacting mortar for the 2^{nd} specimen and with fiber reinforced self-compacting mortar for the 3^{rd} specimen (Figure 2.19). Then they were kept as in lab conditions to set and cure for another 28 days with the 1^{st} specimen. Afterwards, all 3 specimens were removed from water and undergone bending test at the 56^{th} day.

This group also contained 6 concrete cubes of the dimensions 7.5×7.5×7.5 cm. After being cast, they were left in the molds for 24 hours at the room temperature. Next, they were demolded and left for 27 days to cure in the water tank at a temperature of 20 °C. At the 28^{th} day from casting, all specimens were removed from water. The 1^{st} and 2^{nd} cubes were tested with compression test to find the 28^{th} day compressive strength of the concrete. The rest 4 cubes were tested with splitting tensile tests. Later, 6 of the half-cubes resulted from this test were repaired starting by their split surfaces being cleaned using air compressor. Then, the split surfaces being submerged in water for 5 seconds. After that, half-cubes get placed into their molds (Figure 2.20, Figure 2.19). The rest gap was filled with self-compacting mortar for 3 cube specimens and fiber reinforced self-compacting mortar for the other 3 cube specimens. They get the same previously mentioned setting and curing process for 28 days. At the 56^{th} day concrete casting (28^{th} day of repair mortar casting), tensile splitting tests were carried out.

One self-compacting mortar and one fiber reinforced self-compacting mortar specimens were also cast in the dimensions of 16×4×4 cm. Then, bending and compression tests were conducted at the 28^{th} day.

2.6.2 Group B Tests

This group contains 6 concrete flexural beam specimens were cast in the dimensions of 30.5×7.5×5.5 cm by sticking a polystyrene foam board of the width 2 cm in the molds as shown in Figure 2.17. The specimens were kept in the molds for 24 hours at the room temperature. After demolding, the specimens were kept for 27 days in the curing tank at a temperature of 20 °C. At the 28^{th} day from casting, all specimens were removed from water, 4 specimens were drilled and cleaned, in the same manner of group A's specimen's treatment, to maintain good adherence between surfaces of concrete and repair mortar.

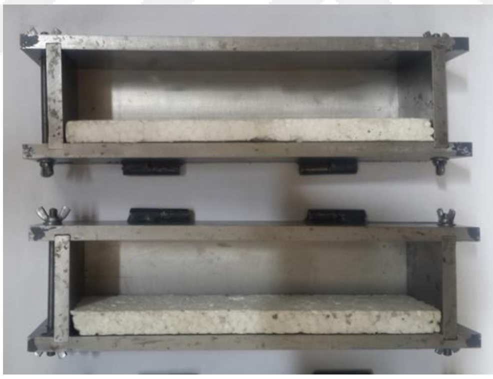

Figure 2.17 Steel molds of the dimensions 30.5×7.5×5.5 cm (Personal archive, 2017)

Figure 2.18 1^{st} group's 3 drilled beam specimens at the 28^{th} day (Personal archive, 2017)

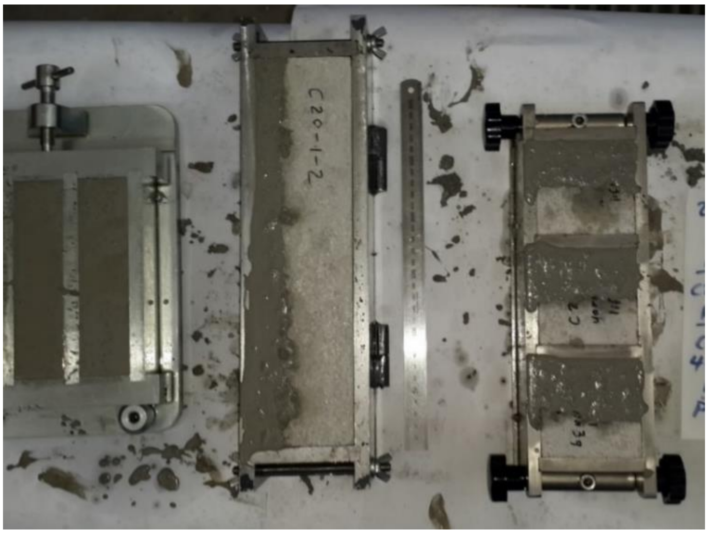

Figure 2.19 Repaired specimens at the 28th day (Personal archive, 2017)

Figure 2.20 Tensile split resultant cube specimens before repairing (Personal archive, 2017)

Then, the drilled 4 specimens were placed into their old molds (Figure 2.21) and the rest gap of the molds were cast by self-compacting mortar for 2 beam specimens (Figure 2.19) and by waste plastic fiber reinforced self-compacting mortar for the other 2 specimens. Then the 4 repaired specimens were kept as previously mentioned in laboratory conditions to set (Figure 2.22) and cure for another 28 days in water with the other not repaired 2 specimens. Afterwards, all 6 flexural beam specimens were removed from water and mechanical tests were conducted at the 56th day of concrete casting (28th day of repair mortar casting).

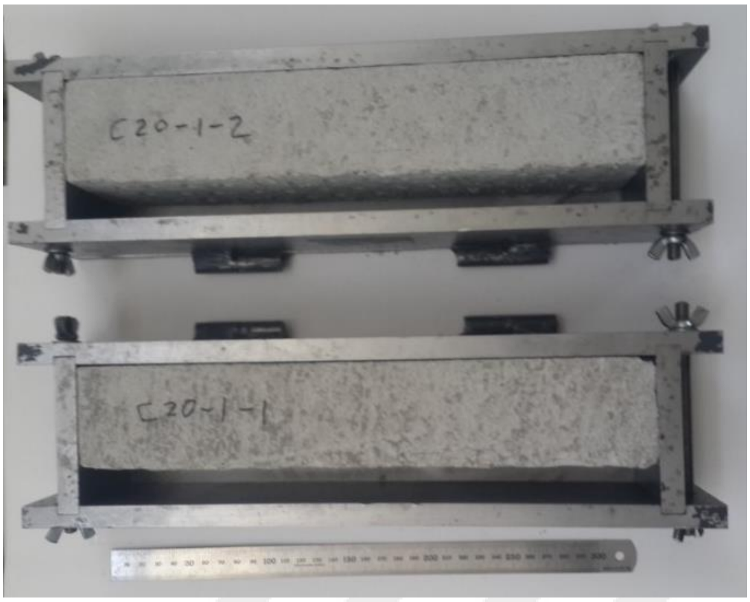

Figure 2.21 Beam specimens at the 28th day before being repaired (Personal archive, 2017)

This group also contains 9 concrete cubes of the dimensions 7.5×7.5×7.5 cm. after being cast, they were left in their molds for 24 hours at the room temperature. Next, they were demolded and left for 27 days in the curing tank at a temperature of 20 °C. At the 28th day from casting, all 9 cube specimens were removed from water. Splitting tensile tests were conducted to 6 of them. Then, 6 half-cubes resulted from this test were chosen and 3 of them were repaired by self-compacting mortar and 3 by fiber reinforced self-compacting mortar. Repairing process was achieved by the half-cubes being placed into their molds shown in Figure 2.20 after the resultant specimens being cleaned by air compressor and then the rest gap was filled by the 2 types of used self-compacting mortar. Later on, they get the same previously mentioned setting (Figure 2.23) and curing process for another 28 days. At the 56th day of concrete casting (28th day of repairing by mortar), tensile splitting tests were carried out for the all 9 cube concrete specimens.

One self-compacting mortar and one fiber reinforced self-compacting mortar specimens were also cast in the dimensions of 16×4×4 cm. Then, bending and compression tests were conducted at the 28th day.

Figure 2.22 Beam specimens at the 29th day after repaired and set (Personal archive, 2017)

Figure 2.23 Cube specimens at the 29th day after repaired and set (Personal archive, 2017)

2.6.3 Group C Tests

This group contained 9 concrete flexural beam specimens were cast in the dimensions of 30.5 cm × 7.5 cm × 5.5 cm by sticking a polystyrene foam board of the width 2 cm in the molds as shown in Figure 2.17. In order to maintain a good adherence between repairing mortar and concrete, polystyrene foam boards in this group were pierced at regular distances of 1 cm, diameter of 0.3 mm and approximate depth of 5 mm at the surface that meets the concrete surface in the mold. So, the resulted specimens were surface-roughened by protrusions that have same approximate dimensions of the bores on polystyrene foam board. 4 of the 9 polystyrene foam boards also had 13 nails at a distance of 3 cm from each other placed in a way that make the head part of the nail will be out of the concrete specimens by 2 cm after cast (Figure 2.24). Specimens were cast and kept in the molds for 24 hours at room temperature. After demolding, the specimens were left for 27 days in the curing tank at a temperature of 20 °C. At the 28th day from casting, all specimens were removed from water. Then, specimens were placed into their molds and the rest gap of the molds was filled by self-compacting mortar for 2 nailed and 2 surface-roughened beam specimens. The other 2 nailed and 2 surface-roughened beams specimens were repaired by waste plastic fiber reinforced self-compacting mortar. Then all 8 specimens were kept in lab conditions to set and cure for another 28 days with the other not repaired 1 specimens. Afterwards, all 9 flexural beam specimens were removed from water and the mechanical tests were conducted at the 56th day of concrete casting (28th day of repairing by mortar).

This group also contains 6 concrete cubes of the dimensions 7.5 cm × 7.5 cm × 7.5 cm. After being cast, they were left in the molds for 24 hours at room temperature. Next, they were demolded and left for 27 days in the curing tank at a temperature of 20 °C. At the 28th day from casting, all specimens were removed from water and 4 of them undergo splitting tensile tests. Then, 3 of the 6 half-cubes resulted from this test were repaired by self-compacting mortar by getting placed into their molds and the rest gap was filled with self-compacting mortar. and the other 3 half-cubes were repaired by waste plastic fiber reinforced self-compacting mortar. Next, the 6 cubes got the same previously mentioned setting and curing processes for 28 days by being kept in water beside the other non-repaired cubes. At the 56th day of casting concrete (28th day of repairing by mortar), tensile splitting tests were carried out for all 9 cube concrete specimens.

One self-compacting mortar and one fiber reinforced self-compacting mortar specimens were also cast in the dimensions of 16×4×4 cm. Then, bending and compression tests were conducted at the 28th day. Tables 2.11 and 2.12 summarizes three groups resulted tests.

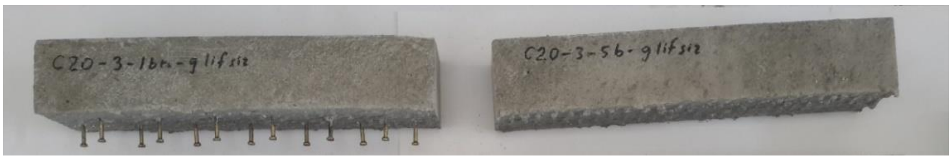

Figure 2.24 Nailed and surface-roughened specimens after 24 hours from casting (Personal archive, 2017)

Table 2.11 Number of tested concrete beam specimens for concrete repairing tests

Type of specimen	Repair mortar	Group A	Group B	Group C	Total
Ordinary of dims. 30.5×7.5×7.5cm	-	1			1
Ordinary of dims. 30.5×7.5×5.5cm	-		2	1	3
Drilled of dims. 30.5×7.5×5.5cm	Fiber reinforced	1	2		3
	Fiberless	1	2		3
Nailed of dims. 30.5×7.5×5.5cm	Fiber reinforced			2	2
	Fiberless			2	2
Roughened of dims. 30.5×7.5×5.5cm	Fiber reinforced			2	2
	Fiberless			2	2

Table 2.12 Concrete cube specimens for repairing tests

Test date and type	Repair mortar	Group A	Group B	Group C	Total
28^{th} day compression	-	2			2
28^{th} day tensile split	-	4	6	4	14
56^{th} day tensile split	-		3	2	6
	Fiber reinforced	3	3	3	9
	Fiberless	3	3	3	9

2.7 Mechanical Tests

Shimadzu Autograph AGS-300kNX mechanical testing machine shown in Figure 2.25 was used. the specifications of the apparatus are shown in Table 2.13. The testing software used was TRAPEZIUM X.

Figure 2.25 Shimadzu testing machine (Personal archive, 2017)

Table 2.13 Shimadzu Autograph AGS-300kNX Apparatus specifications

Capacity		300 kN
Loading Method		Direct, high-precision, constant-rate strain control using non-backlash precision ball-screw drive
Sampling Speed		1000Hz max.
Speed Accuracy		±0.1%
Force Measurement Accuracy	**High-Precision Type (1/500, ±0.5%)**	Within ±0.5% indicated test force (at 1/250 to 1/1 load cell rating), Conforms to EN 10002-2 Grade 0.5, ISO 7500-1 Class 0.5, BS 1610 Class 0.5, and ASTM E4, JIS B7721 Class 0.5.
	Standard-Precision Type (1/500, ±1%)	Within ±1% indicated test force (at 1/500 to 1/1 load cell rating), Conforms to EN 10002-2 Grade 1, ISO 7500-1 Class 1, BS 1610 Class 1, and ASTM E4, JIS B7721 Class 1.
Crosshead	**Speed Range**	0.001 to 500 mm/min (stepless)
	Max. Return Speed	550mm/min

2.7.1 Bending Tests

For mortar specimens, the bending test speed was fixed at 0.2 mm/min. Test was stopped when specimen deflection reaches 2 mm. Span length was 140 mm. 20 N was applied to all specimens at 0 stroke before carrying on the test. Figure 2.26 shows a mortar sample failed by bending test.

For concrete specimens, the bending test speed was fixed at 0.1 mm/min. Test was stopped when specimen deflection reaches 1.8 mm. Span length was 263 mm. Bending tests were performed according to the instructions of ASTM C1609M - 12.

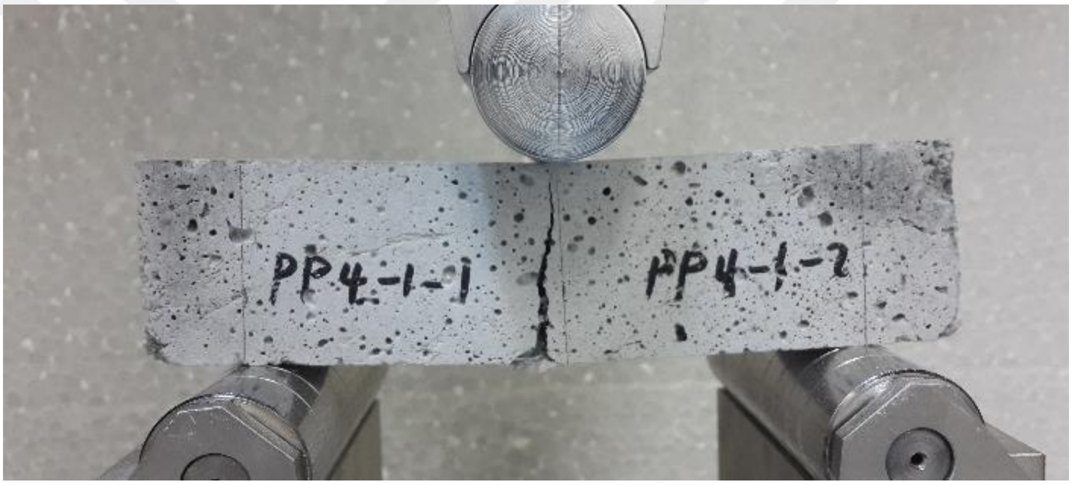

Figure 2.26 Mortar sample failed by bending test (Personal archive, 2016)

Results of bending tests were analyzed in terms of flexural strength and flexural toughness. Flexural strength was calculated from the equation 2.1.

$$f_b = 1.5\frac{P.L}{b.d^2} \quad (2.1)$$

Where; (f_b) is the flexural strength in MPa, (P) is the load in N, (L) is the span length in mm, (b) is the average width of the specimen at the fracture in mm, and (d) is the average depth of the specimen at the fracture in mm.

Flexural toughness is the area under the load-displacement curve (Figure 2.27). Displacement in mortar analysis was considered until 2 mm, in concrete analysis it was considered until 1.8 mm.

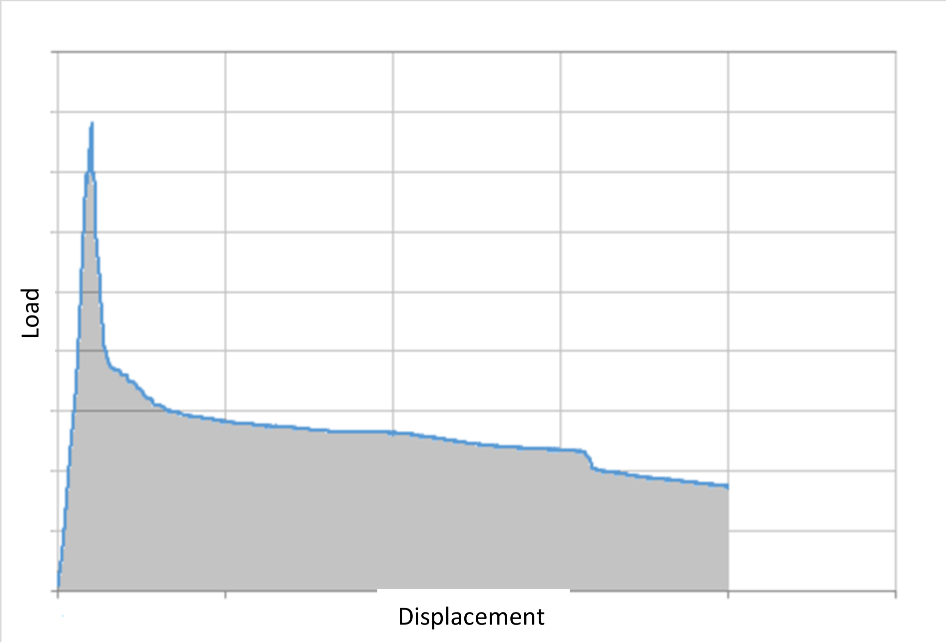

Figure 2.27 Area under load-displacement curve (flexural toughness)

2.7.2 Compression Tests

For mortar, compressive strength tests were performed using portions of the prisms broken in flexure. Velocity was set as 0.5 mm/min, and tests were set to be stopped when the force fall to 50% of the obtained maximum force. Figure 2.28 shows a mortar sample failed by compression test. Compression tests of concrete where applied on cubes, concrete tests had the same testing parameters used for mortar specimens. Compression tests were performed according to the instructions of ASTM C349 - 14.

Results of compression tests were analyzed in terms of compressive strength and compressive toughness. Compressive strength was calculated from the equation 2.2.

Figure 2.28 Mortar sample failed by compression test (Personal archive, 2016)

$$\sigma = \frac{P}{b^2} \tag{2.2}$$

Where; (σ) is the compressive strength in MPa, (P) is the maximum load in N and (b) is the dimensions of the cube specimen in mm.

Compressive toughness is the area under the load-displacement curve (Figure 2.29). It was considered until maximum load drop to 50%.

2.7.3 Splitting Tensile Tests

The tests speed was fixed at 2.5 mm/min. Test was stopped when specimen fails. Figure 2.30 shows a concrete sample failed by tensile splitting test.

Results of split tensile tests were analyzed in terms of split tensile strength and it was calculated from the equation 2.3.

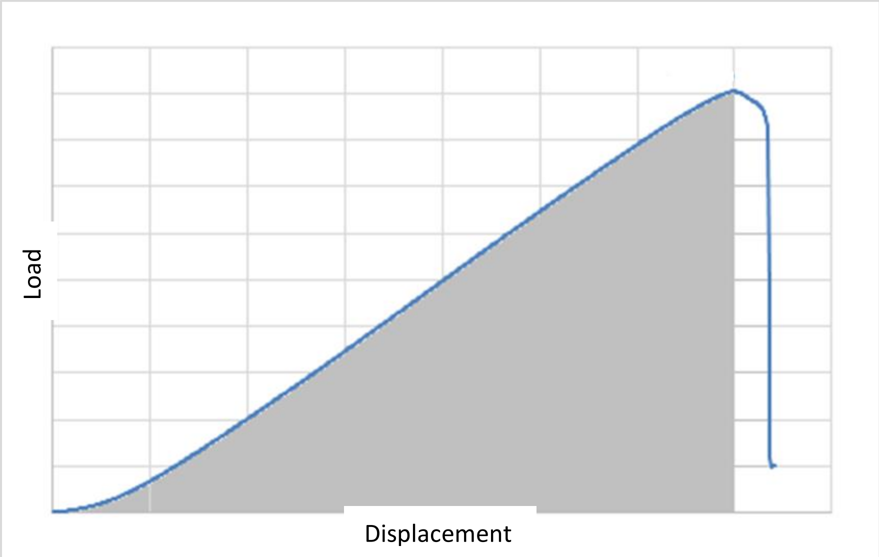

Figure 2.29 Area under load-displacement curve until max. load (flexural toughness until max. load)

$$f_t = \frac{P}{b^2} \quad (2.3)$$

Where; (f_t) is the split tensile strength in MPa, (P) is the split load in N and (b) is the dimensions of the cube specimen in mm.

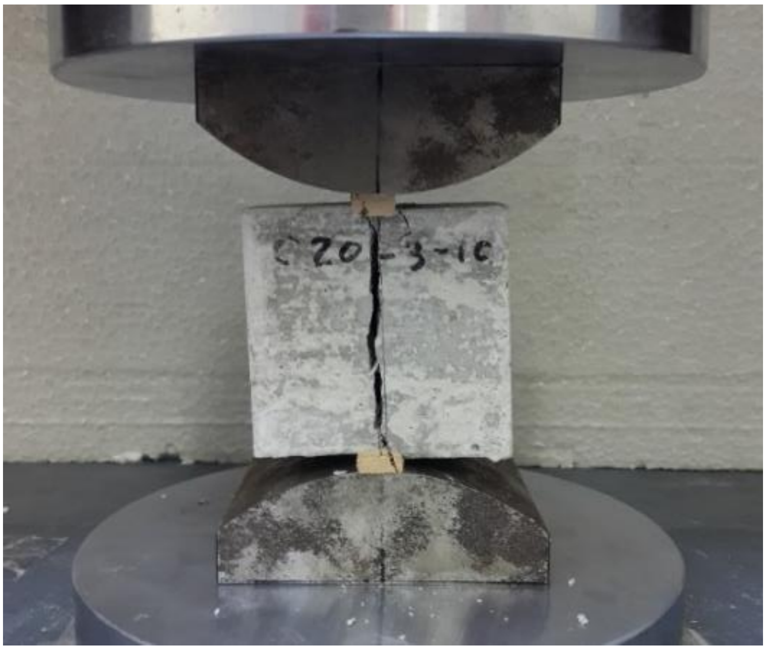

Figure 2.30 Concrete sample failed by tensile splitting test (Personal archive, 2017)

CHAPTER THREE
RESULTS AND DISCUSSION

This chapter discusses the experimental results of the influence of waste plastic fibers on the mechanical properties of reinforced structural mortar.

As mentioned earlier in chapter two, two series of experiments were accomplished. In the first series, mortar mixtures were designed by changing four variables:

1- **Waste plastic type:**
(PET, PET/PE, PP, PE and PA)

2- **Plastic fiber's aspect ratio for artificially produced waste plastic fibers:**
(5×10, 5×15 and 5×20) for PET, and (5×10 and 5×15) for PET/PE.

3- **Plastic surface treatment for industrial waste plastic fibers:**
Surface treated PP and PE.

4- **Fiber volume ratio:**
- 0%, 0.2%, 0.5%, 0.8%, 1% and 1.5% for artificially produced waste plastic fibers.
- 0%, 0.2%, 0.5%, 0.8%, 1%. 1.5% and 2% for industrial waste plastic fibers.

Then, bending and compression tests were applied to the specimens and the results were analyzed and discussed from the aspects of flexural strength, flexural toughness, compressive strength and compressive toughness.

In the second series, experiments were conducted to study the ability to achieve designs of SCM and waste PP fiber reinforced SCM by changing the following variables:

1- **Plasticizer ratio by weight of binder (1%, 1.25% and 1.5%)**
2- **Waste PP fiber incorporation (0%, 0.2%, 0.3% and 0.4%)**

Then, bending and compression tests were applied to the specimens, analyzed and discussed from the aspects of flexural strength, flexural toughness, compressive strength and compressive toughness.

After that, one conventional concrete mixture was designed to be repaired by SCM and by a chosen waste PP fiber reinforced SCM mixture as detailed previously in chapter two and shown in Tables 2.11 and 2.12.

Then, bending, splitting tensile and compression tests were applied to the repaired concrete specimens. Results were analyzed and discussed from the aspects of flexural strength, flexural toughness, splitting tensile strength, compressive strength and compressive toughness of repaired concrete.

3.1 Waste PET Bottle Reinforced Mortar Test Results

3.1.1 Bending Test Results

Figure 3.1 presents the flexural strength vs. fiber volume ratio behavior of all waste PET fiber reinforced flexural prisms. Graphs shows that the use of a 2% volume ratio of the dimensions 5×15 mm and 5×20 PET fiber was found to reveal a flexural strength of about 18.6% and 11.1%, respectively, higher than that of the control mortar (M0) flexural prisms. The highest volume flexural strength value for 5×10 mm fiber incorporated mortar was at 1.5% by 12.8% increment from control mortar.

Figure 3.2 presents the flexural toughness vs. fiber volume ratio behavior of all waste PET fiber reinforced flexural prisms. Graphs shows that, in general, there is an increment in flexural toughness with fiber volume ratio and with the aspect ratio of fibers. The use of a 2% volume ratio of the dimensions 5×20 mm and 5×15 PET fiber was found to reveal a flexural toughness of about 2401% and 1865%, respectively, higher than that of the control mortar. The highest volume flexural toughness value for 5×10 mm fiber incorporated mortar was at 1.5% by 827% increment from control mortar.

This enhancement in the flexural strength and toughness by increasing PET fiber volume ratio can be attributed to the bridging effect caused by the fibers and to the better mechanical bond strength between the fibers and the cement matrix.

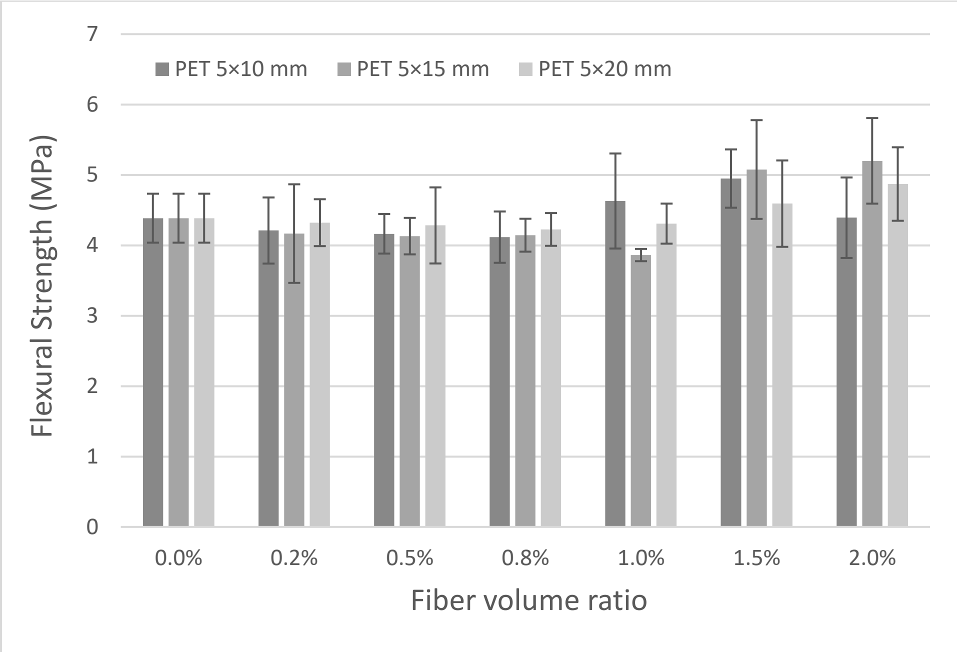

Figure 3.1 Flexural strength vs. PET fiber volume ratio for 3 different aspect ratios

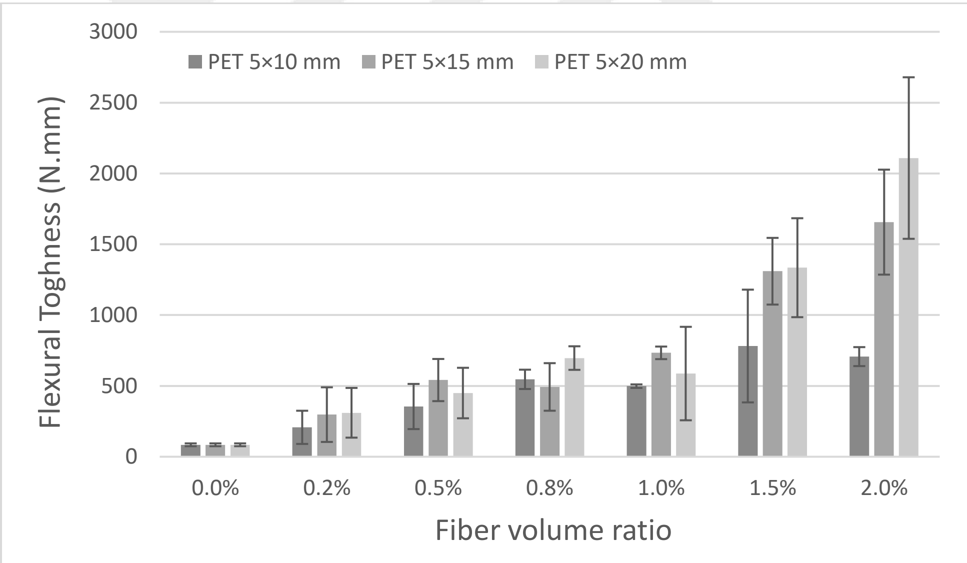

Figure 3.2 Flexural toughness vs. PET fiber volume ratio for 3 different aspect ratios

3.1.2 Compression Test Results

Figure 3.3 presents the compressive strength vs. fiber volume ratio behavior of all waste PET fiber reinforced specimens. Graph shows that the compressive strength decreased with fiber volume ratio incorporation into mortar for all used aspect ratios.

The same patterns of compressive strength vs. fiber volume ratio are noticed in the results of compressive toughness vs. fiber volume ratio graphs shown in Figure 3.4.

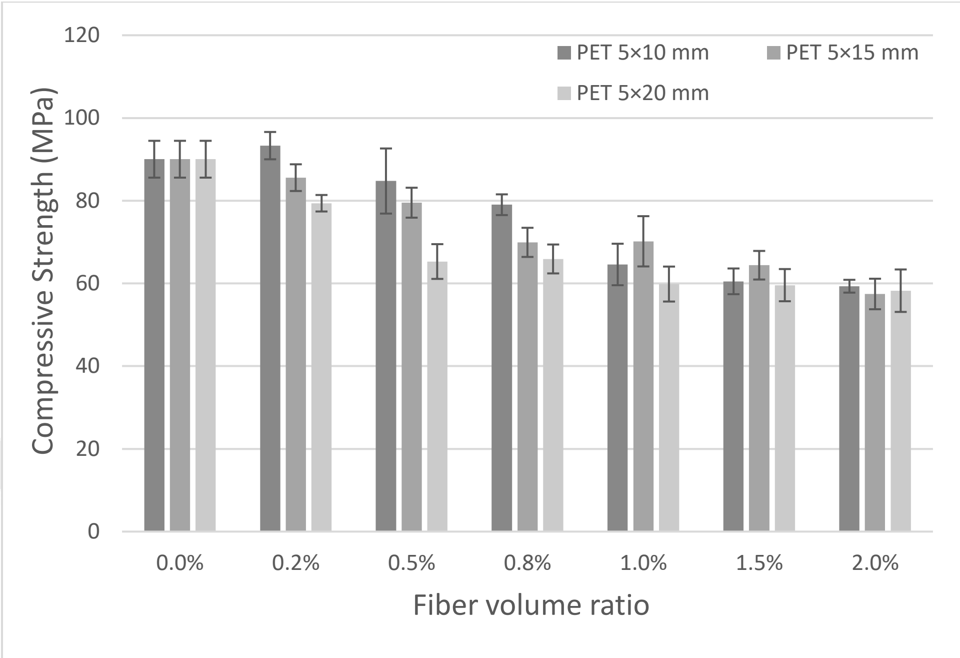

Figure 3.3 Compressive strength vs. PET fiber volume ratio for 3 different aspect ratios

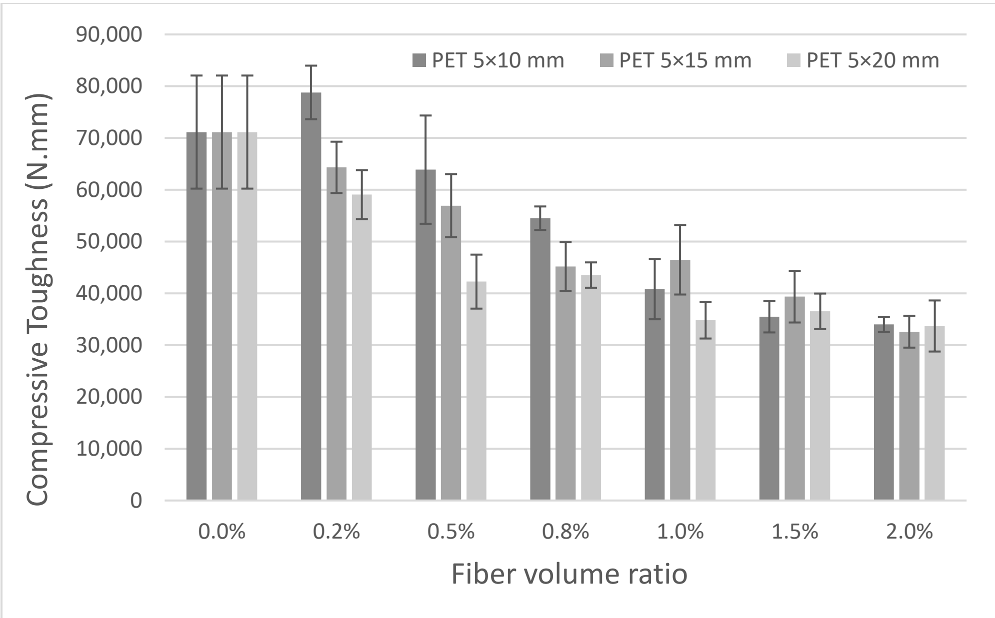

Figure 3.4 Comp. toughness vs. PET fiber volume ratio for 3 different aspect ratios

This decline in the compressive strength and compressive toughness by increasing PET fiber volume ratio can be attributed to the weak behavior of fibers as emptiness when resisting compression. It can be noticed also from ratios less than 1% that the compressive strength and toughness values decrease with the increment of the length of the incorporated fibers.

3.2 PET/PE Waste Reinforced Mortar Test Results

3.2.1 Bending Test Results

Figure 3.5 presents the flexural strength vs. fiber volume ratio behavior of all waste PET/PE fiber reinforced mortars. Graph shows that the flexural strength was not considerably affected by fiber volume ratio for all used aspect ratios.

Figure 3.6 presents the flexural toughness vs. fiber volume ratio behavior of all waste PET/PE fiber reinforced flexural prisms. Graph shows that there is an increment in flexural toughness with fiber volume ratio and with the aspect ratio of fibers. The use of a 2% volume ratio of the dimensions 5×15 mm and 5×10 PET/PE fiber led to an increase in the flexural toughness of about 616% and 561%, respectively, in comparison to that of the control mortar.

This enhancement in the flexural toughness by increasing PET/PE fiber volume ratio can be explained by the crack bridging effect of fibers.

3.2.2 Compression Test Results

Figure 3.7 presents the compressive strength vs. fiber volume ratio behavior of all waste PET/PE fiber reinforced specimens. Graph shows that the compressive strength decreased with fiber volume ratio incorporation into mortar for all used aspect ratios.

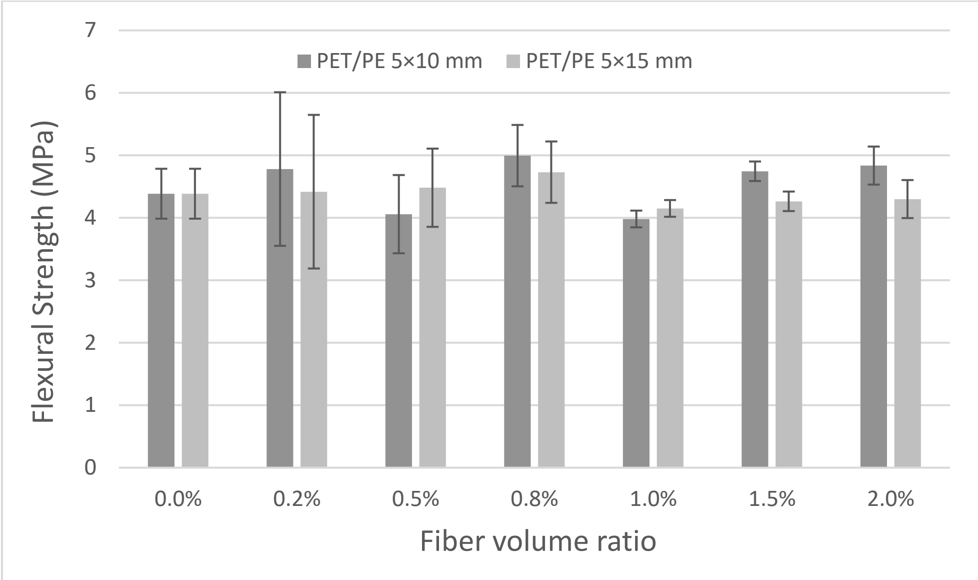

Figure 3.5 Flexural strength vs. PET/PE fiber volume ratio for 2 different aspect ratios

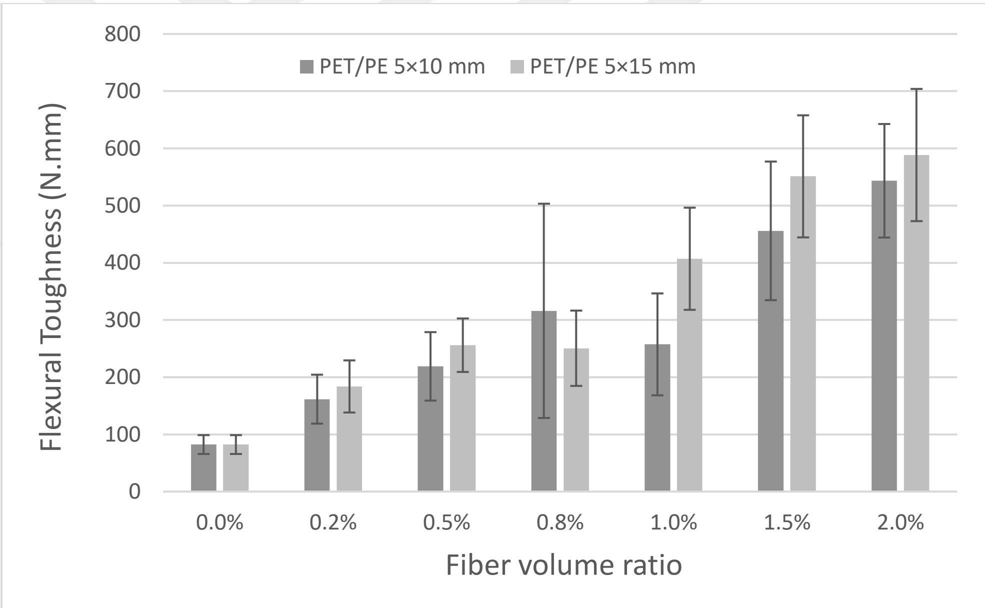

Figure 3.6 Flexural toughness vs. PET/PE fiber volume ratio for 2 different aspect ratios

The same patterns of compressive strength vs. fiber volume ratio are noticed in the results of compressive toughness vs. fiber volume ratio graph shown in Figure 3.8.

This decline in the compressive strength and compressive toughness by increasing PET/PE fiber volume ratio can be attributed to the behavior of fibers as weakness zones. It can also be noticed that the compressive strength and toughness values decrease with the increment of aspect ratio of incorporated fibers.

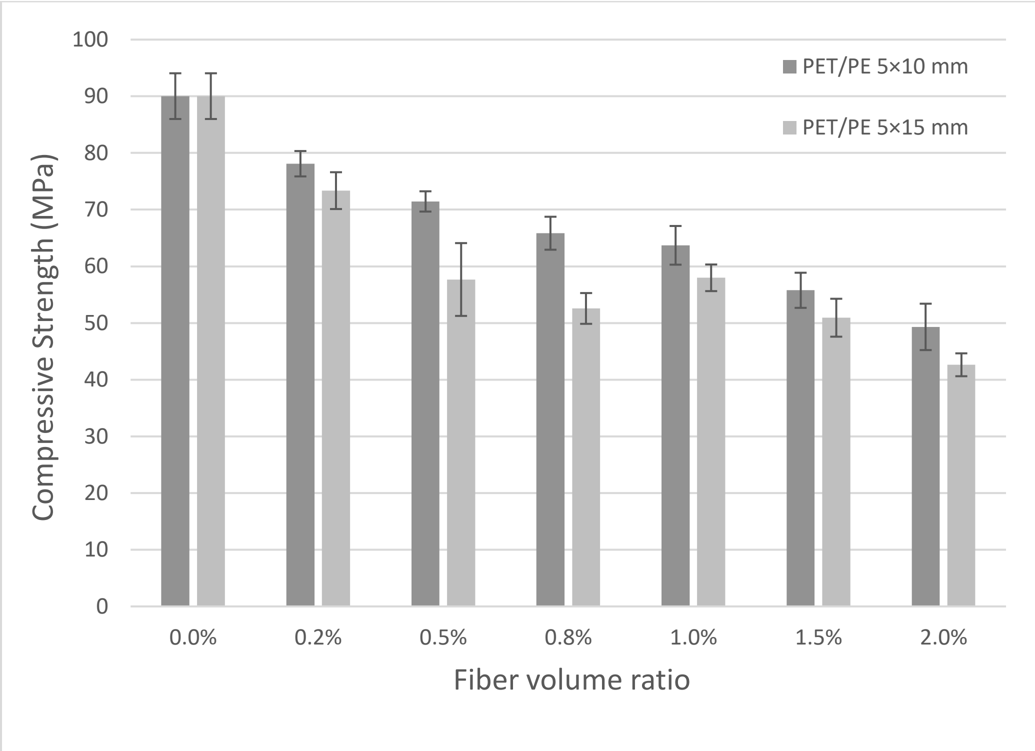

Figure 3.7 Compressive strength vs. PET/PE fiber volume ratio for 2 different aspect ratios

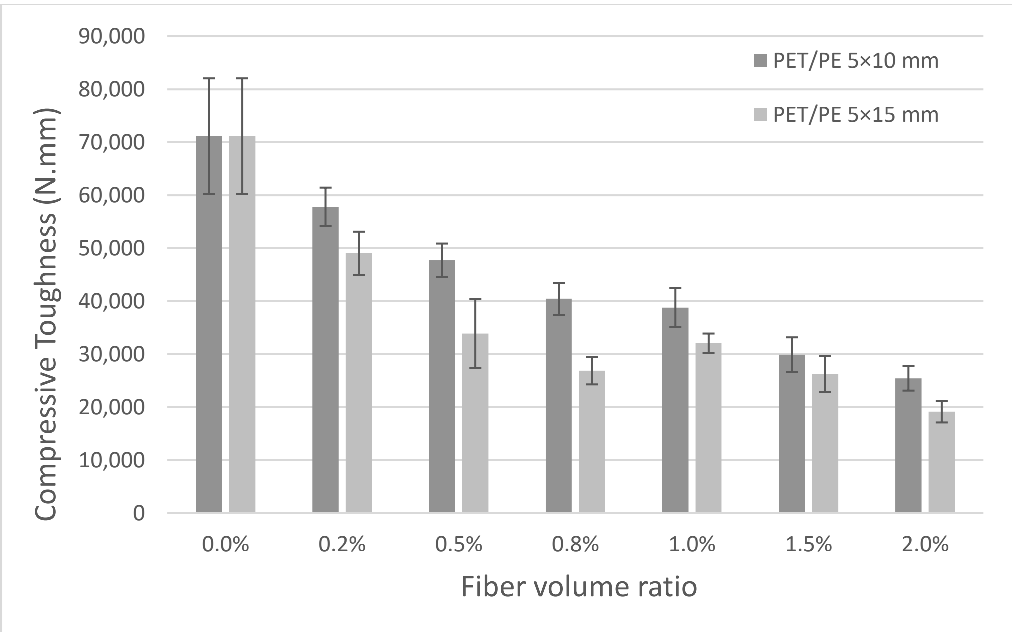

Figure 3.8 Comp. toughness vs. PET/PE fiber volume ratio for 2 different aspect ratios

3.3 Industrial Waste Plastic Reinforced Mortar Test Results

3.3.1 Bending Test Results

Figure 3.9 presents the flexural strength vs. fiber volume ratio behavior of PP, PE and PA fiber reinforced mortars. PP fiber graph shows increment in flexural strength with fiber volume ratio after a drop at 0.2% incorporation ratio. PE graph shows that the flexural strength is not considerably affected by fiber volume ratio. PA fiber graph shows decrement in flexural strength with fiber volume ratio. The maximum flexural strength is displayed at 1.5% PP fiber incorporated specimens higher than control specimens by 8.4%. Flexural strength at 1.5% PE fiber incorporated specimens is higher than control specimens by 4.1%. Flexural strength at 1.5% PA fiber incorporated specimens is less than control specimens by 41%.

Figure 3.10 presents the flexural toughness vs. fiber volume ratio behavior of PP, PE and PA fiber reinforced flexural prisms. Graph shows that there is an increment in flexural toughness with fiber volume ratio. PP fiber incorporated specimens had the maximum increment with fiber volume ratio in comparison to PE and PA. The use of a 1.5% volume ratio of PP, PE and PA fiber led to a flexural toughness of 1841%, 571% and 357%, respectively, higher than that of the control mortar.

Superiority of PP fiber on PE and PA fibers in terms of flexural strength and flexural toughness can be attributed to the high aspect ratio comparing to PE and PA fibers. Enhancement in the flexural toughness with fiber volume ratio can be attributed to the bridging effect which delayed crack propagation.

Figure 3.11 presents the flexural strength vs. fiber volume ratio behavior of PP and TPP fiber reinforced mortar. Graph shows that treatment process did not demonstrate a significant change in the flexural strength of PP.

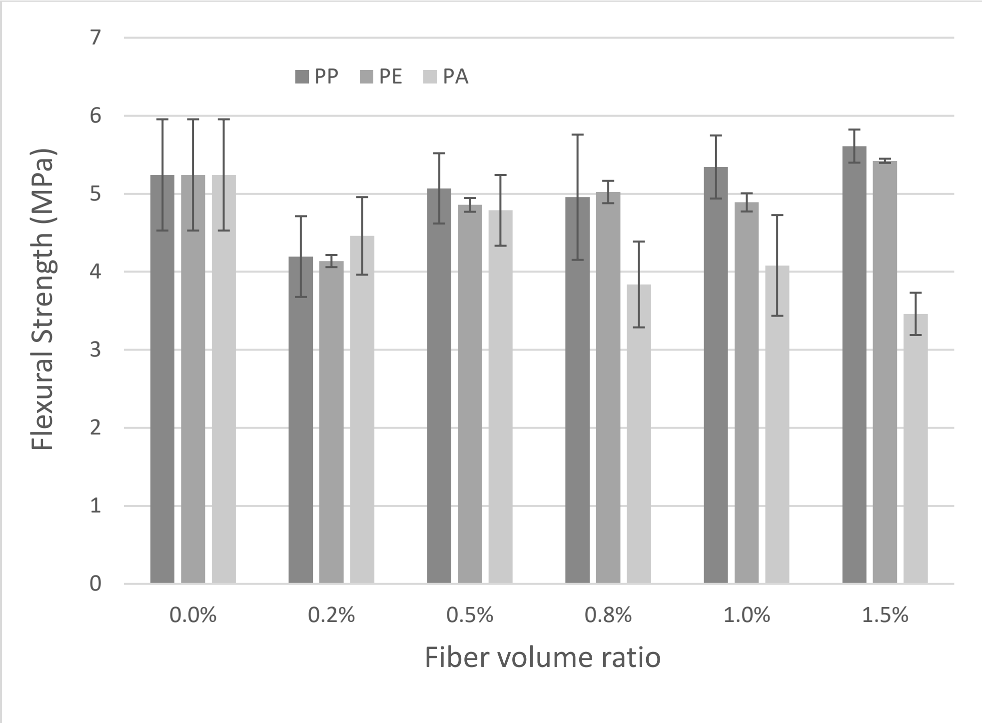

Figure 3.9 Flexural strength vs. PP, PE and PA fiber volume ratio incorporated in mortar

Figure 3.12 presents the flexural toughness vs. fiber volume ratio behavior of PP and TPP fiber reinforced mortar. Graph shows that treatment process have a negative effect on the flexural strength of PP.

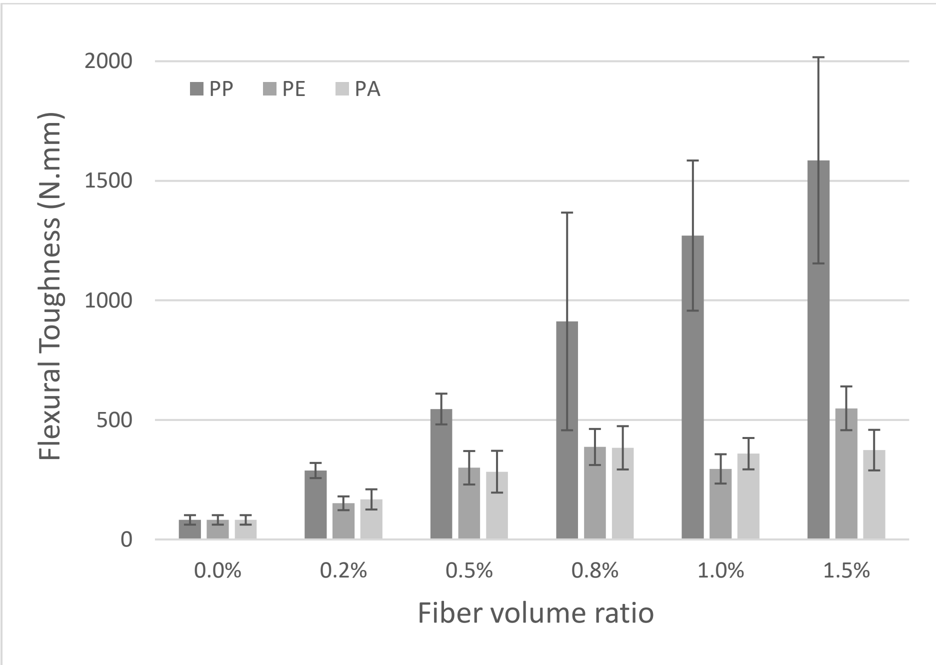

Figure 3.10 Flexural toughness vs. PP, PE and PA fiber volume ratio incorporated in mortar

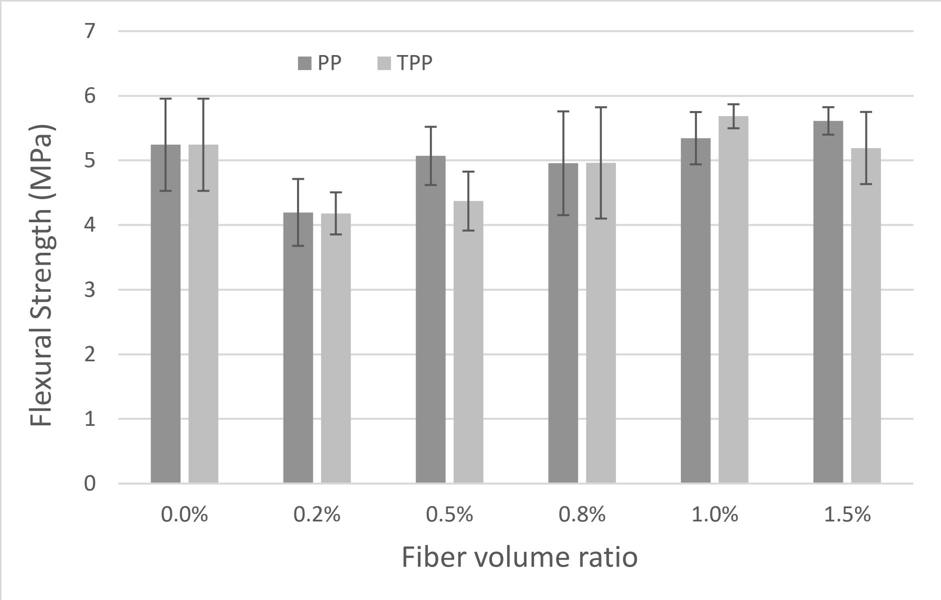

Figure 3.11 Flexural strength vs. PP and TPP fiber volume ratio incorporated in mortar

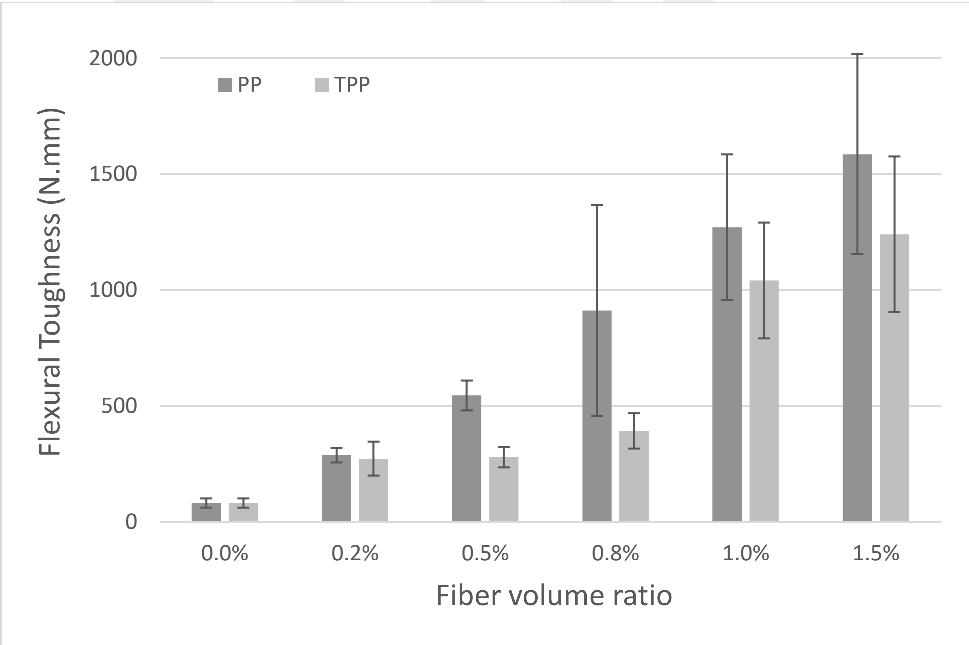

Figure 3.12 Flexural toughness vs. PP and TPP fiber volume ratio incorporated in mortar

Figure 3.13 presents the flexural strength vs. fiber volume ratio behavior of PE and TPE fiber reinforced mortar. Graph shows that treatment process did not demonstrate a significant change in the flexural strength of PE.

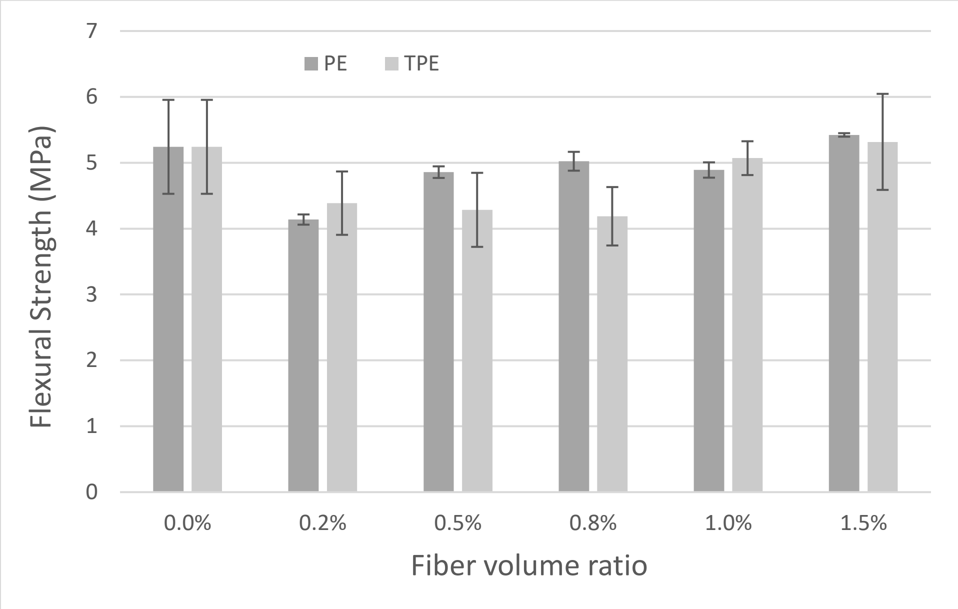

Figure 3.13 Flexural strength vs. PE and TPE fiber volume ratio incorporated in mortar

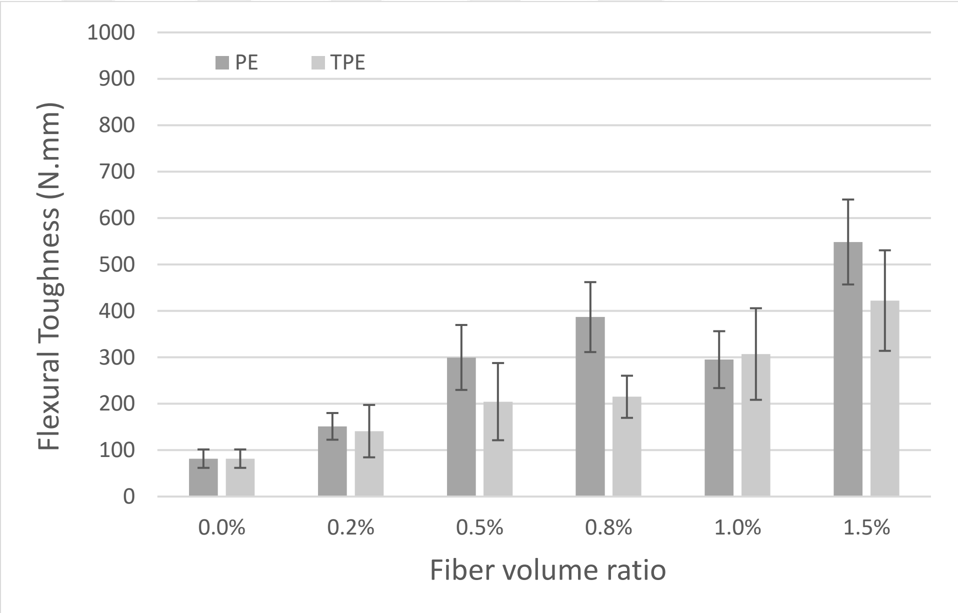

Figure 3.14 Flexural toughness vs. PE and TPE fiber volume ratio incorporated in mortar

3.3.2 Compression Test Results

Figure 3.15 presents the compressive strength vs. fiber volume ratio behavior of PP, PE and PA fiber reinforced specimens. Graphs show that the compressive strength decreased with fiber volume ratio for all used waste plastic types. Sharper drop in the compressive strength of PE with fiber volume ratio is noticed. The same patterns of compressive strength vs. fiber volume ratio are noticed in the results of compressive toughness vs. fiber volume ratio graphs shown in Figure 3.16 and the same discussion can be applied.

This decline in the compressive strength and compressive toughness by increasing PP, PE and PA fiber volume ratio can be attributed to the behavior of fibers as weak zones.

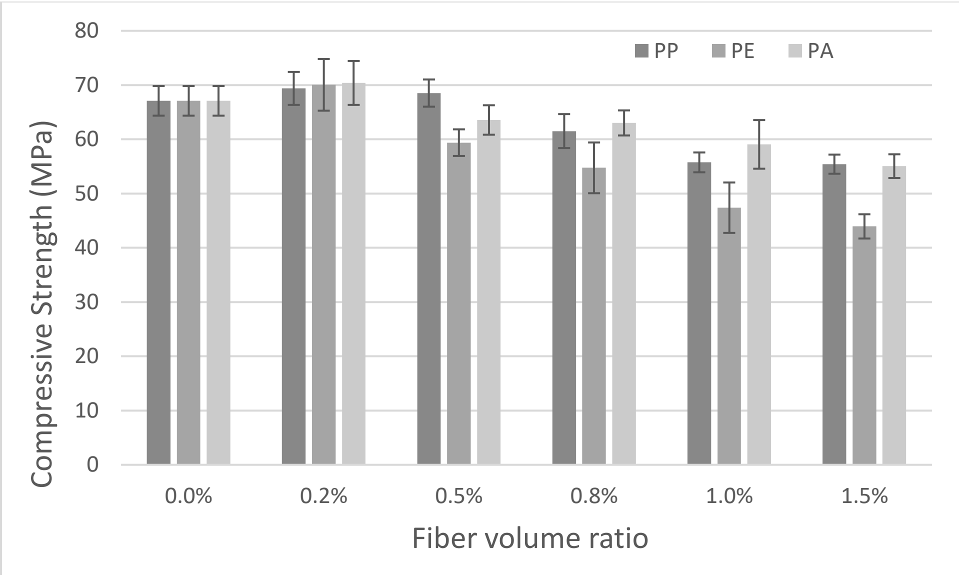

Figure 3.15 Compressive strength vs. PP, PE and PA fiber volume ratio incorporated in mortar

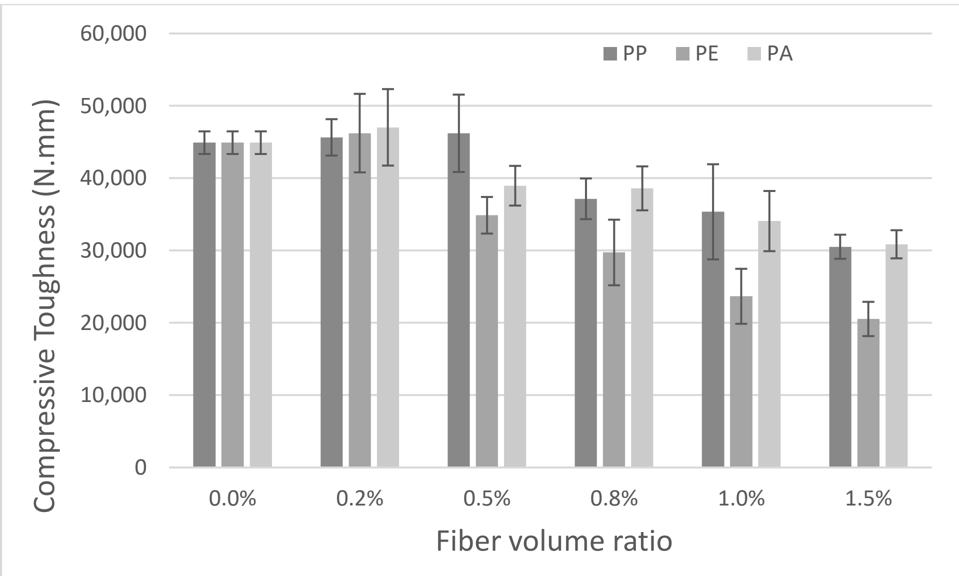

Figure 3.16 Compressive toughness vs. PP, PE and PA fiber volume ratio incorporated in mortar

Figure 3.17 presents the compressive strength vs. fiber volume ratio behavior of PP and TPP fiber reinforced specimens. Graph shows that the surface treatment of fibers' surface increased the compressive strength of PP fiber incorporated mortar.

Figure 3.18 presents the compressive toughness vs. fiber volume ratio behavior of PP and TPP fiber reinforced specimens. Graph shows that the surface treatment of fibers' surface increased the compressive toughness of PP fiber incorporated mortars.

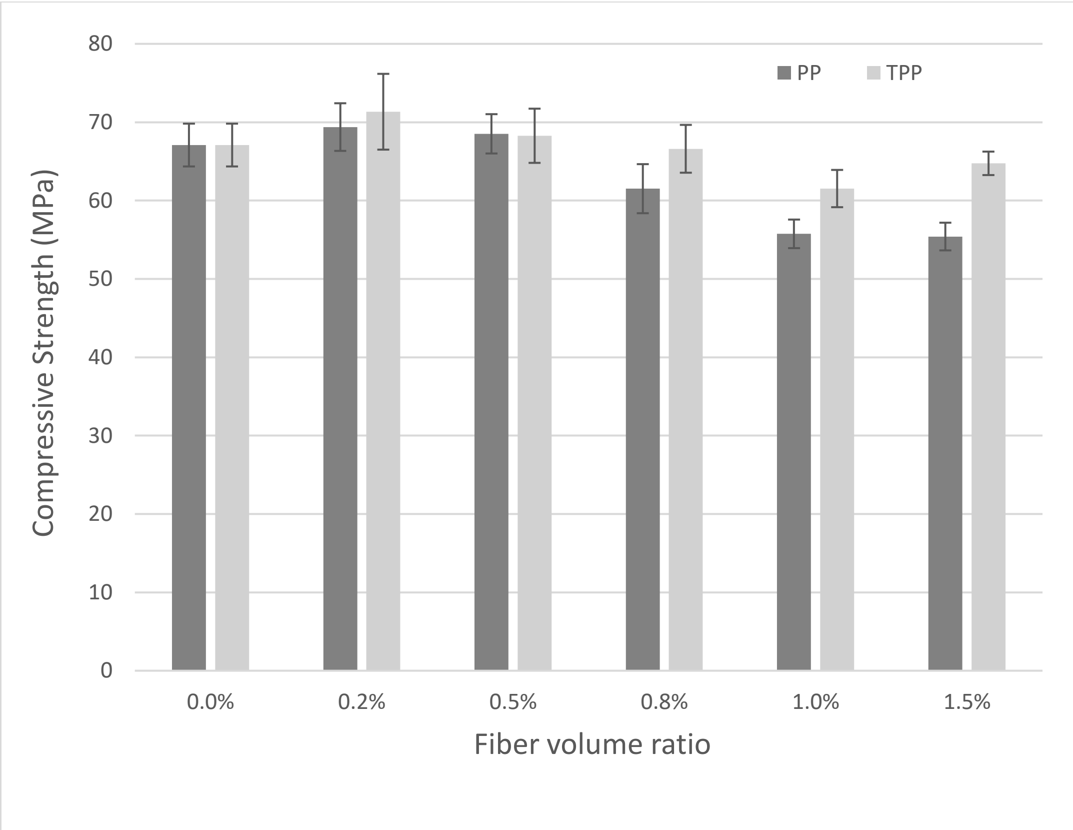

Figure 3.17 Compressive strength vs. PP and TPP fiber volume ratio incorporated in mortar

Figure 3.19 presents the compressive strength vs. fiber volume ratio behavior of PE and TPE fiber reinforced specimens. Graphs shows that the surface treatment of fibers' surface increased the compressive strength of PP fiber incorporated mortars.

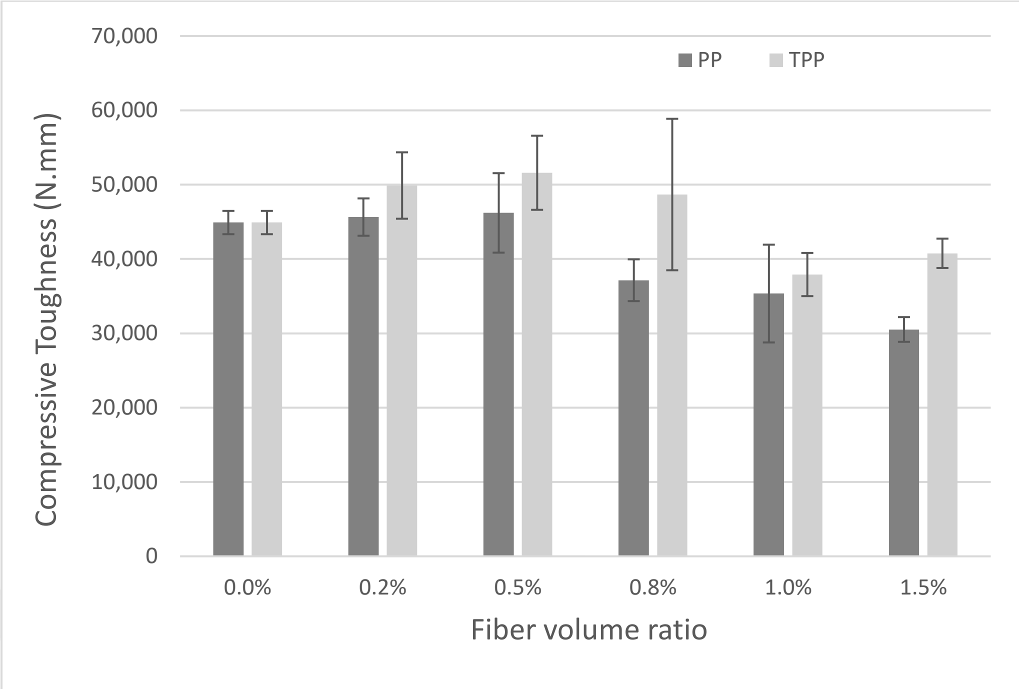

Figure 3.18 Compressive toughness vs. PP and TPP fiber volume ratio incorporated in mortar

Figure 3.20 presents the compressive toughness vs. fiber volume ratio behavior of PE and TPE fiber reinforced specimens. Graph shows that the surface treatment of fibers' surface increased the compressive toughness of PE fiber incorporated mortars.

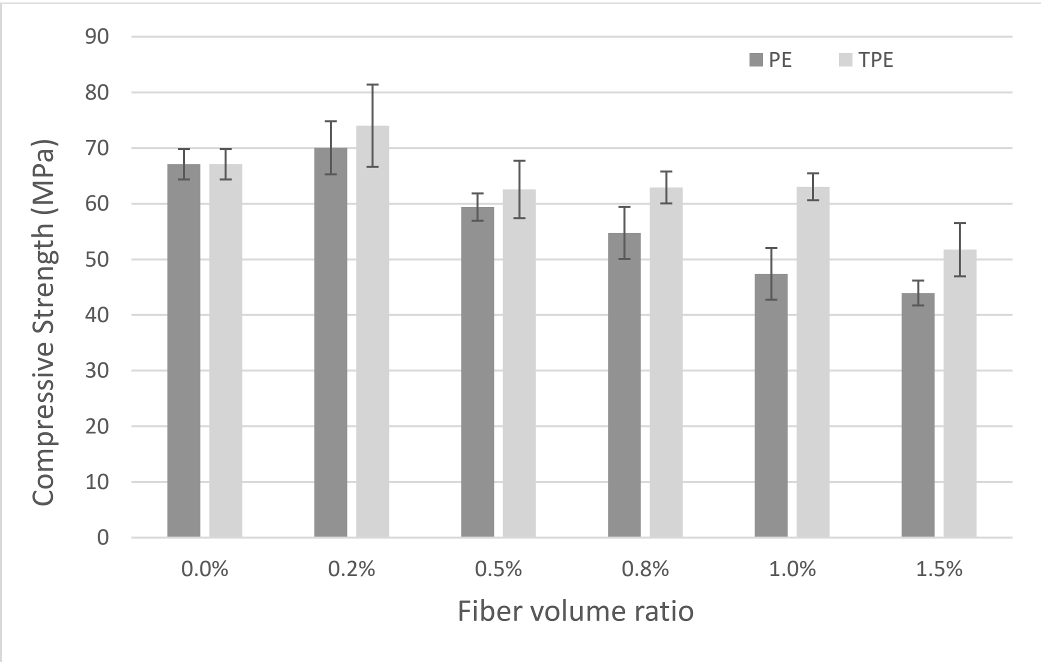

Figure 3.19 Compressive strength vs. PE and TPE fiber volume ratio incorporated in mortar

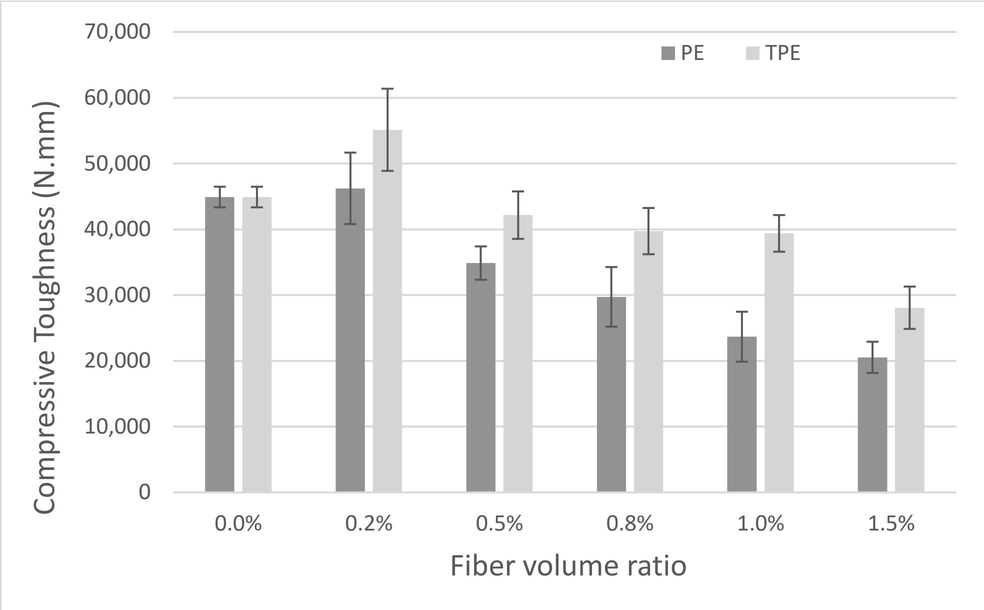

Figure 3.20 Compressive toughness vs. PE and TPE fiber volume ratio incorporated in mortar

3.4 Overall Waste Plastic Performance Results

3.4.1 Bending Test Results

The relationship between flexural strength and the artificially produced fiber volume ratios are shown in Figure 3.21. It can be observed that the use of PET and PET/PE fibers did not significantly affect the flexural strength. The maximum flexural strength was achieved when 2% of PET 5×15 mm is used by 18.6% higher than control mortar.

The relationship between flexural toughness and the artificially produced fiber volume ratios are shown in Figure 3.22. It can be observed that the use of PET and PET/PE fibers significantly raised the flexural strength. The use of 2% of PET 5×20, PET 5×15, PET 5×10, PET/PE 5×15 and PET/PE 5×10 mm raised flexural toughness by 2402%, 1864%, 739%, 616% and 561% respectively in comparison to control mortar.

The relationship between load and stroke for all used artificially produced fiber reinforced flexural mortar specimens at 2% incorporation ratio are shown in Figure

3.23. It can be observed that the post-peak ductility and energy absorption was higher in PET fibers than in PET/PE fibers, and increased with fiber aspect ratio.

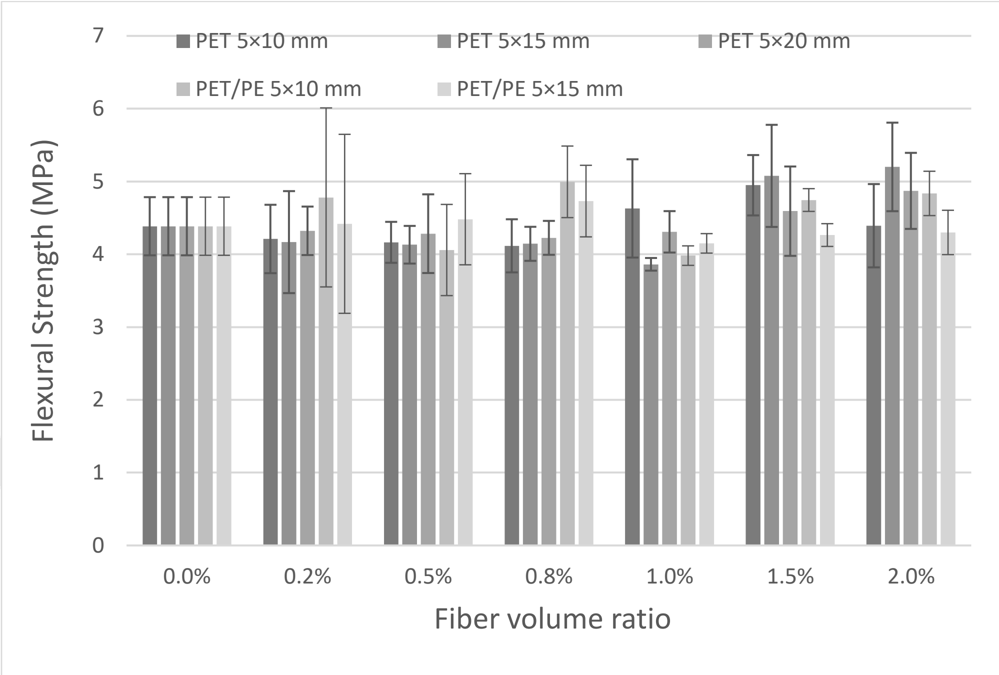

Figure 3.21 Flexural strength vs. all artificially produced fiber volume ratio incorporated in mortar

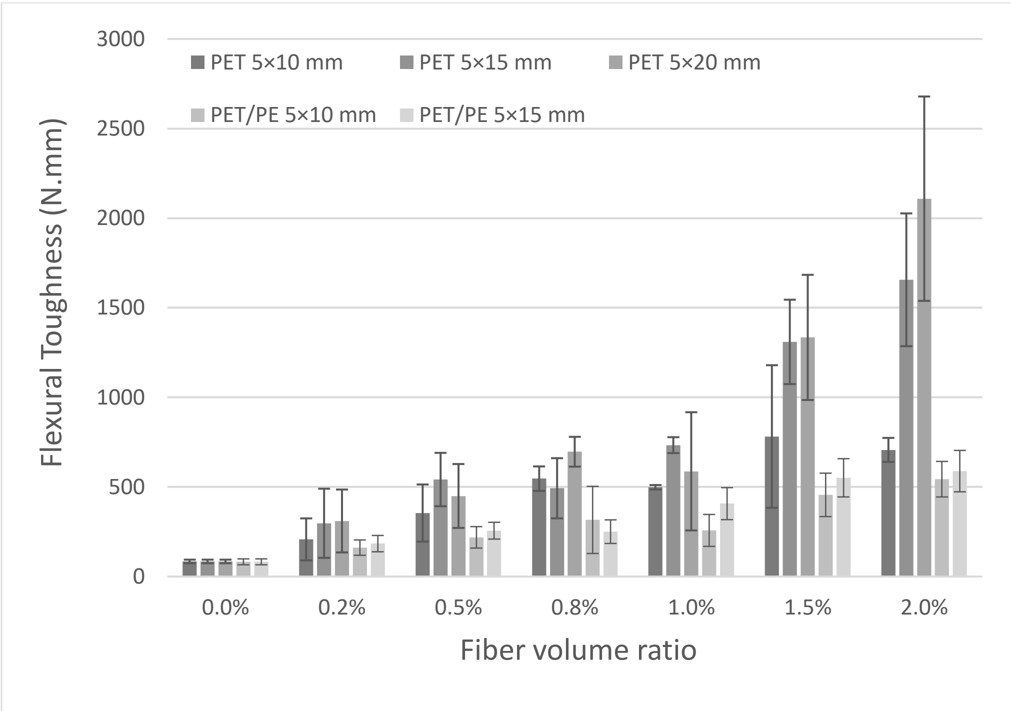

Figure 3.22 Flexural toughness vs. all artificially produced fiber volume ratio incorporated in mortar

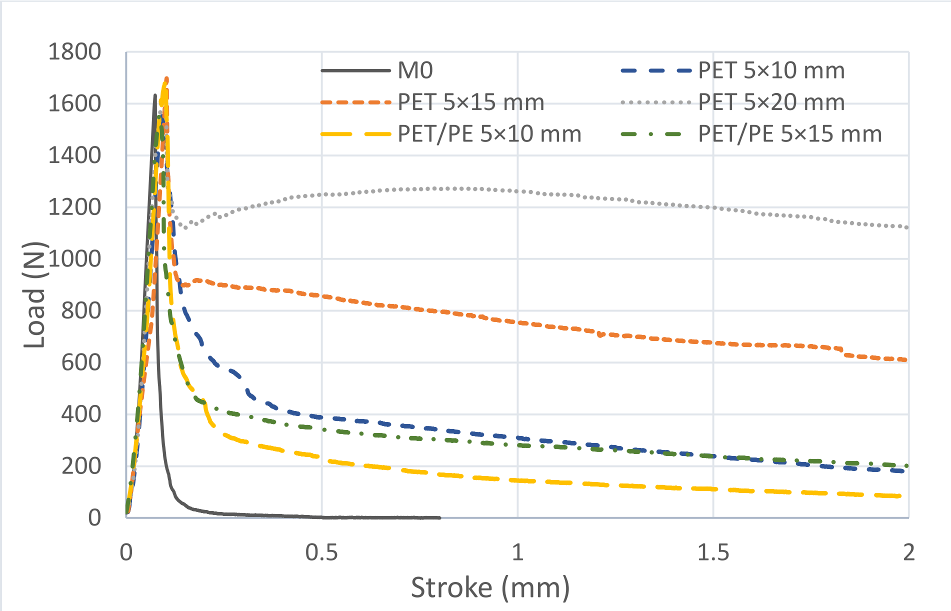

Figure 3.23 Load vs. stroke at 2% artificially produced fiber volume ratio in bending tests

The relationship between flexural strength and all used industrial fiber volume ratios are shown in Figure 3.24. It can be observed that the use of PP, PE, PA, TPP and TPE did not show improvement in the flexural strength. The maximum flexural strength was 8.4% higher than the control mortar when 1.5% of PP was incorporated.

The relationship between flexural toughness and all used industrial fiber volume ratios are shown in Figure 3.25. It can be observed that the use of PP, PE, PA, TPP and TPE fibers significantly raised the flexural strength. The use of PP, PE, PA, TPP and TPE raised flexural toughness by 1841%, 571%, 739%, 357% and 417% respectively in comparison to control mortar.

The relationship between load and stroke for all used industrial fiber reinforced flexural mortar specimens at 1.5% incorporation ratio are shown in Figure 3.26. It can be observed that the post-peak ductility and energy absorption is higher in PP and TPP fibers than the other fibers. This increase can be explained by the high aspect ratio of used waste polypropylene fiber.

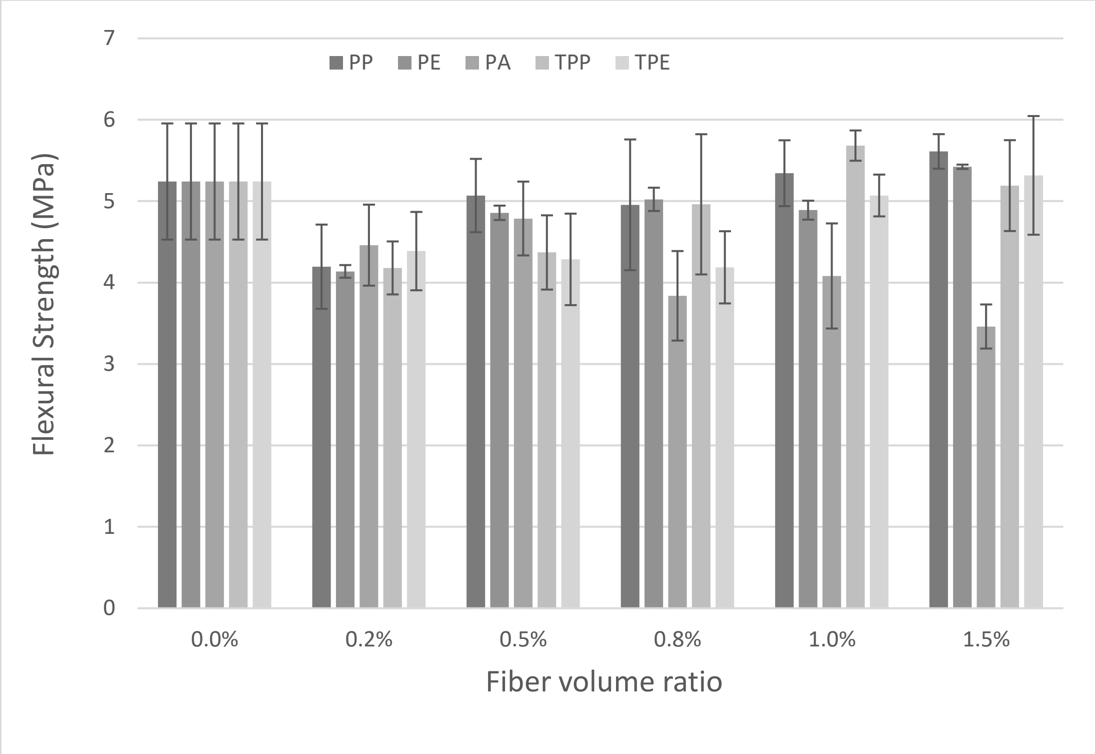

Figure 3.24 Flexural strength vs. all industrial fiber volume ratio incorporated in mortar

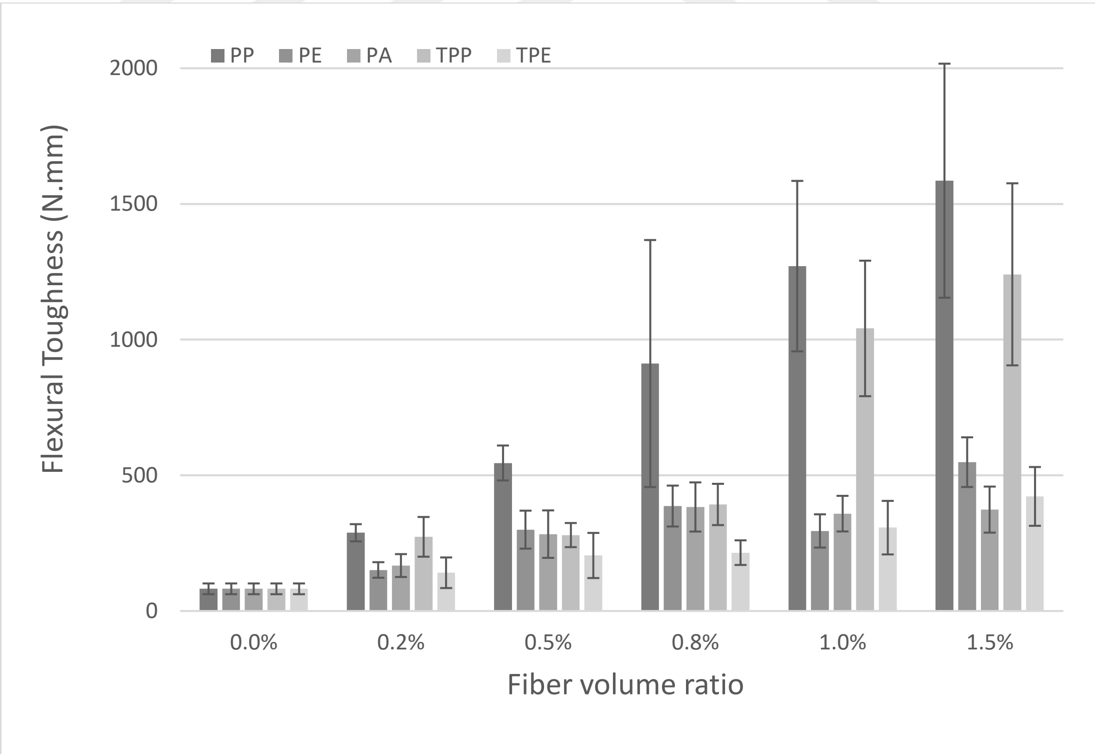

Figure 3.25 Flexural toughness vs. all industrial volume ratio incorporated in mortar

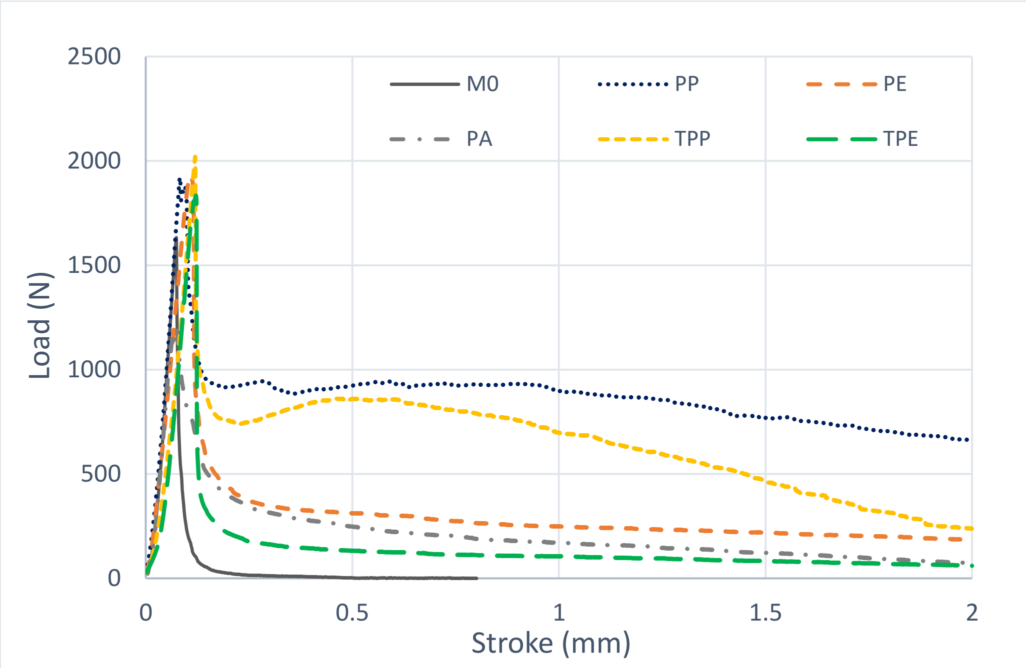

Figure 3.26 Load vs. stroke at 1.5% industrial fiber volume ratio in bending tests

3.4.2 Compression Test Results

The relationship between compressive strength and all used artificially produced fiber volume ratios are shown in Figure 3.27. It can be observed that the use of PET and PET/PE fibers did not positively affect the compressive strength. The maximum compressive strength was achieved when 0.2% of PET 5×10 mm was used by 3.7% higher than control mortar.

The relationship between compressive toughness and all used artificially produced fiber volume ratios are shown in Figure 3.28. It can be observed that the use of PET and PET/PE fibers significantly reduced the compressive toughness in comparison to control mortar.

The relationship between load and stroke for all used artificially produced fiber reinforced compressive mortar specimens at 0.2% incorporation ratio are shown in Figure 3.29. It can be observed that the post-peak ductility and energy absorption is very low.

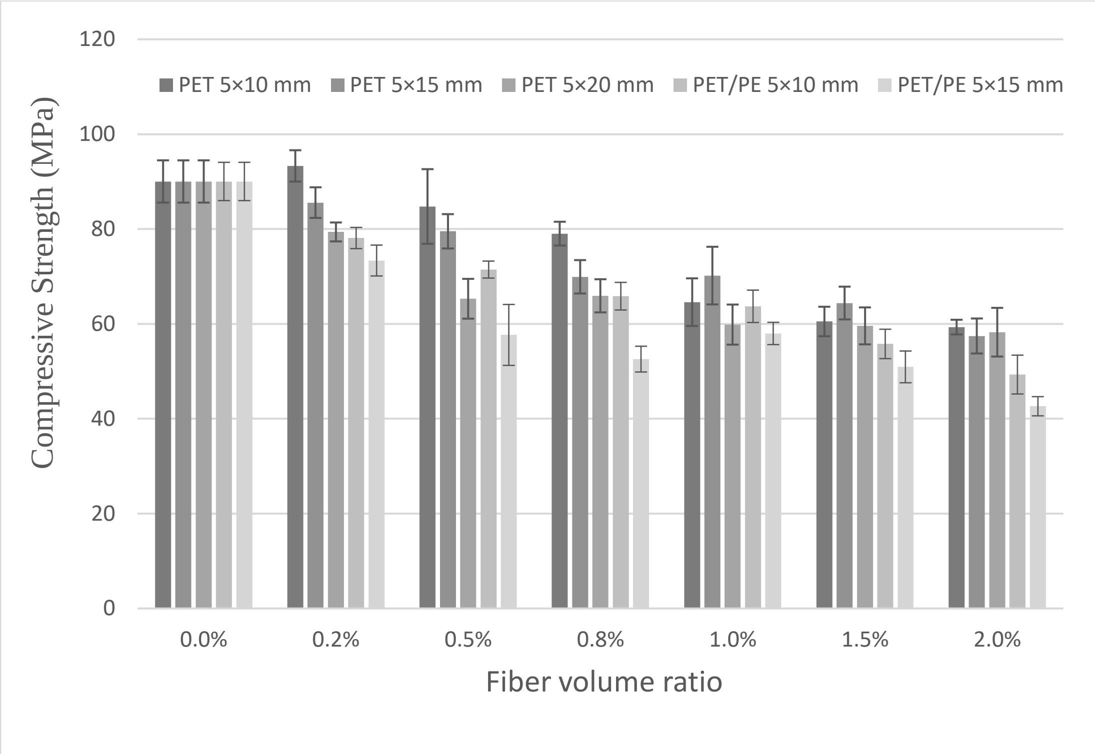

Figure 3.27 Compressive strength vs. all artificially produced fiber volume ratio incorporated in mortar

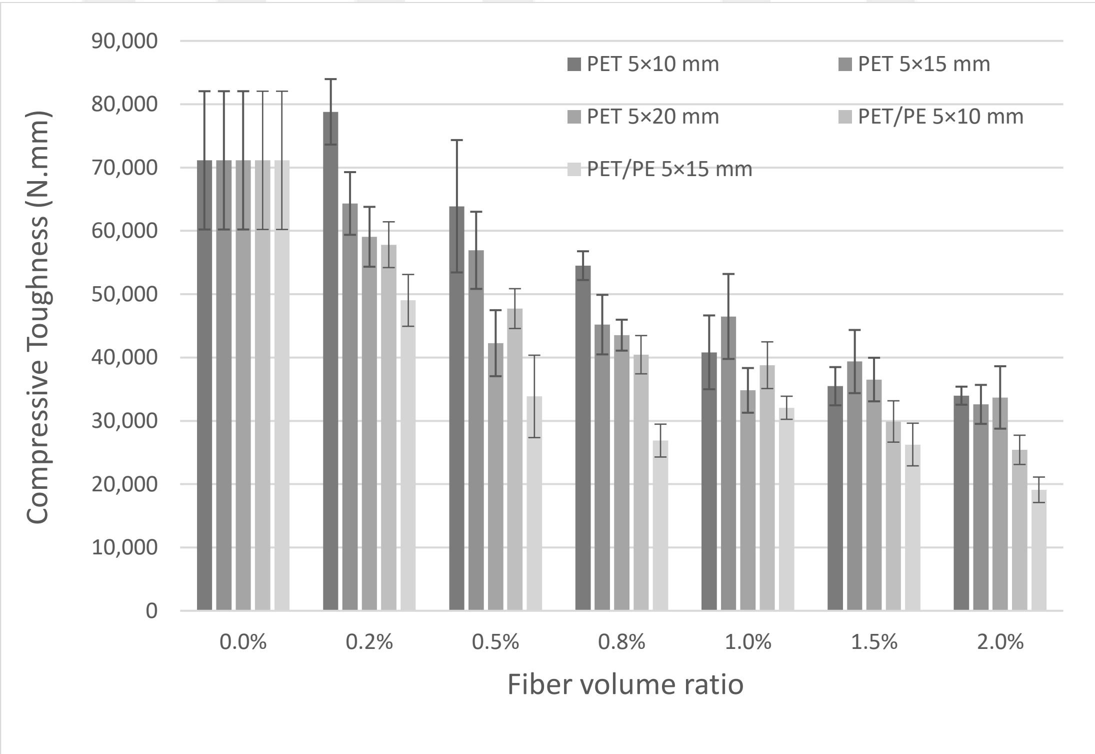

Figure 3.28 Compressive toughness vs. all artificially produced fiber volume ratio incorporated in mortar

The relationship between compressive strength and all used industrial shaped fiber volume ratios are shown in Figure 3.30. It can be observed that the use of PP, PE, PA, TPP and TPE fibers affected the compressive strength positively only at fiber volume ratio of 0.2%. At 0.2% incorporation ratio, the compressive strength was higher than the control mortar by 3.4%, 4.4%, 4.9%, 6.3% and 10.3% respectively.

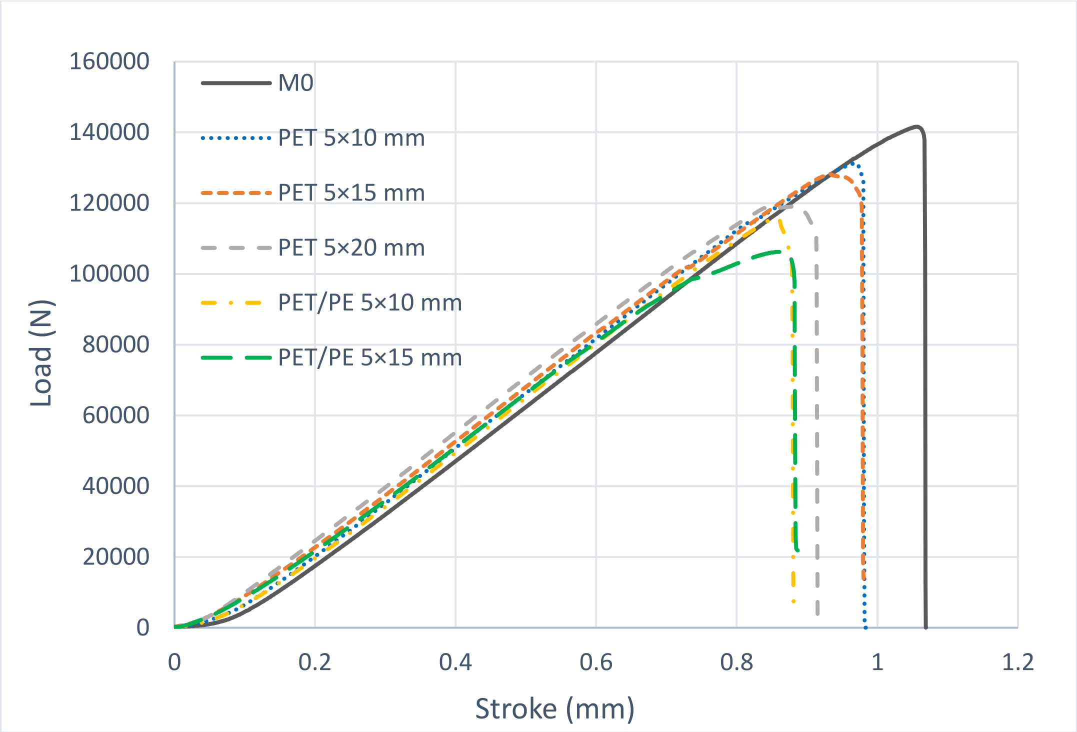

Figure 3.29 Load vs. stroke at 0.2% artificially produced fiber vol. ratio in compression tests

The relationship between compressive toughness and all used industrial fiber volume ratios are shown in Figure 3.31. It can be observed that the use of PP, PE, PA, TPP and TPE fibers affected the compressive toughness positively only at fiber volume ratio of 0.2%. At 0.2% incorporation ratio, the compressive toughness was higher than the control mortar by 1.6%, 2.9%, 4.7%, 11.1% and 22.8% respectively.

The relationship between load and stroke for all used industrial fiber reinforced compressive mortar specimens at 0.2% incorporation ratio are shown in Figure 3.32. It can be observed that the post-peak ductility and energy absorption increased in PP and TPP incorporated mortar specimens.

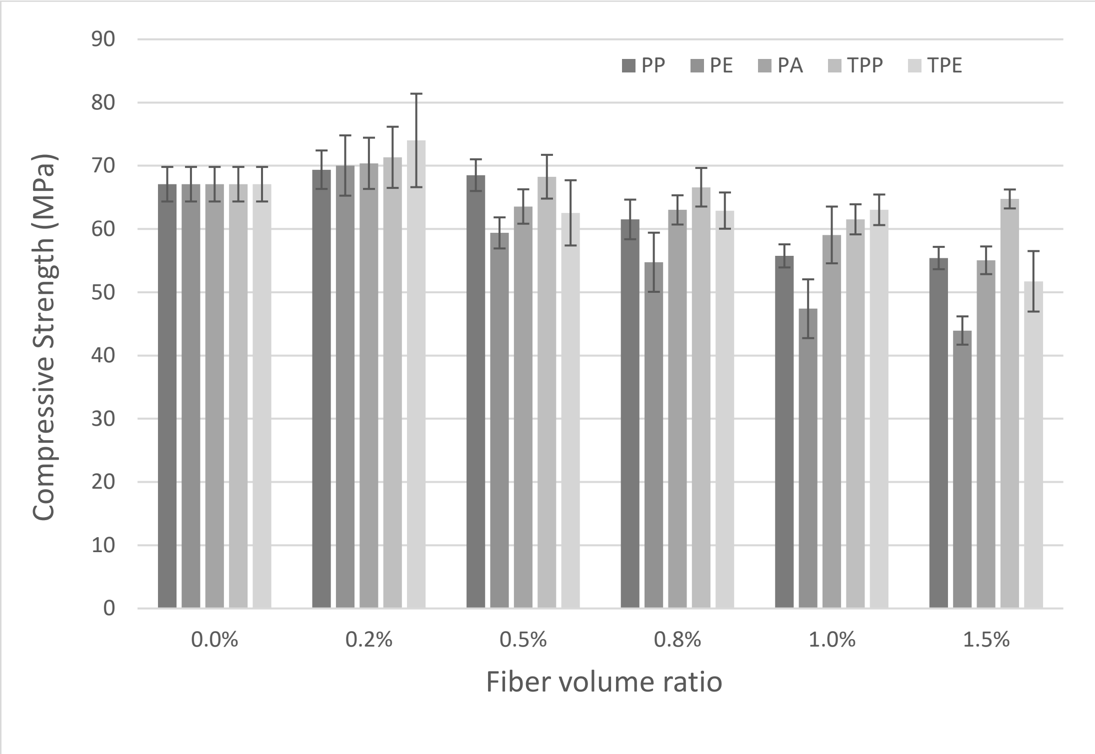

Figure 3.30 Compressive strength vs. all industrial volume ratio incorporated in mortar

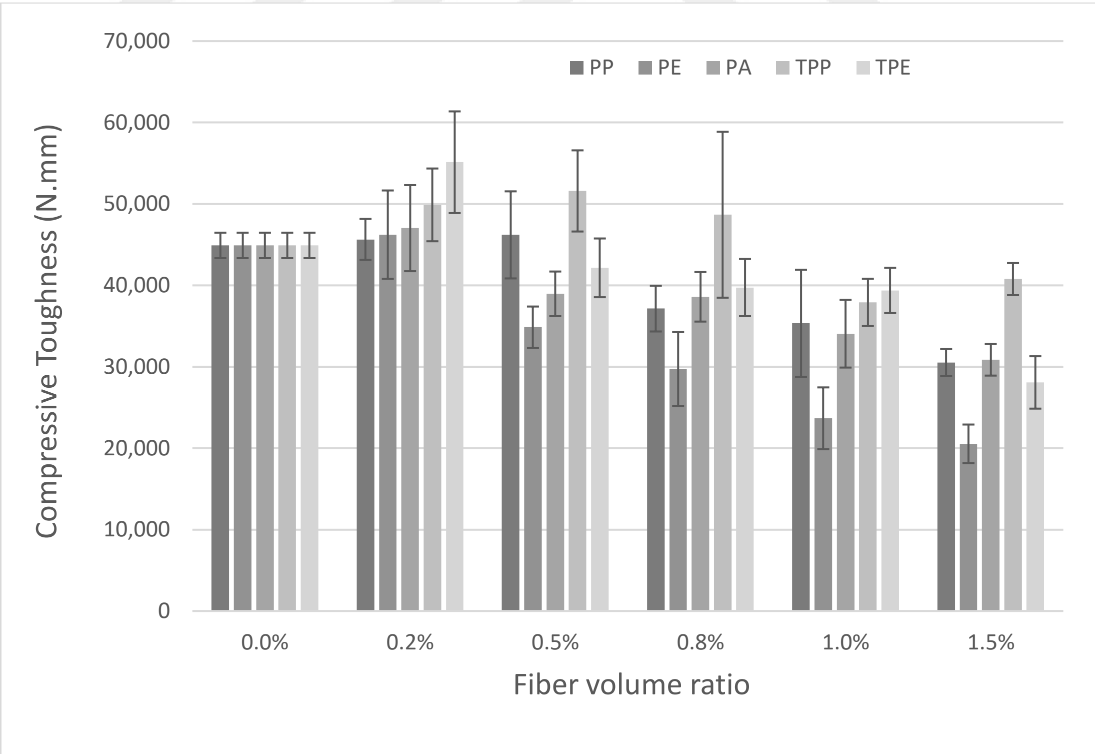

Figure 3.31 Compressive toughness vs. all industrial volume ratio incorporated in mortar

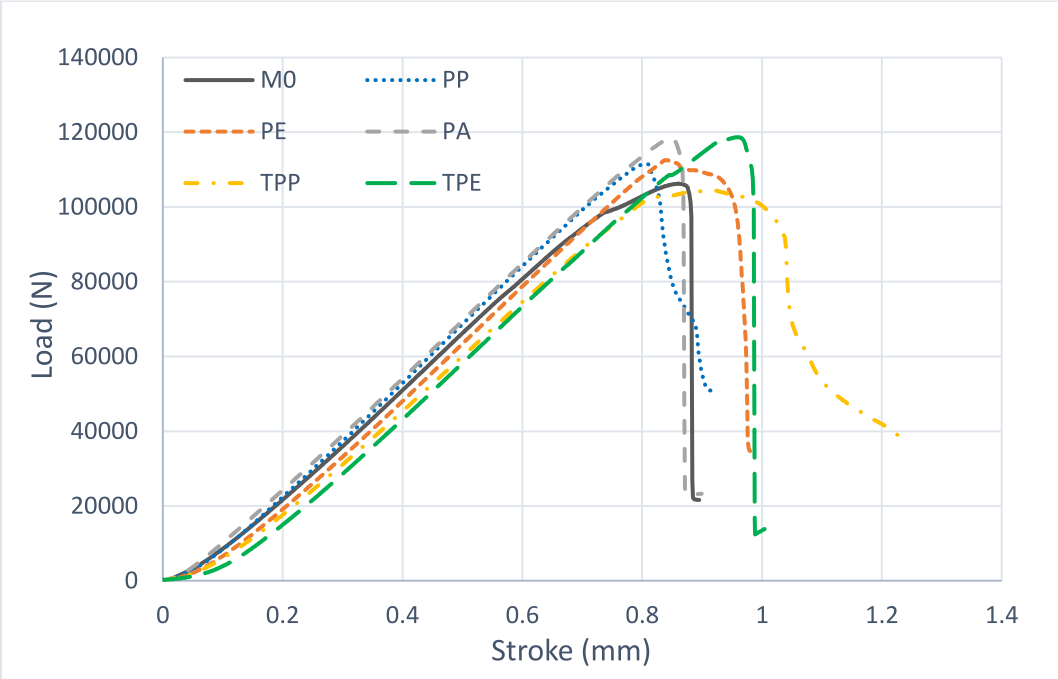

Figure 3.32 Load vs. stroke at 1.5% industrial fiber volume ratio in compression tests

3.5 Self-Compacting Mortar (SCM) Tests Results

In order to examine the ability of waste fiber reinforced mortar to reinforce concrete, Self-compacting mortar was designed and tested. It was decided to be reinforced SCM with waste PP fiber according to the highest flexural toughness results shown among all waste fiber reinforced mortar tests. SCM tests was conducted to decide the optimistic ratio of fiber that shows the greatest flow value (shown in Table 2.10) with improved flexural toughness and without segregation of the constituents.

3.5.1 Bending Test Results

Figure 3.33 presents the flexural strength vs. fiber volume ratio behavior of waste PP fiber reinforced mortars. The graph shows decrese in flexural strength with fiber volume ratio.

Figure 3.34 presents the flexural toughness vs. fiber volume ratio behavior of waste PP fiber reinforced flexural prisms. The graph shows increment in flexural toughness with fiber volume ratio. The use of a 0.4% volume ratio of PP fiber led to an increment in flexural toughness by 279%.

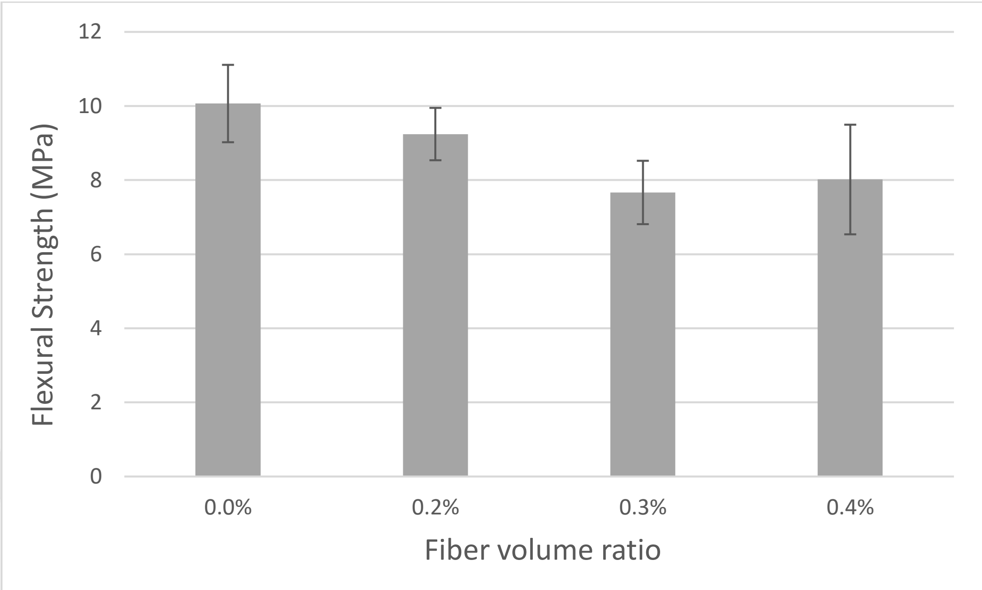

Figure 3.33 Flexural strength vs. PP fiber volume ratio incorporated in SCM

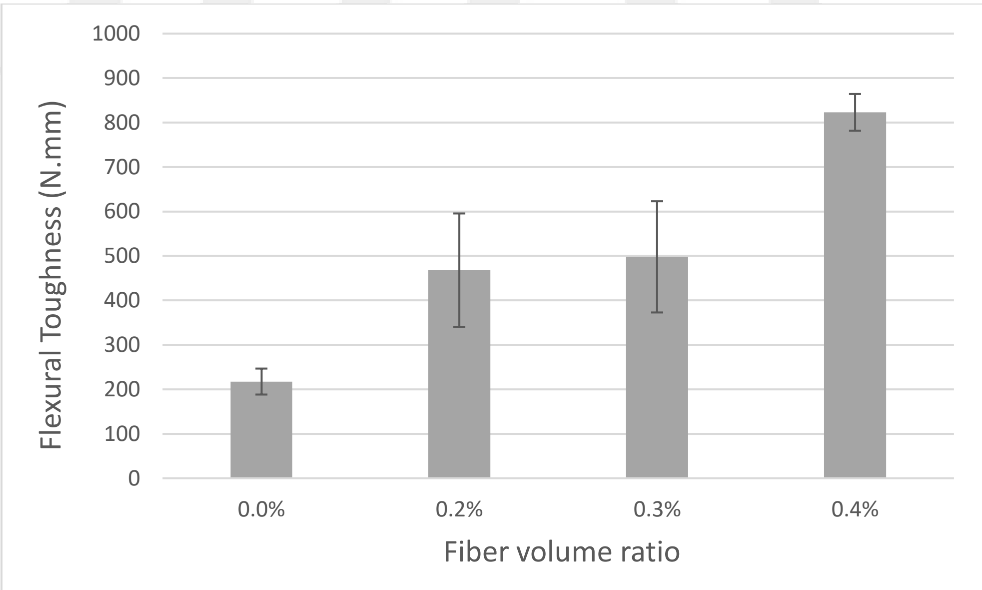

Figure 3.34 Flexural toughness vs. PP fiber volume ratio incorporated in SCM

3.5.2 Compression Test Results

Figure 3.35 presents the compressive strength vs. fiber volume ratio behavior of PP fiber reinforced flexural prisms. The graph shows that the maximum compressive strength was achieved at 0.3% PP fiber incorporation ratio which was 2.9% higher than control mortar.

Figure 3.36 presents the compressive toughness vs. fiber volume ratio behavior of PP fiber reinforced flexural prisms. The graph shows similar results of those of compressive strength with fiber volume ratio. The use of a 0.4% volume ratio of PP fiber led to an increment in compressive toughness by 1.2%.

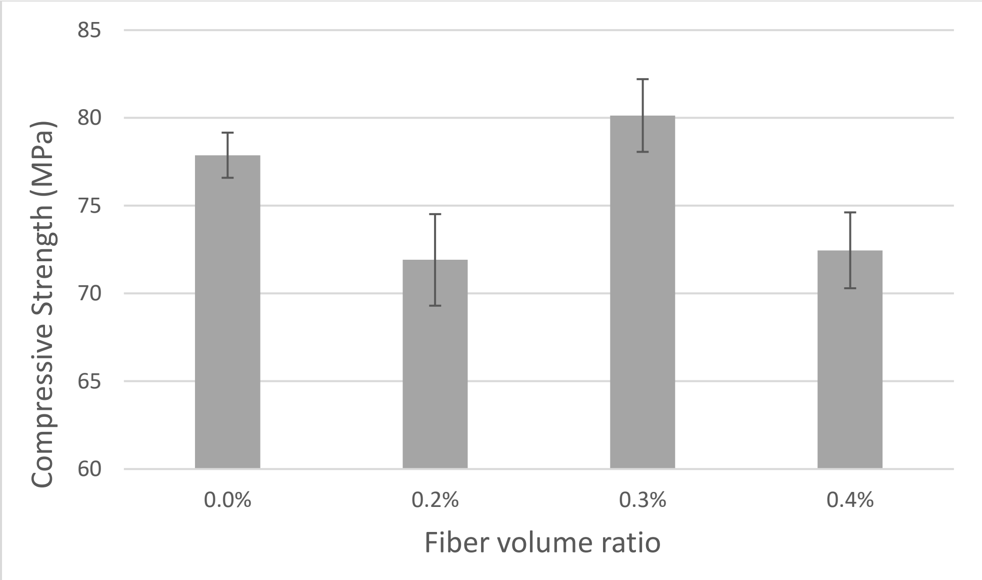

Figure 3.35 Compressive strength vs. PP fiber volume ratio incorporated in SCM

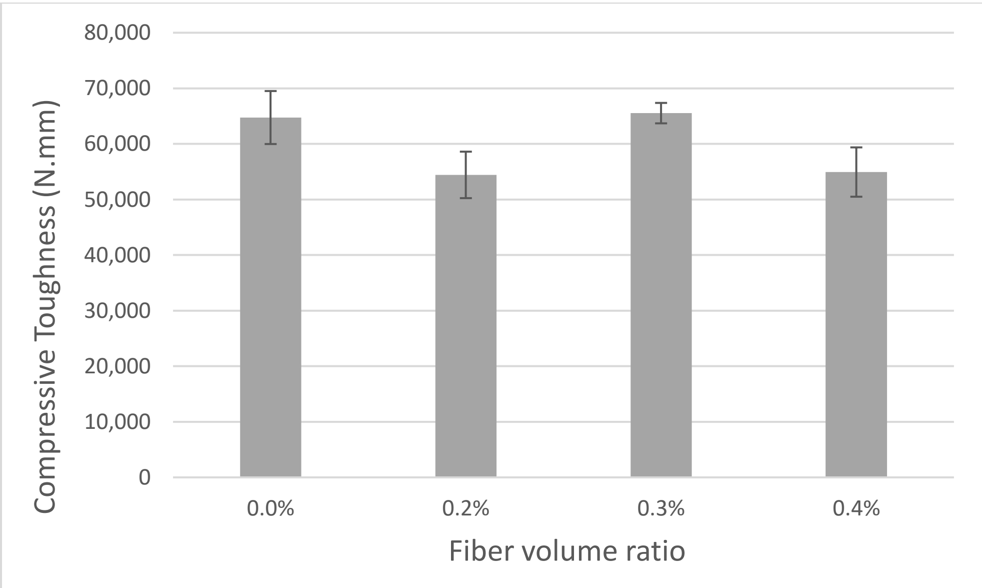

Figure 3.36 Compressive toughness vs. PP fiber volume ratio incorporated in SCM

3.6 Mortar Repaired Concrete Tests Results

Depending on the results of waste PP fiber volume ratio reinforced SCM, it was decided to initiate concrete repairing experiments by repairing concrete using plain SCM. and 0.3% waste PP fiber volume ratio reinforced SCM. For concrete beam specimens, strong contact between concrete and SCM was achieved by different ways.

3.6.1 Bending Test Results

3.6.1.1 Repair SCM Results

Figure 3.37 presents the flexural strength vs. fiber volume ratio behavior of SCM flexural prisms. Graph shows relatively similar flexural strength values for plain SCM and waste 0.3% volume ratio PP fiber reinforced SCM.

Figure 3.38 presents the flexural toughness vs. fiber volume ratio behavior of waste PP fiber reinforced flexural prisms. Graph shows relatively greater flexural toughness value of waste PP reinforced SCM than that of the plain SCM by 164%.

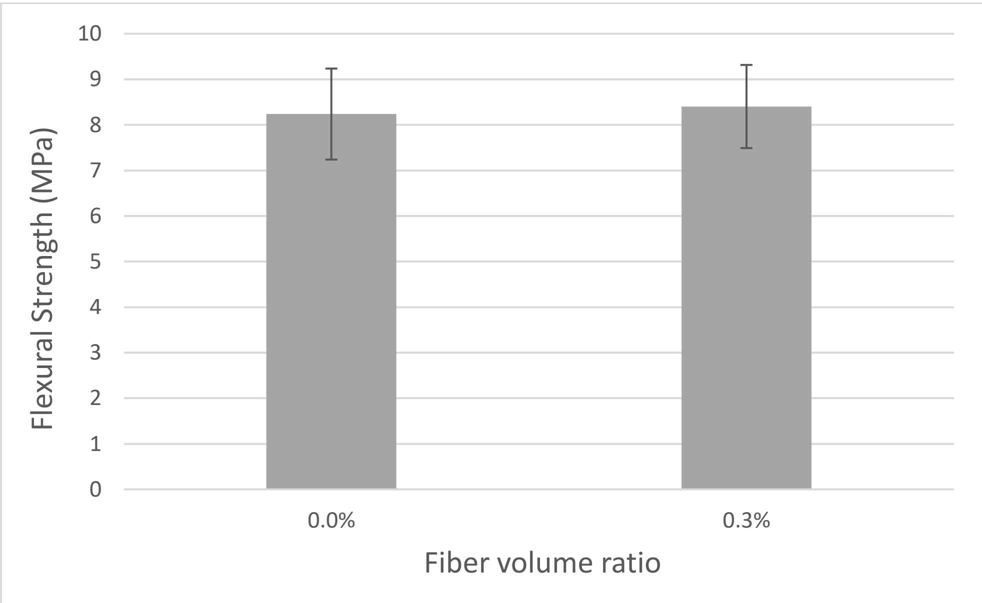

Figure 3.37 Flexural strength vs. PP fiber volume ratio incorporated in repairing SCM

3.6.1.2 Repaired Flexural Concrete Beam Specimens Results of Group A

In this group, three types of beam specimens were used, un-repaired, plain SCM-repaired drilled, and waste PP fiber reinforced SCM-repaired drilled concrete beam (CB). Contact between concrete specimen and SCM was implemented by drilling method which was explained in section 2.6.

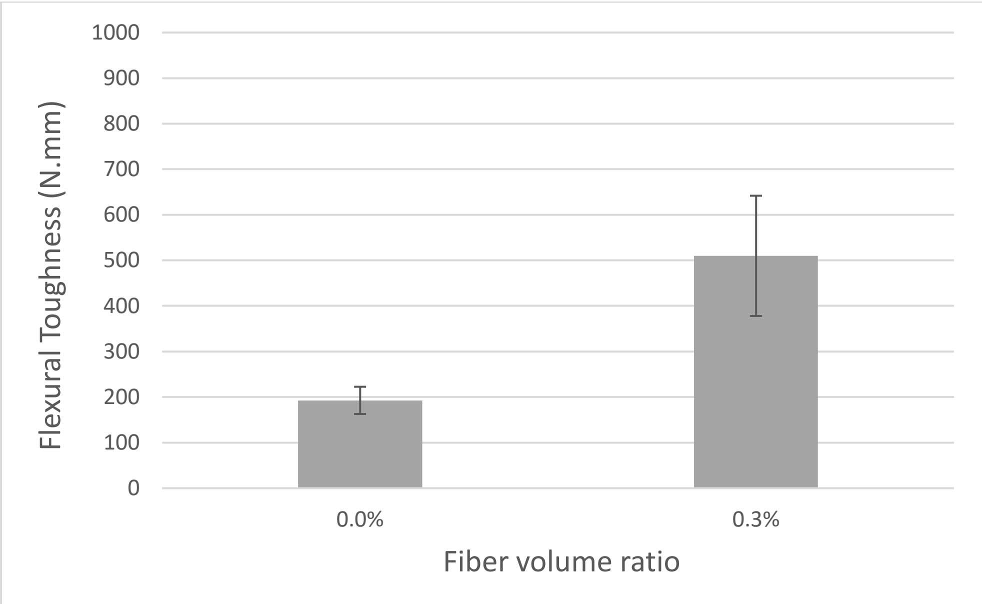

Figure 3.38 Flexural toughness vs. waste PP fiber volume ratio incorporated in repairing SCM

Figure 3.39 presents the flexural strength for the three CB specimens used in this group. Results show relatively similar flexural strength values for the un-repaired CB specimen and the plain SCM-repaired drilled CB specimen. PP-reinforced SCM-repaired drilled CB showed a greater flexural strength value than that of the un-repaired CB specimen by 16.1%.

Figure 3.40 presents the flexural toughness for the three CB specimens used in this group. It can be observed that the repairing by PP-reinforced SCM significantly improved the flexural toughness by 37% in comparison to the un-repaired CB. Repairing by plain SCM did not improve the flexural toughness.

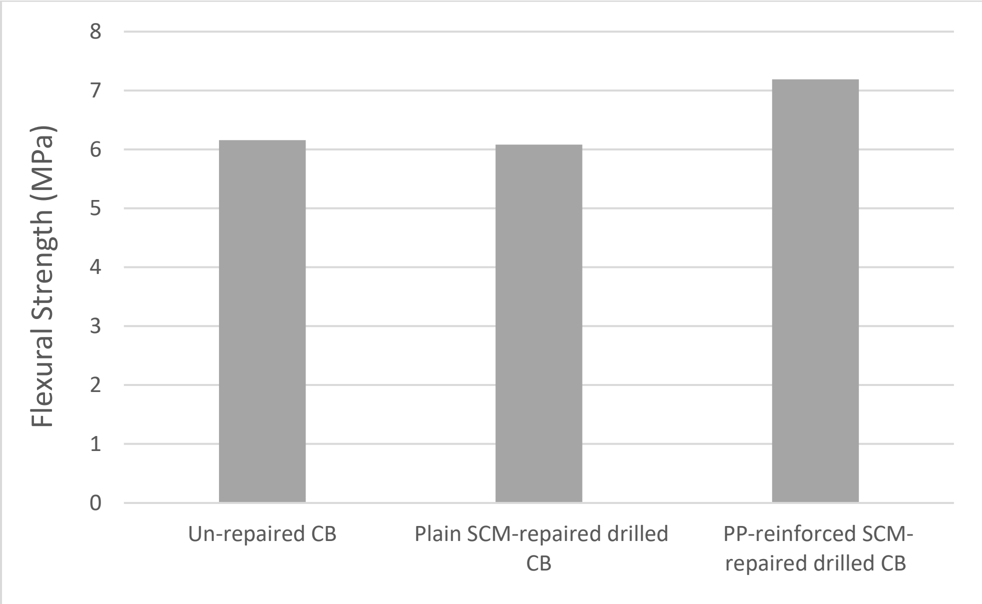

Figure 3.39 Flexural strength of group A's concrete beam specimens

3.6.1.3 Repaired Flexural Concrete Beam Specimens Results of Group B

In this group, three types of beam specimens were used, 2cm-depth-reduced, plain SCM-repaired drilled, and waste PP fiber reinforced SCM-repaired drilled CB specimens. Contact between concrete specimen and SCM was implemented by drilling method explained previously in section 2.6.

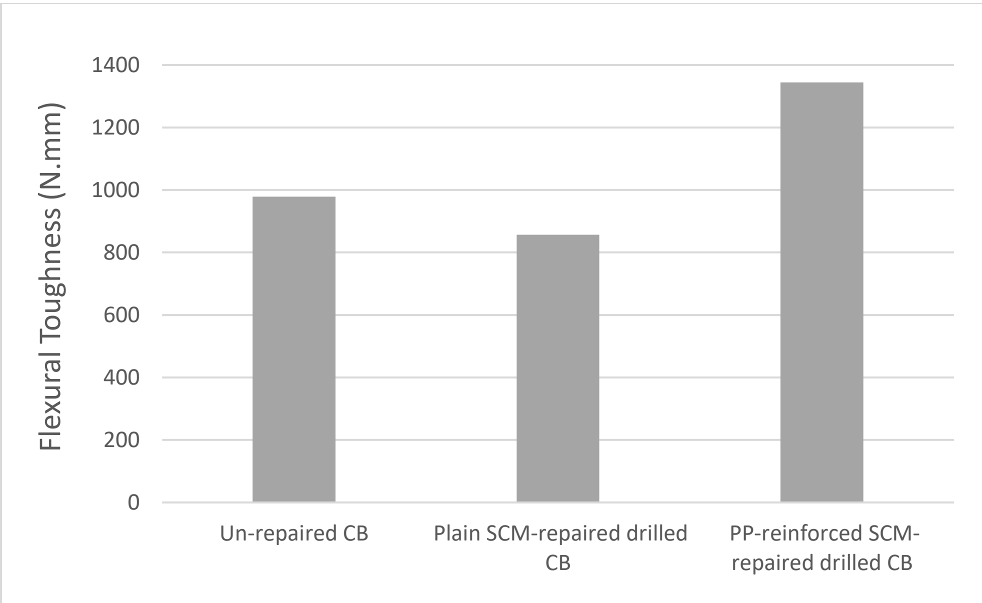

Figure 3.40 Flexural toughness of group A's concrete beam specimens

Figure 3.41 presents the flexural strength for the three CB specimen types used in this group. PP-reinforced SCM-repaired drilled CB showed a greater flexural strength value than that of the un-repaired CB specimens by 118% and greater than plain SCM-repaired CB specimens by 11.1%.

Figure 3.42 presents the flexural toughness for the three CB specimens used in this group. It can be observed that PP-reinforced SCM-repaired drilled CB showed a greater flexural toughness value than that of the un-repaired CB specimens by 113% and greater than plain SCM-repaired CB specimens by 69%.

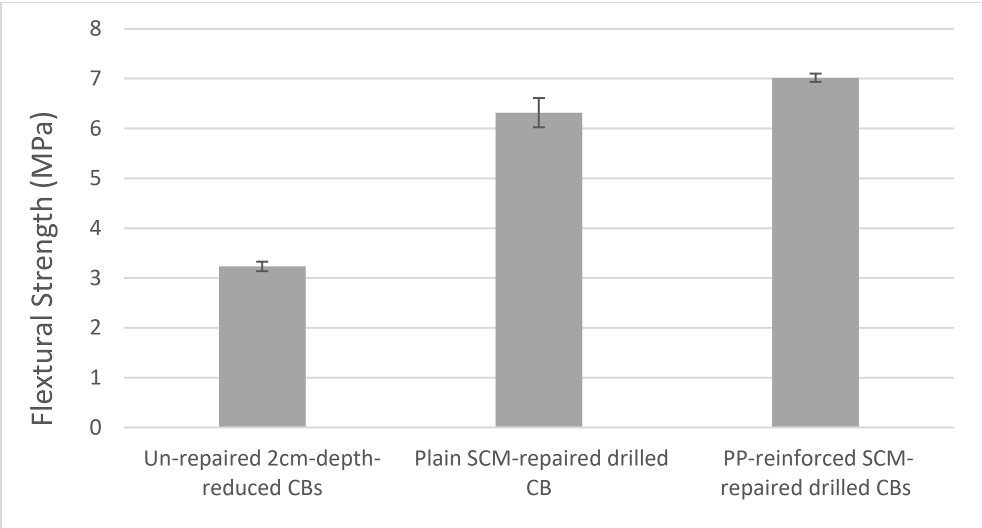

Figure 3.41 Flexural strength of group B's concrete beam specimens

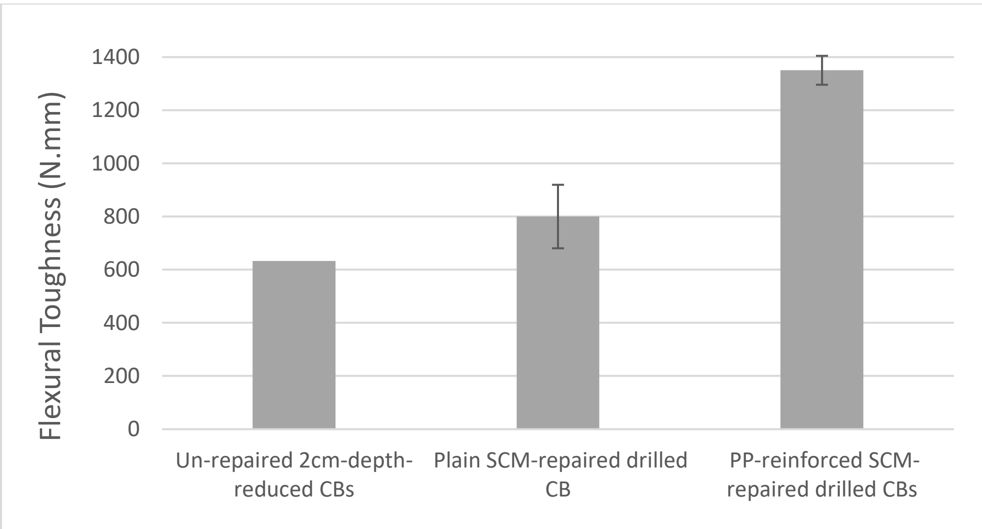

Figure 3.42 Flexural toughness of group B's concrete beam specimens

3.6.1.4 Repaired Flexural Concrete Beam Specimens Results of Group C

In this group, five types of beam specimens were used, 2cm-depth-reduced, plain SCM repaired nailed, PP-reinforced SCM-repaired nailed, plain SCM repaired surface-roughened, and PP-reinforced SCM-repaired surface-roughened BC specimens. Contact between concrete specimen and SCM was implemented by nailing and roughening the surface of specimens as explained previously in section 2.6.

Figure 3.43 presents the flexural strength for the five CB specimen types used in this group. All repaired CBs showed relatively similar flexural strength. Plain SCM-repaired surface-roughened CB showed the maximum flexural strength value which is greater than that of the un-repaired CB specimens by 188%.

Figure 3.44 presents the flexural toughness for the CB specimens used in this group. It can be observed that PP-reinforced SCM-repaired surface-roughened CB showed a greater flexural toughness value than that of the un-repaired CB specimens by 137%.

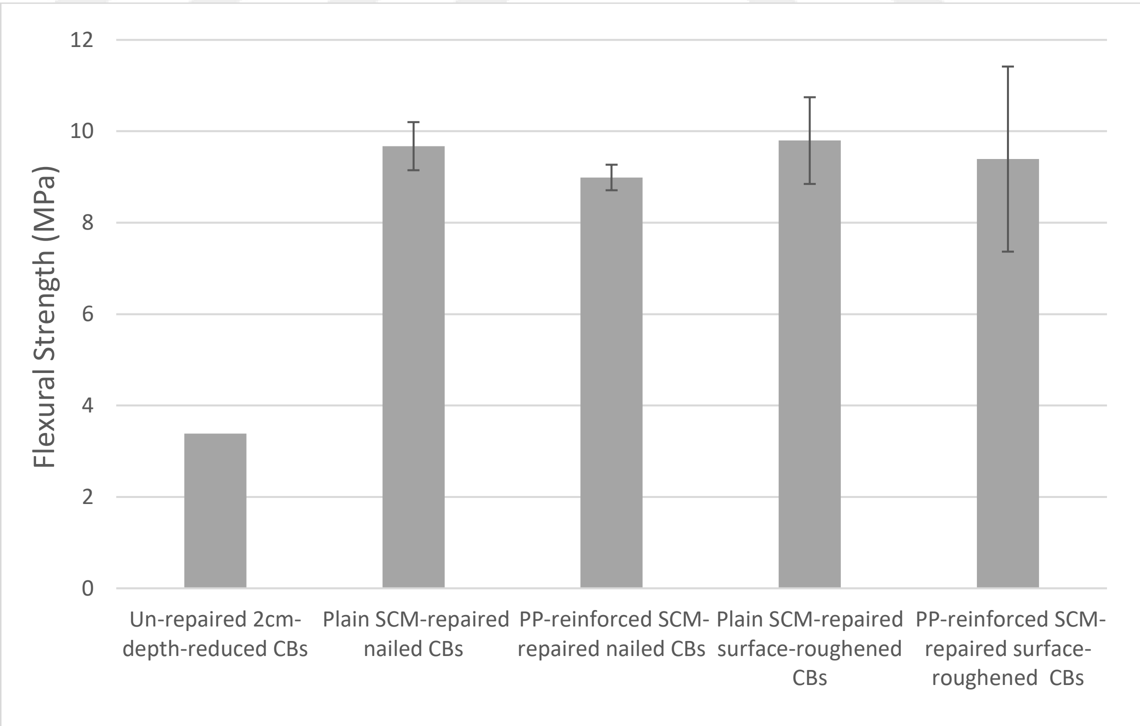

Figure 3.43 Flexural strength of group C’s concrete beam specimens

3.6.1.5 Overall Repaired Flexural Concrete Beam Specimens Results

In this series of experiments, eight types of beam specimens were used, un-repaired, 2cm-depth-reduced, plain SCM-repaired, PP fiber reinforced SCM-repaired, plain SCM repaired nailed, PP-reinforced SCM-repaired nailed, plain SCM repaired surface-roughened, and PP-reinforced SCM-repaired surface-roughened BC specimens. Contact between concrete specimen and SCM was implemented by drilling, nailing and roughening the surface of specimens as explained previously in section 2.6.

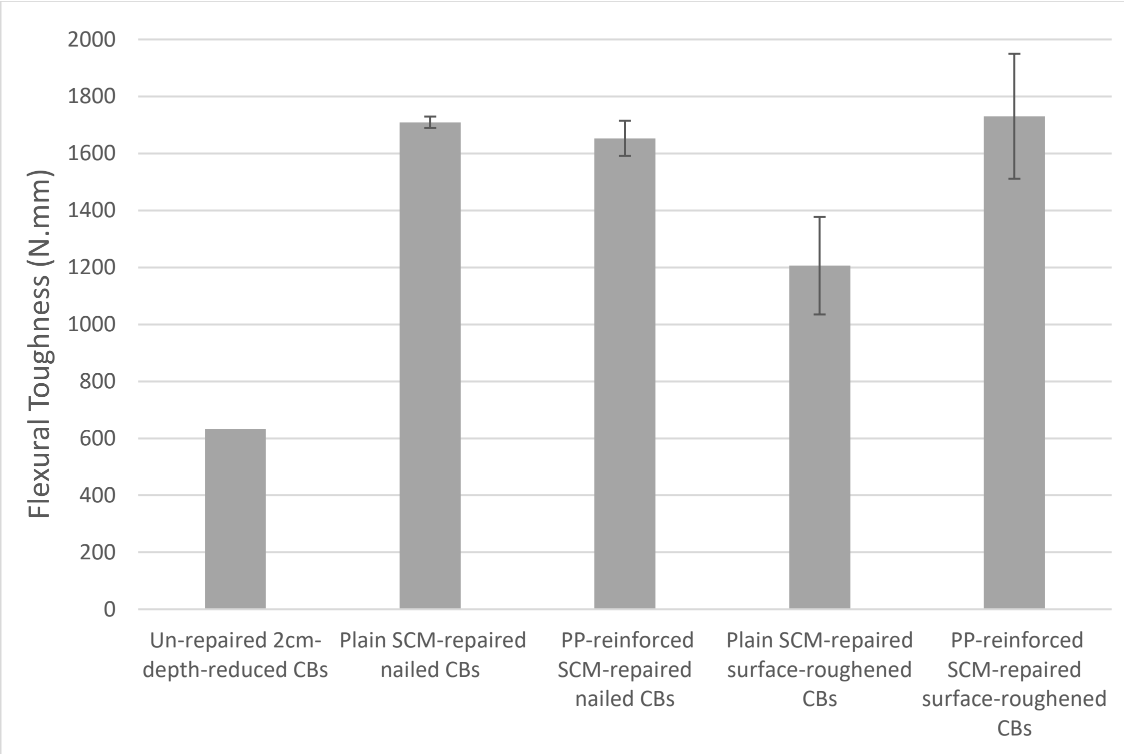

Figure 3.44 Flexural toughness of group C's concrete beam specimens

Figure 3.45 and 3.46 present the flexural strength and toughness for the eight CB specimen types used in this series. It can be observed that the use of surface roughening of CB's surface repaired by plain SCM showed the maximum flexural strength and high flexural toughness.

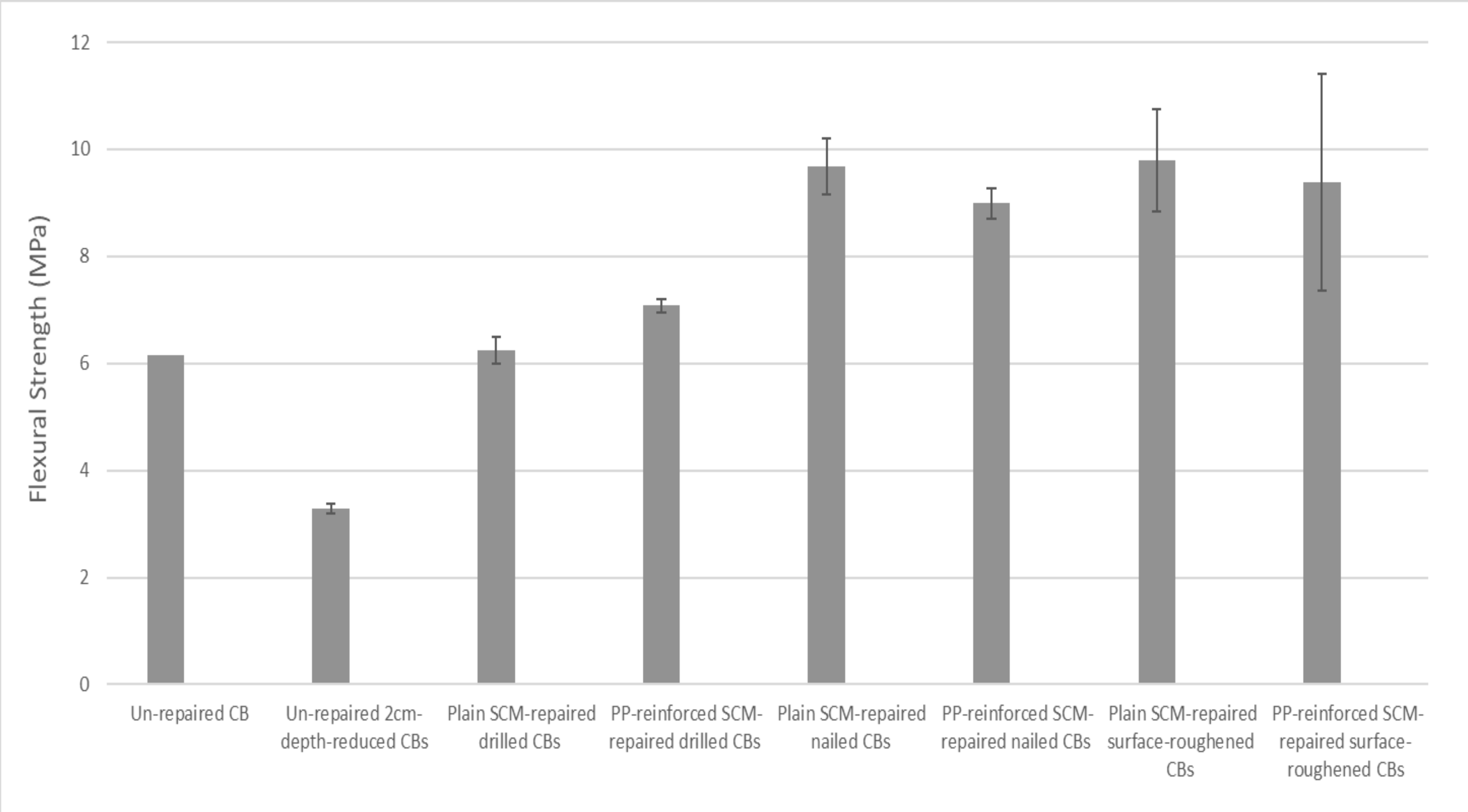

Figure 3.45 Flexural strength of groups, A, B and C’s concrete beam specimens

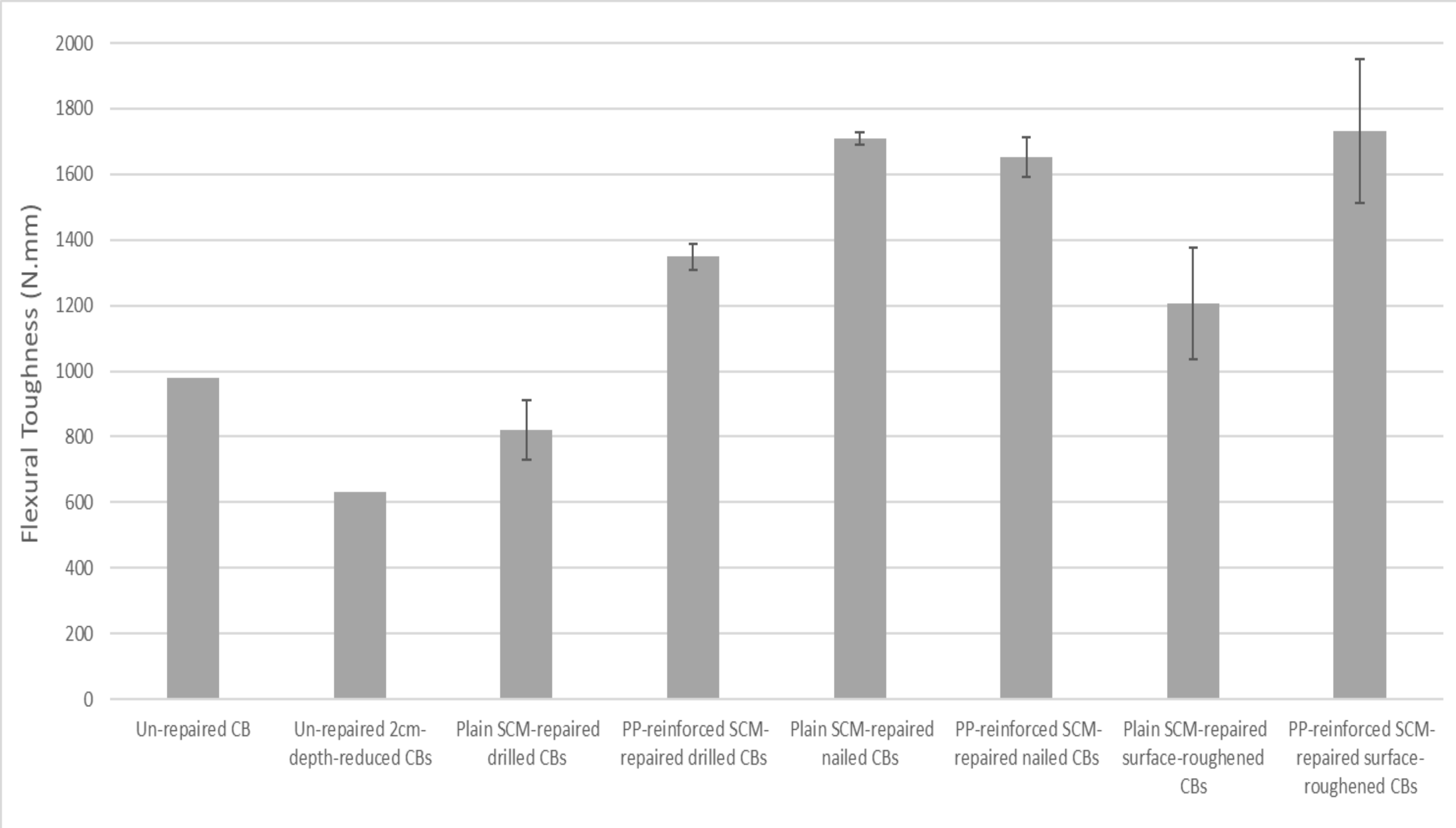

Figure 3.46 Flexural toughness of groups, A, B and C’s concrete beam

3.6.2 Splitting Tensile Test Results

Splitting tensile tests were conducted on cube specimens. Cubes were tested at the 28th day, then the resultant half-cubes were repaired. In group A it was assured to repair the bigger part of the resultant half cubes so the repaired cube would be mostly concrete. In group B it was assured to repair even halves cubes, so the repaired cubes would be half-concrete. In group C it was assured to repair the smaller half cubes so the repaired cubes would be mostly mortar. Then, repaired and un-repaired cubes were tested at the 56^{th} day.

Figure 3.47 presents the splitting tensile strength for the 28^{th} day control, 56^{th} day control, plain SCM repaired, and PP-reinforced SCM-repaired cubes used in group A (mostly concrete cubes). Respectively, the splitting tensile strength for every cubes set are 6.3, 7.1, 4.8 and 5.1 MPa. That indicates 6.3% increase for PP-reinforced SCM-repaired cubes over plain SCM repaired cubes.

Figure 3.48 presents the splitting tensile strength for the 28^{th} day control, 56^{th} day control, plain SCM repaired, and PP-reinforced SCM-repaired cubes used in group B (even halves cubes). Respectively, the splitting tensile strength for every cubes set is 6.7, 7.3, 2.0 and 2.4 MPa. That indicates 20% increase for PP-reinforced SCM-repaired cubes over plain SCM repaired cubes.

Figure 3.49 presents the splitting tensile strength for the 28^{th} day control, 56^{th} day control, plain SCM repaired, and PP-reinforced SCM-repaired cubes used in group C (mostly mortar cubes). Respectively, the splitting tensile strength for every cubes set is 6.4, 6.9, 4.4 and 4.6 MPa. That indicates 4.5% increase for PP-reinforced SCM-repaired cubes over plain SCM repaired cubes.

Figure 3.50 presents over all view of the splitting tensile strength for all the 28^{th} day control, 56^{th} day control, plain SCM repaired, and PP-reinforced SCM-repaired cubes used in groups A, B and C. Respectively, the splitting tensile strength for every cubes set is 6.5, 7.1, 3.8 and 4.1 MPa. That indicates 7.9% increase for PP-reinforced SCM-repaired cubes over plain SCM repaired cubes.

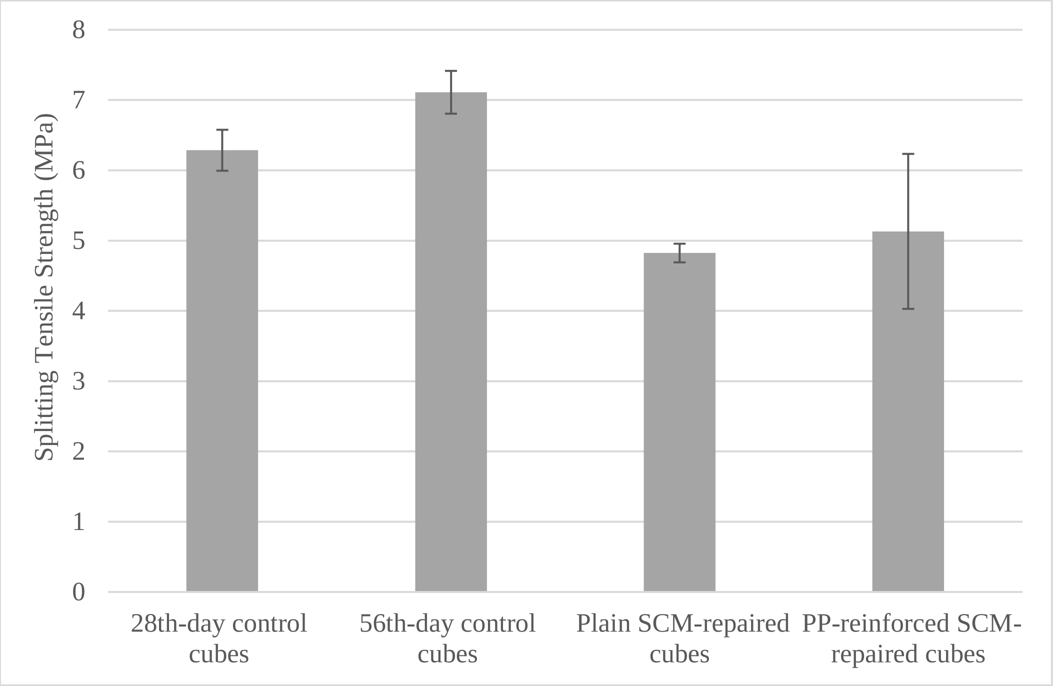

Figure 3.47 Splitting tensile strength of group A’s concrete cubes (mostly concrete cubes)

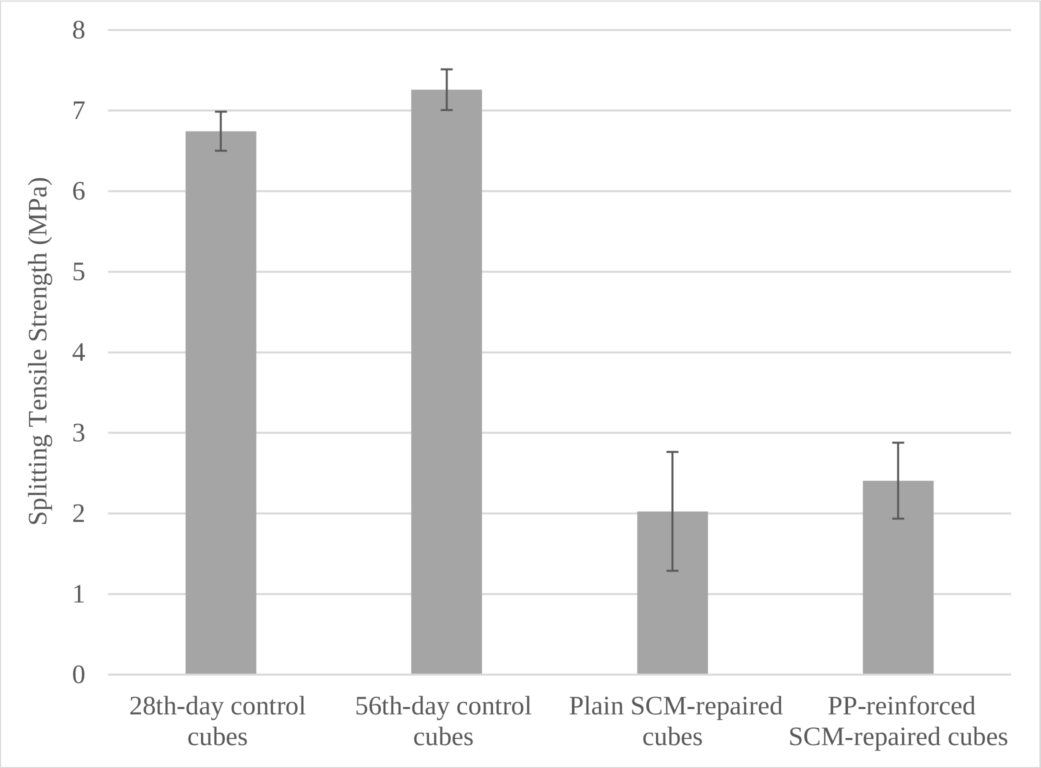

Figure 3.48 Splitting tensile strength of group B’s concrete cubes (even halves cubes)

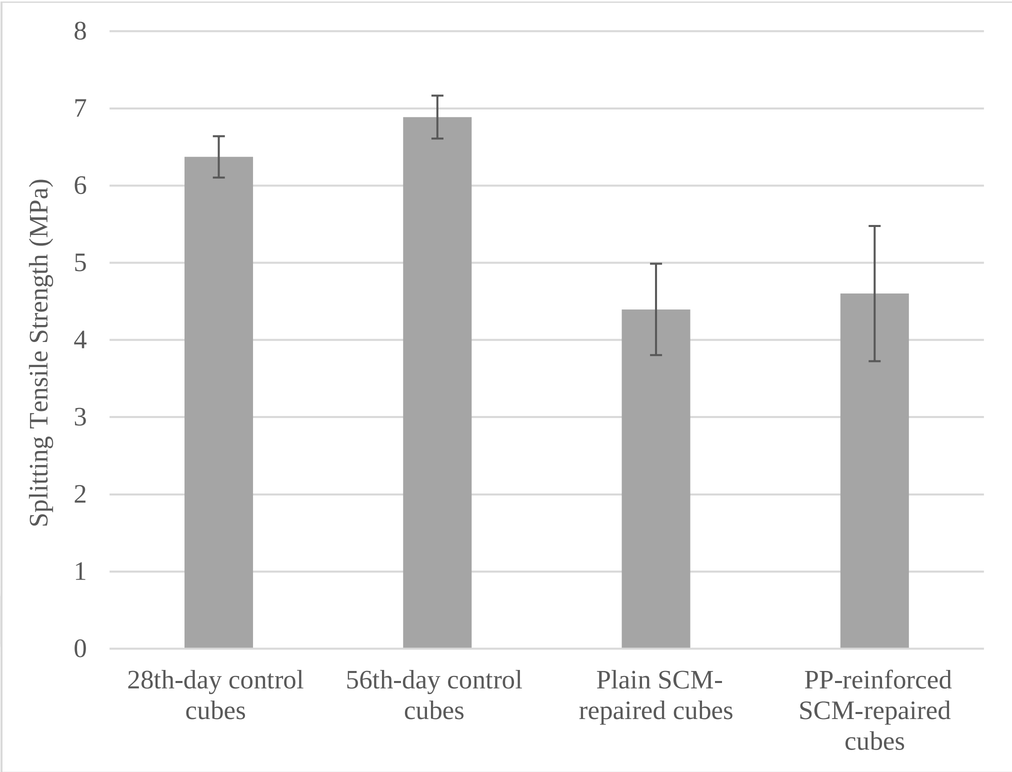

Figure 3.49 Splitting tensile strength of group C's concrete cubes (mostly mortar cubes)

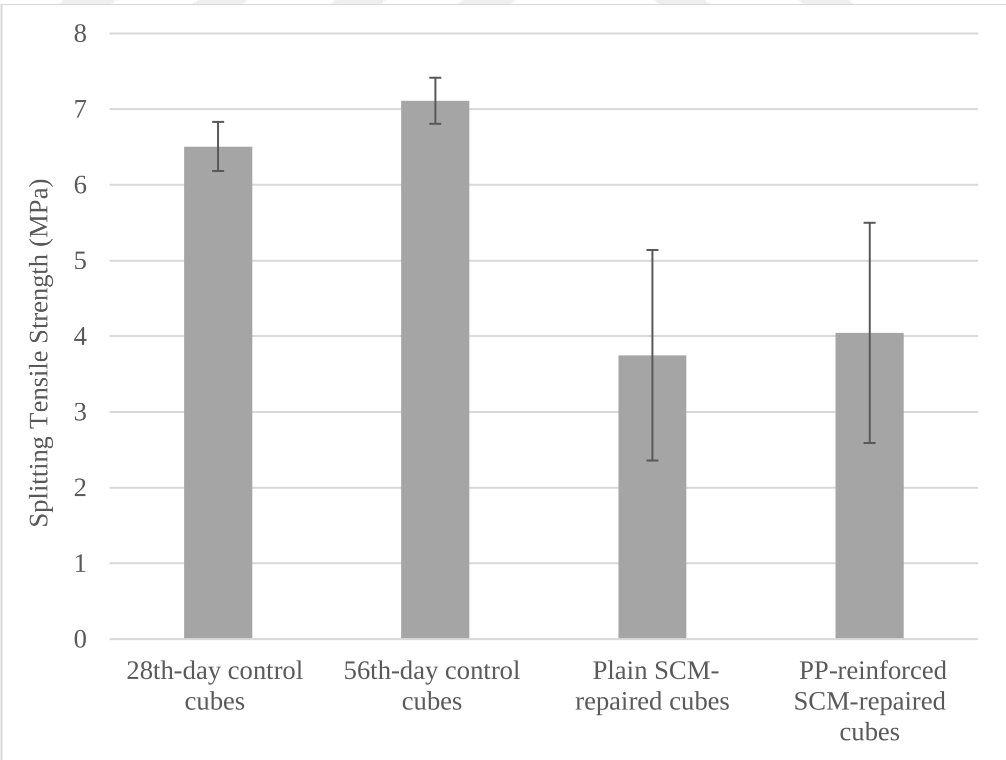

Figure 3.50 Splitting tensile strength of groups, A, B and C's concrete cubes

3.6.3 Compression Test Results

Compression tests were carried out on plain concrete cubes to test its compressive strength which was 35.3 MPa. Then, compression tests were conducted on the two beam parts resulting from every bending test for SCM specimens and for repaired concrete specimens. Concrete specimens were put in the testing machine with the repaired part being down. SCM specimens and the repaired specimen's compression tests results are discussed.

Figure 3.51 and Figure 3.52 present the compressive strength and toughness vs. fiber volume ratio behavior of SCM compressive specimens. Graphs show relatively similar compressive strength and toughness values for plain SCM and waste 0.3% volume ratio PP fiber reinforced SCM.

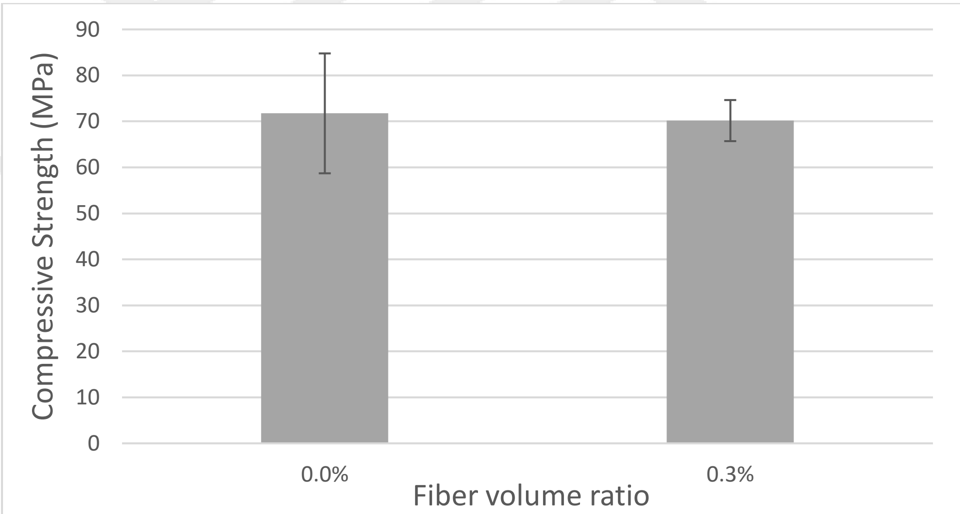

Figure 3.51 Compressive strength vs. PP fiber volume ratio incorporated in repairing SCM

Figures 3.53 and 3.54 present the compressive strength and toughness for the eight CB specimen types used previously in the bending tests. It can be observed that compression test values did not importantly change among specimens. PP-reinforced SCM-repaired nailed CBs had the maximum compressive strength of 40.7 MPa.

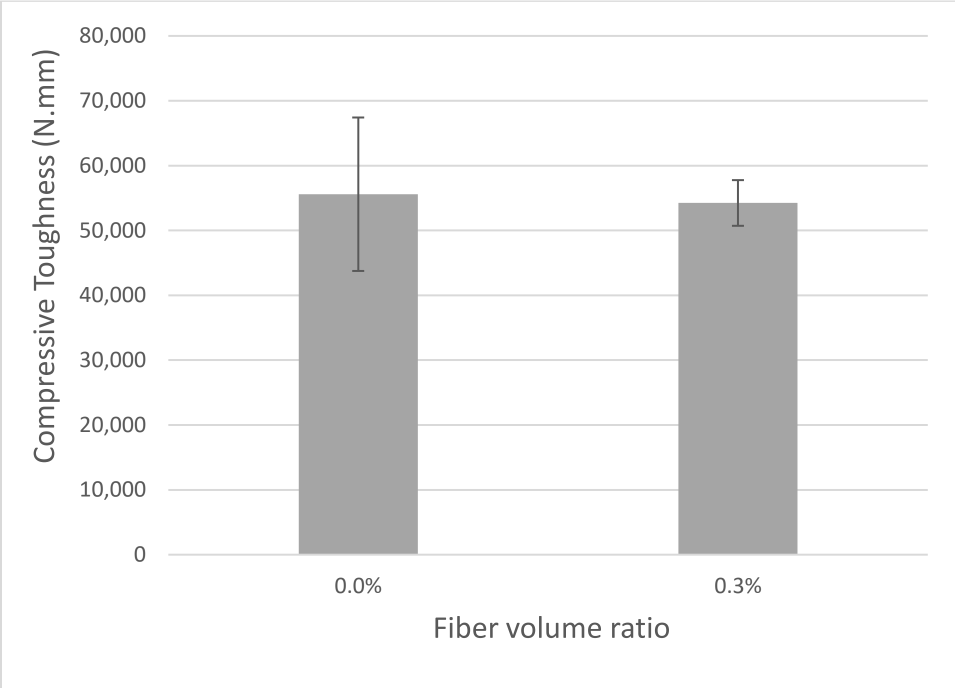

Figure 3.52 Compressive toughness vs. PP fiber volume ratio incorporated in repairing SCM

PP-reinforced SCM-repaired drilled CBs had the maximum compressive toughness of 208960 N.mm. From Figures 3.55 and 3.56 that presents pictures of specimens failed by compression test it can be obviously noticed that PP fibers enhanced the resistance to cracking which resulted in greater compressive strength values.

Figure 3.53 and Figure 3.54 present the compressive strength and toughness for the eight CB specimen types used previously in the bending tests. It can be observed that compression test values did not change. PP-reinforced SCM-repaired nailed CBs had the maximum compressive strength of 40.7 MPa. PP-reinforced SCM-repaired drilled CBs had the maximum compressive toughness of 208960 N.mm. From Figures 3.55 and 3.56 that presents pictures of specimens failed by compression test it can be obviously noticed that PP fibers enhanced the resistance to cracking which resulted in greater compressive strength values.

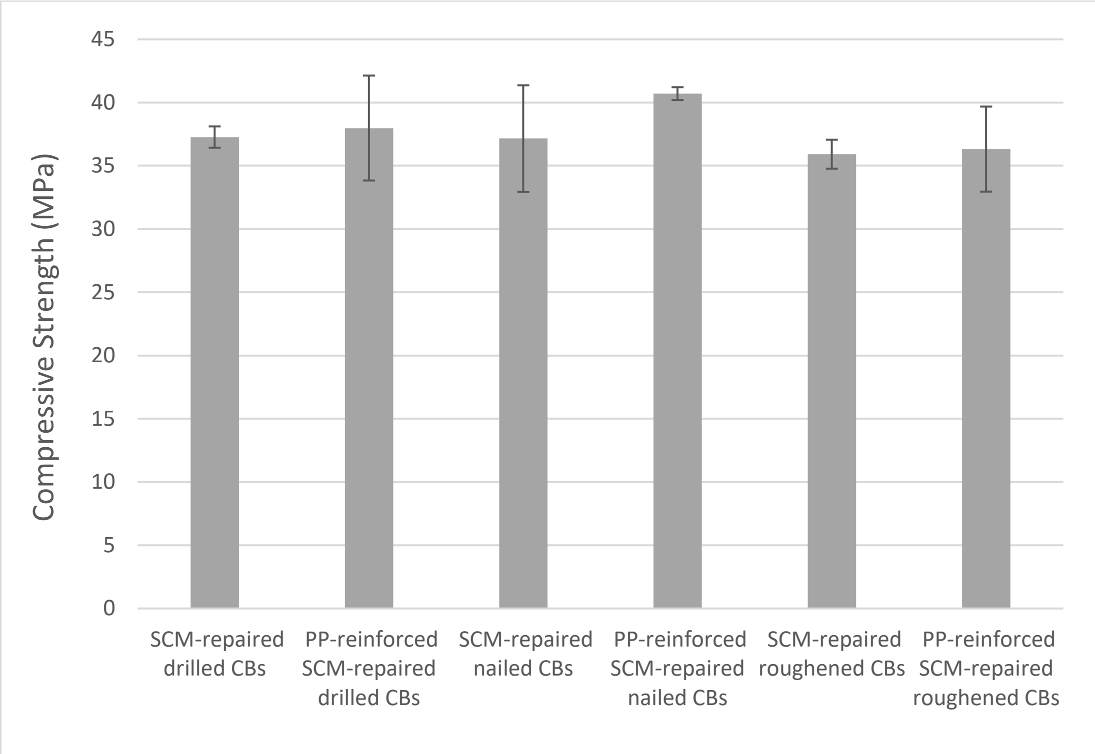

Figure 3.53 Compressive strength of groups A, B and C's concrete specimens

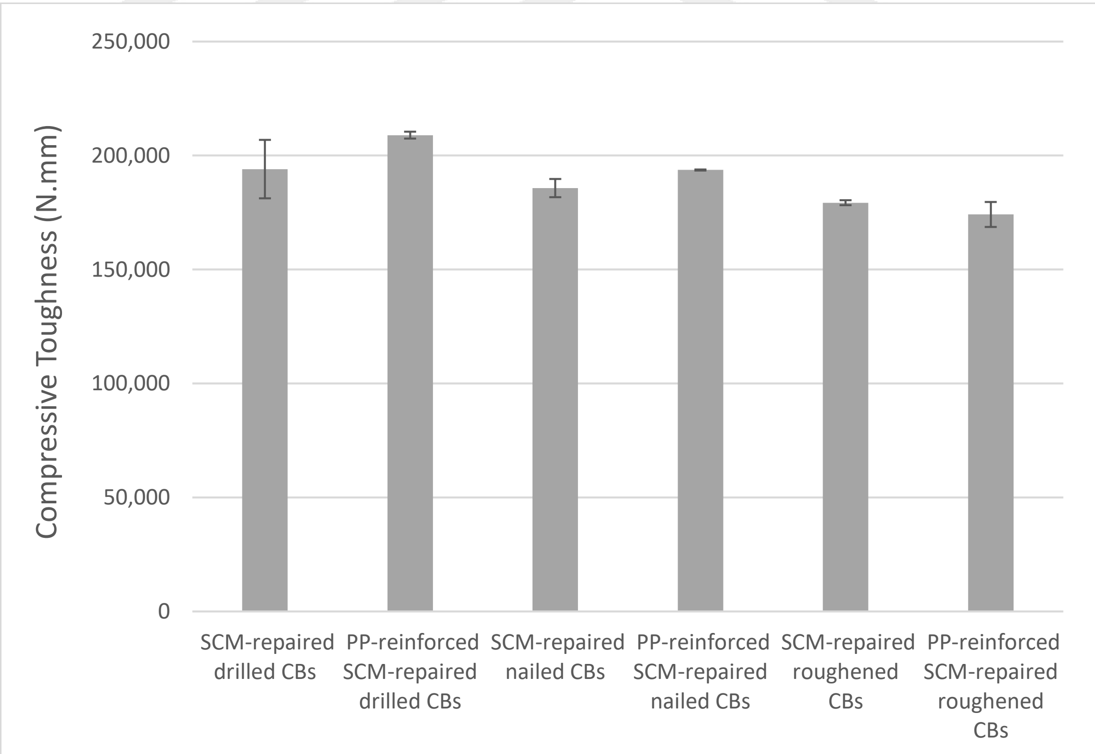

Figure 3.54 Compressive toughness of groups A, B and C's concrete specimens

Figure 3.55 Failed SCM repaired concrete specimen under compression test (Personal archive, 2017)

Figure 3.56 Failed PP- reinforced SCM repaired specimen under comp. test (Personal archive, 2017)

CHAPTER FOUR
CONCLUSIONS

The effect of waste plastic fiber on the mechanical properties of structural repair mortar was examined in this research. Two categories of waste plastic fibers were used; first, artificially produced waste plastic fibers consisting of PET with the dimensions 5×10 mm, 5×15 mm and 5×20 mm and PET/PE with the dimensions 5×10 mm and 5×15 mm, all by the fiber volume ratio of 0.2%, 0.5%, 0.8%, 1%, 1.5% and 2%. Second, industrial plastic fibers consisting of PP, PE, PA, TPP and TPE by the fiber volume ratio of 0.2%, 0.5%, 0.8%, 1% and 1.5% was used.

Two series of experiments were conducted; in the first series, mortar mixtures were designed to incorporate all waste plastic fibers used in the research. Bending tests were conducted on the prismatic samples and compression tests were conducted on the parts of the samples resulted from bending tests. Flexural and compressive strength and toughness were analyzed and discussed. In the second series of experiments, tests were conducted to design plain self-compacting mortar (SCM) and waste PP fiber reinforced SCM. Then, conventional concrete specimens were tested after being repaired by the designed SCM and waste PP fiber reinforced SCM. Concrete repairing by the two types of SCM was achieved by different ways; drilling, nails planting and roughening concrete repaired surface. Control specimens were unrepaired complete beam specimen and unrepaired 2cm-depth-reduced concrete specimens. Bending tests were conducted on the repaired beam specimens and compression tests were conducted on the parts of the beams resulted from bending tests. Splitting tensile tests were also conducted on repaired half-cube concrete specimens and complete concrete cube specimens for control. Flexural and compressive strength and toughness and splitting tensile strength were analyzed and discussed.

The major conclusions of the mechanical characteristics drawn from the first series of experiments carried out on waste plastic fibers incorporated mortar were:

- The use of waste PET, PET/PE fibers did not importantly affect flexural strength of mortar with fiber volume ratio. The use of waste PP, PE and PA fibers did not improve flexural strength of mortar with fiber volume ratio.
- The use of waste PET, PET/PE, PP, PE and PA fibers improved flexural toughness significantly. Results indicated a proportional relationship between fiber volume ratio and flexural toughness. Also, a proportional relationship between aspect ratio of fibers and flexural toughness is noticed. Maximum rise of 2402% was noticed when PET 5×20 mm fibers were incorporated at 2% volume ratio and maximum rise of PP was at 1.5% volume ratio by 1841% from conventional mortar.
- The use of waste PET, PET/PE, PP, PE and PA fibers decreased compressive strength and toughness of mortar with fiber volume ratio. Enhancement in the compressive strength and toughness of mortar was noticed when incorporated PP and PE were chemically treated in comparison to the untreated PP and PE fibers.

The major conclusions of the mechanical characteristics drawn from the experiments carried out on plain and waste PP fiber incorporated SCM specimens in the second series of experiments are:

- The use of waste PP fibers in SCM caused a gradual decline in flexural strength that reached the maximum drop by 28.8% at 0.3% volume ratio incorporation.
- The use of waste PP fibers in SCM improved flexural toughness significantly. Results indicated a proportional relationship between fiber volume ratio and flexural toughness. The maximum rise of PP reinforced SCM's flexural toughness was reached at 0.4% volume ratio by 279% in compare to plain SCM.
- The use of waste PP fibers in SCM caused a rise in compressive strength by 2.9% at 0.3% volume ratio incorporation and did not improve compressive toughness.

The major conclusions of the mechanical characteristics drawn from the second series of experiments carried out on plain and waste-PP-fiber reinforced-SCM repaired concrete beam (CB) specimens in the second series of experiments are:

- Repairing CBs by plain and by waste-PP-fiber reinforced SCM showed enhancement in the flexural strength in comparison to the unrepaired CB. Repairing CBs by plain SCM did not show important change from repairing by waste-PP-fiber reinforced-SCM in terms of flexural strength. CBs whose contact with SCM achieved by nailing and roughening showed better flexural strength than drilled CBs. An enhancement was displayed in the flexural toughness of CBs when repaired by waste-PP-fiber reinforced SCM in comparison to CBs repaired by plain SCM for surface-roughened and drilled CBs.
- 56^{th} day concrete cube specimens repaired by waste-PP-fiber reinforced SCM showed splitting tensile strength 8% better than the 56^{th} day plain SCM reinforced concrete cube specimens.

Numerous studies have been carried out on this subject in the recent years. These works showed that the use of recycled plastic fibers as building materials intensifies attention. The findings of this study show that using waste plastic as reinforcing fiber led to some better mortar mechanical properties. The use of some waste plastic materials as reinforcing fiber significantly increased the flexural properties and the post-peak ductility of mortar.

More research is still needed in this subject to study the other properties of waste plastic fiber reinforced mortar such as air content, pulse velocity, abrasion resistance, creep, shrinkage, durability.

REFERENCES

Al-Tulaian B.S., Al-Shannag M.J., Al-Hozaimy A.R. (2016). Recycled plastic waste fibers for reinforcing Portland cement mortar. *Construction and Building Materials 127, 102–110.*

ASTM C230 / C230M-14. (2014). Standard Specification for Flow Table for Use in Tests of Hydraulic Cement. *ASTM International*, USA.

ASTM C349-14. (2014). Standard Test Method for Compressive Strength of Hydraulic-Cement Mortars (Using Portions of Prisms Broken in Flexure). *ASTM International*, USA.

ASTM C1609 / C1609M-12. (2012). Standard Test Method for Flexural Performance of Fiber-Reinforced Concrete (Using Beam With Third-Point Loading). *ASTM International*, USA.

ASTM D792-13. (2013). Standard Test Methods for Density and Specific Gravity (Relative Density) of Plastics by Displacement. *ASTM International*, USA.

ASTM C1437-15. (2015). Standard Test Method for Flow of Hydraulic Cement Mortar, *ASTM International*, USA.

Choi, Y.W., Moon, D.J., Chung, J.S., Cho, S.K. (2005). Effects of waste PET bottles aggregate on the properties of concrete. *Cement and Concrete Research, 35, 776–781.*

Choi, Y.W., Moon, D.J., Kim, Y.J., Lachemi, M. (2009). Characteristics of mortar and concrete containing fine aggregate manufactured from recycled waste polyethylene terephthalate bottles. *Construction and Building Materials, 23, 2829–283.*

Ge, Z., Sun, R., Zhang, K., Gao, Z., Li, P. (2013). Physical and mechanical properties of mortar using waste Polyethylene Terephthalate bottles. *Construction and Building Materials, 44, 81–86.*

Gu L., Ozbakkaloglu T. (2016). Use of recycled plastics in concrete: A critical review. *Waste Management 51, 19–42.*

Felekoglu B., Tosun K., Baradan B. (2009). A comparative study on the flexural performance of plasma treated polypropylene fiber reinforced cementitious composites. *Journal of Materials Processing Technology 209, 5133–5144.*

Foti, D. (2011). Preliminary analysis of concrete reinforced with waste bottles PET fibers, *Construction and Building Materials, 25, 1906–1915.*

Kim J.-H. J., Park C.-G., Lee S.-W., Lee S.-W., Won J.-P. (2008). Effects of the geometry of recycled PET fiber reinforcement on shrinkage cracking of cement-based composites. *Composites: Part B 39, 442–450.*

Kolatar, Ö.A. (2016). *Yapı sağlığının izlenmesi için betonda elektriksel direnç – birim uzama ilişkisinin deneysel olarak araştırılması.* MSc Thesis, Dokuz Eylül University, İzmir.

López-Buendía A.M., Romero-Sánchez, M.D., Climent, V., Guillemb, C. (2013). Surface treated polypropylene (PP) fibres for reinforced concrete. *Cement and Concrete Research, 54, 29–35.*

Ozbakkaloglu T., Gu L., Gholampour A. (2017). Short-Term Mechanical Properties of Concrete Containing Recycled Polypropylene Coarse Aggregates under Ambient and Elevated Temperature. *Journal of Materials in Civil Engineering. 29*(10), *1-10.*

Payrow P., Nokken M. R., Banu D., Feldman D. (2011). Effect of surface treatment on the post-peak residual strength and toughness of polypropylene/polyethylene-blended fiber-reinforced concrete. *Journal of Composite Materials 45*(20)*, 2047–2054.*

Peled A., Guttman H. (1992). Treatments of Polypropylene Fibres to Optimize their Reinforcing Efficiency in Cement Composites. *Cement & Concrete Composites 14, 277-285.*

Safi B., Saidi M., Aboutaleb D., Maallem M. (2013). The use of plastic waste as fine aggregate in the self-compacting mortars: Effect on physical and mechanical properties. *Construction and Building Materials 43, 436–442.*

Saikia, N., de Brito, J. (2012). Use of plastic waste as aggregate in cement mortar and concrete preparation: A review. *Construction and Building Materials, 34, 385–401*.

Saikia, N., de Brito, J. (2014). Mechanical properties and abrasion behavior of concrete containing shredded PET bottle waste as a partial substitution of natural aggregate. *Construction and Building Materials, 52, 236–244.*

Siddique, R., Khatib, J., Kaur, I. (2008). Use of recycled plastic in concrete: A review. *Waste Management, 28, 1835–1852.*

Silva A. M., Brito J., Veiga R. (2014). Incorporation of fine plastic aggregates in rendering mortars. *Construction and Building Materials 71, 226–236.*

Sharma R., Bansal P. P., Use of different forms of waste plastic in concrete - a review. *Journal of Cleaner Production 112*(1)*, 1-10.*

Thorneycroft J., Orr J., Savoikar P., Ball R.J. (2018). Performance of structural concrete with recycled plastic waste as a partial replacement for sand. *Construction and Building Materials 161, 63–69.*

Türk Standardı TS 802. (2009). Beton karışım tasarımı hesap esasları. *Türk Standartları Enstitüsü,* Ankara.

Turkish Standard TS EN 13395-1. (2004). Products and systems for the protection and repair of concrete structures - Test methods - Determination of workability - Part 1: Test for flow of thixotropic mortars. *Türk Standartları Enstitüsü,* Ankara.

Verdolotti, L., Iucolano F., Capasso I., Lavorgna M., Iannace S., Liguorib B. (2014). Recycling and Recovery of PE-PP-PET-based Fiber Polymeric Wastes as Aggregate Replacement in Lightweight Mortar: Evaluation of Environmental Friendly Application. Environmental Progress & Sustainable Energy *33*(4), *1445–1451*.

Wang J.-Y., Chia K.-S., Liew J.-Y. R., Zhang M.-H. (2013). Flexural performance of fiber-reinforced ultra lightweight cement composites with low fiber content. *Cement & Concrete Composites 43, 39–47.*